ENHANCEMENT OF BIOMETHANE PRODUCTION FROM CATTLE MANURE DIGESTION VIA GRANULAR ACTIVATED CARBON AMENDMENT

A THESIS SUBMITTED TO
THE GRADUATE SCHOOL OF NATURAL AND APPLIED SCIENCES
OF
MIDDLE EAST TECHNICAL UNIVERSITY

BY

YASİN ODABAŞ

IN PARTIAL FULFILLMENT OF THE REQUIREMENTS
FOR
THE DEGREE OF MASTER OF SCIENCE
IN
ENVIRONMENTAL ENGINEERING

NOVEMBER 2022

Approval of the thesis:

ENHANCEMENT OF BIOMETHANE PRODUCTION FROM CATTLE MANURE DIGESTION VIA GRANULAR ACTIVATED CARBON AMENDMENT

submitted by **YASİN ODABAŞ** in partial fulfillment of the requirements for the degree of **Master of Science** i**n Environmental Engineering, Middle East Technical University** by,

Prof. Dr. Halil Kalıpçılar
Dean, Graduate School of **Natural and Applied Sciences** _____

Prof. Dr. Bülent İçgen
Head of the Department, **Environmental Engineering** _____

Assist. Prof. Dr. Yasemin Dilşad Yılmazel Tokel
Supervisor, **Environmental Engineering, METU** _____

Examining Committee Members:

Prof. Dr. Ülkü Yetiş
Environmental Engineering, METU _____

Assist. Prof. Dr. Yasemin Dilşad Yılmazel Tokel
Environmental Engineering, METU _____

Prof. Dr. Ayşegül Aksoy
Environmental Engineering, METU _____

Prof. Dr. Ayşenur Uğurlu
Environmental Engineering, Hacettepe University _____

Assist. Prof. Dr. Nazife Işık Semerci
Energy Engineering, Ankara University _____

Date: 17.11.2022

I hereby declare that all information in this document has been obtained and presented in accordance with academic rules and ethical conduct. I also declare that, as required by these rules and conduct, I have fully cited and referenced all material and results that are not original to this work.

Name Last name: Yasin Odabaş

Signature :

ABSTRACT

ENHANCEMENT OF BIOMETHANE PRODUCTION FROM CATTLE MANURE VIA GRANULAR ACTIVATED CARBON AMENDMENT

Odabaş, Yasin
Master of Science, Environmental Engineering
Supervisor: Assoc. Prof. Dr. Yasemin Dilşad Yılmazel Tokel

November 2022, 152 pages

In this study we investigated the impact of granular activated carbon (GAC) application on anaerobic digestion (AD) process of cattle manure. Firstly, the effect of the presence of basal medium on cattle manure digestion was evaluated. It was observed that basal medium addition decreased methane yield and increased lag time. Then, for the enhanced cattle manure digestion, a metal-based conductive material, hematite (Fe_2O_3), and carbon-based material, GAC, were amended into the reactors. From the comparison of these two conductive materials, GAC was selected to be used in this study because of the higher performance in methane production. To study, amendment of GAC the optimum dosage was determined as 40 g/L experimentally. Further, the impact of GAC application on mesophilic (T = 35 ^oC) cattle manure digestion was investigated under both mixing and no mixing conditions and at two different food-to-microorganism (F/M) ratios of 1 and 3 in batch reactors. In the experimental tests, sand particle of similar size as in GAC were also added into the control reactors to assess the impact of supplying extra surface area for biomass attachment. The application of GAC increased the methane yield (139.0 ml CH_4/g VS_{added}) by 28% at F/M ratio of 1 under mixing condition. While the enhancement in methane yield by sand amendment (115.6 ml CH_4/g VS_{added}) was

limited to 6% as compared to the Control1-mix (109.3 ml CH_4/g VS_{added}). A higher increase was attained at F/M ratio of 3 under mixing conditions. In GAC amended reactor methane yield was 71% higher than the control, yet in sand amended reactor methane yield was only 15% higher than control. This implies that the performance enhancement in methane production and lag time is not merely due to surface area and can be attributed to the presence of conductive material. Further, we investigated the impact of GAC at psychrophilic temperature (~18 ^oC) conditions. GAC amendment increased methane yield by 12% and 26% in comparison to conventional anaerobic digestion reactor at F/M ratios of 1 and 3, respectively. Additionally, we have also investigated the impacts of biomass attached GAC, named as BioGAC, on the performance of psychrophilic manure digestion. BioGAC amendment enhanced methane yield by 21% and 33% compared to the control reactor at F/M ratio of 1 and 3, respectively. When GAC and sand applications were compared, higher increase in methane production was observed in GAC added reactors owing to its contribution to direct interspecies electron transfer (DIET) mechanism in the reactors. These results were also supported by cyclic voltammetry (CV) analysis. Finally, 16S ribosomal RNA based methods were used to identify the key microorganisms present in the psychrophilic reactors.

Keywords: Cattle Manure, Anaerobic Digestion, Granular Activated Carbon, Methane, Direct Interspecies Electron Transfer

ÖZ

GRANÜL AKTİF KARBON EKLENMESİ İLE SIĞIR GÜBRESİNİN ÇÜRÜTÜLMESİNDEN BİYOMETAN ÜRETİMİNİN ARTIRILMASI

Odabaş, Yasin
Yüksek Lisans, Çevre Mühendisliği
Tez Yöneticisi: Dr. Öğr. Üy. Yasemin Dilşad Yılmazel Tokel

Kasım 2022, 152 sayfa

Bu çalışmada granüler aktif karbon (GAK) uygulamasının sığır gübresinin anaerobik çürütme (AÇ) süreci üzerindeki etkisini aratştırdık. İlk olarak, bazal besiyerin varlığının sığır gübresi üzerindeki etkisi değerlendirilmiştir. Bazal besiyeri ilavesinin metan verimini azalttığı ve reaktör başlama süresini artırdığı gözlendi. Daha sonra, metal bazlı iletken madde, hematit (Fe_2O_3) ve karbon bazlı iletken madde olan, GAK, sığır gübresi çürütülmesinin artırılması için reaktörlere eklendi. Bu iki iletken maddenin kıyaslanmasından, daha yüksek perfromans sağladığı için GAK bu çalışmada kullanılmak üzere seçilmiştir. GAK eklenmesinin etkilerini incelemek için optimum dozaj deneysel olarak 40 g/L olarak belirlendi. Ayrıca, GAK uygulaması mezofilik (35 ^oC) sığır gübresi çürütülmesinde hem karıştırma varken hem de karıştırma olmadan iki farklı besin-aşı oranı (1 ve 3) sağlanarak kesikli reaktörlerde incelenmiştir. Deneysel testlerde, biyokütlenin tutunabilmesi için ekstra yüzey alanı sağlanmasının etkisi GAK ile benzer boyutta kum parçacıklarının kontrol reaktörlerine eklenmesiyle incelenmiştir. GAK ilavesi karıştırma uygulandığında B/A oranı 1 olduğunda metan verimliliğini %28 artırmıştır. Kum parçacıklarının eklenmesi ile ise bu artış kontrol reaktörüne kıyasla %6'da kalmıştır. Karıştırma uygulandığında daha fazla artış B/A oranı 3'ken elde edilmiştir. GAK

uygulanan reaktörde metan verimliliği kontrolden %71 daha yüksekken, kum parçacıklarının eklenmesi verimliliği kontrol reaktörüne kıyasla yalnızca %15 artırmıştır. Bu, performans artışının yalnızca sağlanan ekstra yüzey alanından kaynaklanmadığı ve iletken maddenin varlığına atfedilebileceği anlamına gelir. Ayrıca, psikrofilik sıcaklıkta (~18 ºC) GAK uygulamasının etkisini de araştırdık. GAK uygulaması metan verimliliğini kontrol reaktörlerine kıyasla B/A oranın 1 ve 3 olduğu koşullarda sırasıyla %12 ve %26 artırmıştır. Ek olarak, BioGAK olarak adlandırdığımız önceden üzerinde biyokütle oluşturulmuş GAK'ın psikrofilik sığır gübresi çürütülmesi üzerindeki etkisi de incelenmiştir. BioGAK uygulaması metan verimliliğini kontrol reaktörlerine kıyasla B/A oranın 1 ve 3 olduğu koşullarda sırasıyla %21 ve %33 artırmıştır. GAK ve kum uygulamaları karşılaştırıldığında, türler arası doğrudan elektron transferi (TADET) mekanizmasına katkısı nedeniyle GAK eklenen reaktörlerde daha fazla performans artışı gözlemlenmiştir. Bu sonuçlar döngüsel voltametri (DV) analizi ile de desteklenmiştir. Son olarak, psikrofilik reaktörlerde bulunan temel mikroorganizmaların tanımlanabilmesi için 16S ribozomal RNA bazlı yöntemler kullanılmıştır.

Anahtar Kelimeler: Sığır Gübresi, Anaerobik Çürütme, Granüler Aktif Karbon, Metan, Türler Arası Doğrudan Elektron Transferi

To my family…

ACKNOWLEDGMENTS

First of all, I would like to express my sincere gratefulness to Assist. Prof. Dr. Yasemin Dilşad Yılmazel Tokel for her guidance, invaluable support, advices and encouragement during this my master study. It was a honor to work with her and in the environment she provided.

I also would like to acknowledge The Scientific and Technological Research Council of Turkey (TÜBİTAK) for the financial support as part of this thesis study was conducted within the scope of 218M854 project.

I am deeply grateful to the members of our research group Bioprocesss Engineering Research Group (BIOERG); Amin Ghaderikia, Aykut Kaş, Berivan Tunca, Berkan Öden, Feride Ece Kutlar, Işkın Köse, Mert Şanlı for their friendships and support during this period. I also appreciate our undergraduate members of the group: Buse Naval, Elif Taştan and Mehmet Yağcı.

I would like to present exclusive thank to my mother Hayriye Odabaş, my father İsmail Odabaş, my sisters Tuğçe Odabaş and Özge Odabaş, and my brother Emir Kaan Odabaş for their endless encouragement and patience.

Finally, I could not find any words to express my feelings for Beyza Çetiner, but I am deeply gratefulness to her who has been always stand by me and provide ever-constant support especially at most difficult times.

TABLE OF CONTENTS

ABSTRACT v

ÖZ vii

ACKNOWLEDGMENTS x

TABLE OF CONTENTS xi

LIST OF TABLES xiv

LIST OF FIGURES xvi

LIST OF ABBREVIATIONS xix

CHAPTERS

1 INTRODUCTION 1

2 LITERATURE REVIEW 7

2.1 Anaerobic Digestion (AD) 7

2.1.1 Process Description and Stages of AD 7

2.1.2 Important Parameters Affecting AD Performance 9

2.1.3 Variety of Feedstocks in AD 12

2.1.4 Electron Transfer Mechanisms in AD 13

2.1.5 Limitations of AD 16

2.1.6 Methods used for AD Performance Enhancement and its widespread Application 16

2.2 The impact of Conductive Material Amendment on AD Process 21

2.2.1 Impacts of CoMs on AD 21
2.2.2 Types of CoMs 23
2.2.3 Electrochemical Analysis of Microbial Electron Transfer: Cyclic Voltammetry (CV) 24
2.2.4 Microbial Communities of CoM amended AD Reactors 25
3 MATERIALS AND METHODS 27
3.1 Waste and Inoculum Characteristics 27
3.2 Basal medium 30
3.3 Analytical Methods 30
3.3.1 Characterization experiments 30
3.3.2 Determination of Biogas Production and the Content of Biogas 31
3.3.3 Determination of Volatile Fatty Acid (VFA) Concentrations 34
3.4 BioMethane Production Data Analysis 35
3.5 Experimental Sets and Procedures 36
3.5.1 The reactor configuration 37
3.5.2 Set 1: The impact of Basal Medium on Mesophilic Anaerobic Digestion of Cattle Manure 38
3.5.3 Set 2: Enhancement of CM Digestion via Amendment of Conductive Materials: Hematite vs. Granular Activated Carbon 40
3.5.4 Set 3: The Impact of GAC Amendment on Mesophilic AD of CM under Different Organic Loads and the Impact of Mixing on the Performance 44
3.5.5 Set 4: The Impact of GAC Amendment on Psychrophilic Anaerobic Treatability of CM under Different Organic Loads 47
3.6 Cyclic Voltammetry (CV) Analysis 50

3.7 Struvite Precipitation Experiments and Product Analysis 51
3.8 Cost-Revenue analysis 52
3.9 Microbial Community Analysis 54
4 RESULTS AND DISCUSSIONS 57
4.1 Set 1: The Impact of Basal Medium on Mesophilic Anaerobic Digestion of Cattle Manure 57
4.2 Set 2: Enhancement of Mesophilic AD of CM via Amendment of Conductive Materials (CoMs): Hematite vs. GAC 63
4.3 Set 3: Enhancement of CM Digestion via GAC under Different Organic Loads and Mixing 79
4.4 Set 4: The Impact of GAC & BioGAC Amendment on Psychrophilic AD of CM under Different Organic Loads 100
5 CONCLUSION 123
6 RECOMMENDATIONS 125
REFERENCES 127
APPENDICES
A. Calculation for kinetic parameters 147
B. Modified Gompertz Model Fittings for Set 1 148
C. Modified Gompertz Model Fittings for Set 2 149
D. Modified Gompertz Model Fittings for Set 3 150
E. Modified Gompertz Model Fittings for Set 4 152

LIST OF TABLES

TABLES

Table 2.1. Acetogenic and methanogenic reactions possible during AD process... 14
Table 3.1. The characteristics of CM and inoculum used in Set 1 28
Table 3.2. The characteristics of CM and inoculum used in Set 2 28
Table 3.3. The characteristics of CM and inoculum used in Set 3 29
Table 3.4. The characteristics of CM and inoculum used in Set 4 29
Table 3.5. The methods used in the characterization experiments 31
Table 3.6. The experimental design for Set 1 39
Table 3.7. TS and VS results for GAC and hematite 41
Table 3.8. The experimental design for Set 2 42
Table 3.9. The experimental design for Set 3 45
Table 3.10. The experimental design for Set 4 49
Table 4.1. The results of kinetic parameters calculated from the Modified Gompertz modeling for the reactors in Set 1 61
Table 4.2. Methane yields of similar studies when CM was used as feed 62
Table 4.3. Comparison of results from different studies using GAC amendment in AD 67
Table 4.4. Comparison of results from different studies using hematite amendment in AD 69
Table 4.5. Kinetic parameters calculated from the fitting with the modified Gompertz model in Set 2 72
Table 4.6. The results of kinetic parameters calculated from Gompertz modeling for the reactors in Set 3 83
Table 4.7. The results of struvite precipitation in terms of N&P removals and the amount of struvite precipitated in Set 3 98
Table 4.8. The results of kinetic parameters calculated from Gompertz modeling for the reactors in Set 4 106

Table 4.9. Methane yield and methane production rates for AD1-mix, GAC1 and BioGAC1 121
Table 4.10.The costs due to GAC application and heating, revenue from methane production rate and the difference between cost and revenue for AD1-mix, GAC1 and BioGAC1..... 122

LIST OF FIGURES

FIGURES

Figure 2.1. AD stages and the microorganisms responsible for each stage (Adopted from Y. Liu et al., 2021) 8
Figure 2.2. Electron transfer mechanism during AD process; a) MIET via hydrogen, b) MIET via extracellular soluble compounds, and c) DIET via conductive pili d) DIET via electron transfer proteins. (Modified from Lovley, 2017; Stams et al., 2006) 15
Figure 2.3. Microbial electrolysis cell (MECs) as an example of bioelectrochemical systems (BESs) (W. Wang et al., 2022) 19
Figure 2.4. DIET via CoM (Modified from Park, Park, et al., 2018) 20
Figure 3.1. Water displacement device used for the measurement of total biogas production 32
Figure 3.2. An example of calibration curves a) for methane and b) for carbon dioxide 33
Figure 3.3. An example calibration curve for a) acetic acid, b) butyric acid, and c) propionic acid 35
Figure 3.4. Schematic representation of the experimental sets 36
Figure 3.5. a) The serum bottle, stopper and clamp and b) the reactor filled with inoculum and cattle manure for Set 1 37
Figure 3.6. The serum bottle, cap and stopper used in Set 2, Set 3 and Set 4 37
Figure 3.7. The reactor filled with inoculum and cattle manure wrapped with aluminum foil in Set 1 39
Figure 3.8. Particle size distribution for hematite 41
Figure 3.9. a) GAC and b) hematite used as CoM in Set 2 41
Figure 3.10. a) The reactors filled with inoculum and cattle manure and b) the reactors on the shaker in Set 2 43
Figure 3.11. a) The reactors without mixing and b) the reactors with mixing on shaker 46

Figure 3.12. The reactor set-up for acclimation of inoculum 47
Figure 3.13. a) Neoprene stopper, graphite blocks, reference electrode and CV cell used in the analysis and b) during CV analysis reactors connected to a potentiostat 51
Figure 3.14. Precipitate scratched from the filter paper to be analyzed with XRD 52
Figure 4.1. a) Cumulative methane production, b) organic removal and c) methane yield for Set 1 60
Figure 4.2. a) Cumulative methane production , b) organic removal and c) methane yields for the reactors in Set 2 65
Figure 4.3. Final ammonium and phosphorus concentrations in Set 2 74
Figure 4.4. Final pH, electrical conductivity and ORP values in Set 2 76
Figure 4.5. a)-b) Cumulative methane production for F/M of 1 and 3 reactors, c)-d) organic removal for F/M of 1 and 3 reactors and e)-f) methane yields for F/M of 1 and 3 reactors in Set 3 80
Figure 4.6. Cyclic voltammetry analysis of F/M 1 reactors under a) no mixing and b) mixing and F/M 3 reactors under c) no mixing and d) mixing (inset 1st derivative of CV results) 89
Figure 4.7. a)-b) acetic acid concentrations for F/M of 1 and 3 reactors, c)-d) butyric acid concentrations for F/M of 1 and 3 reactors and e)-f) propionic acid concentrations for F/M of 1 and 3 reactors in Set 3 92
Figure 4.8. Total VFA profiles of the reactors with a) F/M 1 and b) F/M 3 in Set 3 94
Figure 4.9. Final pH, electrical conductivity and ORP values in Set 3 95
Figure 4.10. Final ammonium and phosphorus concentrations in Set 3 97
Figure 4.11. XRD analysis of the precipitate collected from the a) AD, b) Sand and c) GAC groups 99
Figure 4.12. Cumulative methane production during the acclimation period 101
Figure 4.13. Cumulative methane production for biofilm formation reactors 102
Figure 4.14. Temperature profile of biofilm formation reactors during the incubation 103

Figure 4.15. Cumulative methane production for a) reactors with F/M of 1 and b) for reactors with F/M ratio of 3, c) organic removal for all reactors and, d) methane yields for all reactors in Set 4 104
Figure 4.16. a) CV curves for reactors with F/M ratio of 1 b) first derivatives of CV curves of F/M ratio of 1 reactors, c) CV curves for reactors with F/M ratio of 3 (d) first derivatives of CV curves of F/M ratio of 3 reactors 108
Figure 4.17. a)-b) acetic acid concentrations for F/M of 1 and 3 reactors, c)-d) butyric acid concentrations for F/M of 1 and 3 reactors and e)-f) propionic acid concentrations for F/M of 1 and 3 reactors in Set 4 110
Figure 4.18. Total VFA profile for the reactors in Set 4 112
Figure 4.19. Final ammonium and phosphorus concentrations in Set 4 114
Figure 4.20. Final pH, electrical conductivity and ORP values in Set 4 115
Figure 4.21. Microbial community structure based on relative abundance of 16S rRNA sequences of the sample in Set 4 at archaeal genus level 118
Figure 4.22. Microbial community structure based on relative abundance of 16S rRNA sequences of the sample in Set 4 at bacterial genus level..... 120
Figure B.1. The fittings of the experimental data and the model data in Set 1 148
Figure C.1. The fittings of the experimental data and the model data in Set 2…. 149
Figure D.1. The fittings of the experimental data and the model data for reactors at F/M ratio of 1 in Set 3……... 150
Figure D.2. The fittings of the experimental data and the model data for reactors at F/M ratio of 3 in Set 3……151
Figure E.1. The fittings of the experimental data and the model data in Set 4..…152

LIST OF ABBREVIATIONS

Abbreviations

AD: Anaerobic digestion

BioGAC: Biofilm attached granular activated carbon

BM: Basal medium

CM: Cattle manure

COD: Chemical oxygen demand

sCOD: Soluble Chemical Oxygen Demand

CoM: Conductive Material

DIET: Direct Interspecies Electron Transfer

F/M: Food to Microorganism Ratio

GAC: Granular Activated Carbon

IFT: Interspecies Formate Transfer

IHT: Interspecies Hydrogen Transfer

MIET: Mediated Interspecies Electron Transfer

TS: Total Solids

VFA: Volatile Fatty Acid

VS: Volatile Solids

CHAPTER 1

INTRODUCTION

In today's world, people are mainly consuming fossil fuels for the purposes of heating and cooking. Consumption of fossil fuels has many globally significant adverse effects such as land degradation, water pollution and greenhouse gas emissions (Rittmann, 2008). Besides the adverse effects of fossil fuels, their reserves are limited, in other words, they are non-renewable. Approximately 80% of global energy need is provided via fossil fuel consumption, and it is expected that the lifespan of fossil fuels is nearly 50 years with the current consumption rate (Holechek et al., 2022).

In order to sustain the demands of all living creatures and for the prevention of fossil fuel effects, the concept of renewable energy such as wind, solar, biomass, geothermal and hydropower is critical (S. S. Kumar et al., 2021). As another note, the management waste materials produced as a result of human activities (agricultural activities etc.) and their environmental impacts should be managed properly (S. S. Kumar et al., 2021). Specifically, the pollution due to the release of nutrients and organic compounds because of animal manure production should be carefully addressed (Loyon, 2018).

Conventional anaerobic digestion (AD) is an effective technology for the treatment of organic wastes and bioenergy production in the form of biogas (Anukam et al, 2019). As a result of AD, biogas containing 60-70% methane (CH_4) and 30-40% carbon dioxide (CO_2) can be produced (Speece, 1983). Different feedstock such as animal manure, municipal solid wastes and wastewater treatment plant sludge can

be used in AD for methane production. Especially, cattle manure (CM) due to its high nutrients, organic content and high level of microbial activity, it has been applied to AD as feed commonly (Zheng et al., 2015). Use of CM as a feed in AD can decrease its environmental impacts and also provide beneficial products such as biogas.

Although AD is a well-known and effective technology for organic waste disposal and simultaneous renewable energy production, it has some limitations. These limitations can be counted as low methane production rate due to slow reaction kinetics, high sensitivity to inhibitory compounds such as ammonium, volatile fatty acids (VFAs), and unstable operations with changing conditions due to accumulation of VFAs (J. H. Park, Kang, et al., 2018; Yin et al., 2020). The slow processing of wastes is a result of little energy gained by anaerobic microbes during AD, and slow growth rate of the microorganisms involved in the AD process ((Yin et al., 2020)). Further, since mostly the optimum growth of AD microorganisms is in the mesophilic temperature range, any decrease in temperature due to seasonal variations can result in instable AD operation (J. H. Park et al., 2020a). These drawbacks are important for effective AD operation, and they should be properly managed.

The production of methane and organic matter decomposition during AD occur via a series of reactions, hydrolysis, acidogenesis, acetogenesis and methanogenesis ((J. H. Park, Kang, et al., 2018)). Hydrolytic bacteria, acidogenic bacteria and acetogenic bacteria are responsible for hydrolysis, acidogenesis and acetogenesis. Methanogenic archaea, on the other hand, is responsible for methanogenesis step (V. Kumar et al., 2021). The syntrophic interactions between bacteria and methanogens are the key for effective AD performance and this interaction is based on electron transfer between different microbial communities (J. H. Park, Kang, et al., 2018). It was considered that electron transfer between fermentative bacteria and methanogens mainly occurs via hydrogen and acetate as soluble carriers ((Thauer et al., 2008)). However, electron transfer via hydrogen and acetate depends on the diffusion limitations of these carriers which creates a limitation on methane production (Yin et al. 2020, Martins et al. 2018). Approximately, a decade ago

scientists discovered a new way of electron exchange in between different microorganisms (Summers et al., 2010). For such kind of electron transfer is bacteria and archaea (methanogens in AD) can use membrane bound proteins called cytochromes and a conductive pili (J. H. Park et al., 2020a). This phenomenon named, direct species electron transfer (DIET) was firstly demonstrated on co-culture of *Geobacter metallireducens* and *Geobacter sulfurreducens*, which were acting as electron-donating and electron-accepting bacteria with the presence of ethanol and fumarate, respectively (Summers et al., 2010). *G. metallireducens* can metabolize ethanol but is unable to use fumarate as an electron acceptor. On the other hand, *G. sulfurreducens* can reduce fumarate, but is unable to metabolize ethanol. The co-culture of *G. metallireducens* and *G. sulfurreducens* could, however, grow in a medium with ethanol as the sole electron donor and fumarate as the sole electron acceptor, which is only possible via DIET (Summers et al., 2010). It was emphasized that DIET is thermodynamically more favorable because electrons are conveyed directly from microorganism to microorganism, and it is an energy efficient mechanism as compared to the mechanism via hydrogen and acetate since there is no need for the production and consumption of intermediate products in DIET mechanism (C. Wang et al., 2020). Later, it has been proven that DIET can also occur in co-cultures of *Geobacter* species and aceticlastic methanogens; *e.g.* in co-cultures of *G. metallireducens* and *Methanosarcina barkeri* (Rotaru, Shrestha, Liu, Markovaite, et al., 2014a), and *G. metallireducens* and *Methanosaeta harundinace* (Rotaru, Shrestha, Liu, Shrestha, et al., 2014). As more research was conducted on this topic, it was proposed that DIET can also be performed between bacteria and archaea in AD systems with the supplementation of conductive materials (CoMs), which will replace the need for membrane bound proteins or conductive pili for electron exchange and act as an electron transfer conduit (Rotaru et al., 2014; Kutlar et al., 2022). Carbon based materials, metal-based materials, and metal oxides can be used as CoM for AD performance improvement in terms of methane production. In most studies, carbon-based materials, mainly biochar and granular activated carbon (GAC) have been used as CoM since these are easily accessible, have an

environmental use at the moment and relatively cheaper as compared to other types of CoMs (Kutlar et al., 2022). It was reported that the amendment of carbon-based conductive materials improved the performance of AD process in terms of increase in methane yield, enhanced methane production rate, reduction in lag time, decrease in VFA accumulation and improved tolerance to inhibitory compounds (Kutlar et al., 2022).

In the literature, biomethane recovery from many different feedstocks have been tested via amendment of a variety of CoMs. However, there is only limited number of studies investigating the impact of CoMs on biomethane recovery from digestion of CM. Especially, studies investigating the impacts of CoMs on psychrophilic anaerobic digestion are very limited. To fill this gap in the literature, the focus of this study was to investigate the major impacts of adding CoMs into anaerobic digesters for enhanced methane production from CM. After a comparative analysis GAC was selected as a carbon-based CoM to further studies and the mechanisms behind the enhancement of methane recovery via amendment of GAC was investigated. In total four sets of laboratory experiments were performed:

- In Set 1 the impacts of nutrient addition via supplying a basal medium (BM) and the amount of organic load on mesophilic (T = 35 ^{o}C) CM digestion was studied.
- In Set 2, the impact of two different CoMs were compared. A carbon-based CoM, GAC, and a metal-based CoM, hematite (Fe_2O_3), were added into the digesters for investigation of their impact on mesophilic AD performance and also the optimum dosage of each was determined.
- In Set 3, the aim was to investigate whether the enhancement in mesophilic anaerobic manure digestion via GAC is only due to surface area provided by GAC for biomass attachment or not. To this purpose, we applied GAC as CoM and also operated control reactors with sand (the same particle size with GAC) application as a non-conductive material. Further, the applicability of GAC on CM digestion under different organic loads (based on food-to-

microorganism (F/M) ratio) was studied under the presence and absence of mixing.

- Sets 1 – 3 were performed under mesophilic conditions. In the final set (Set 4), psychrophilic condition (T ~18 ^{o}C) CM digestion via GAC application under different F/Ms was studied. In this set, to assess the effect of microbial adaptation at psychrophilic temperature on AD performance, biomass attached GAC (BioGAC) was also amended to the reactors and the performances were compared against bare GAC. Further, to determine the key microorganisms involved in psychrophilic AD of CM, the bacterial and archaeal communities on the GAC samples were identified via 16S rRNA based methods.

CHAPTER 2

LITERATURE REVIEW

2.1 Anaerobic Digestion (AD)

2.1.1 Process Description and Stages of AD

AD is a well-known technology for organic decomposition and biogas production (Speece, 1983). It is a sustainable process that has been widely applied for treatment of various wastes as it significantly contributes to global carbon cycle by biomethane production (Speece, 1983). As a result of AD process, biogas containing 60-70% methane and 30-40% carbon dioxide is produced.

AD consists of four stages: hydrolysis, acidogenesis, acetogenesis and methanogenesis in which a consortium of anaerobic microorganisms take place (Y. Liu et al., 2021). The stages and the microorganisms responsible for each stage are given in Figure 2.1.

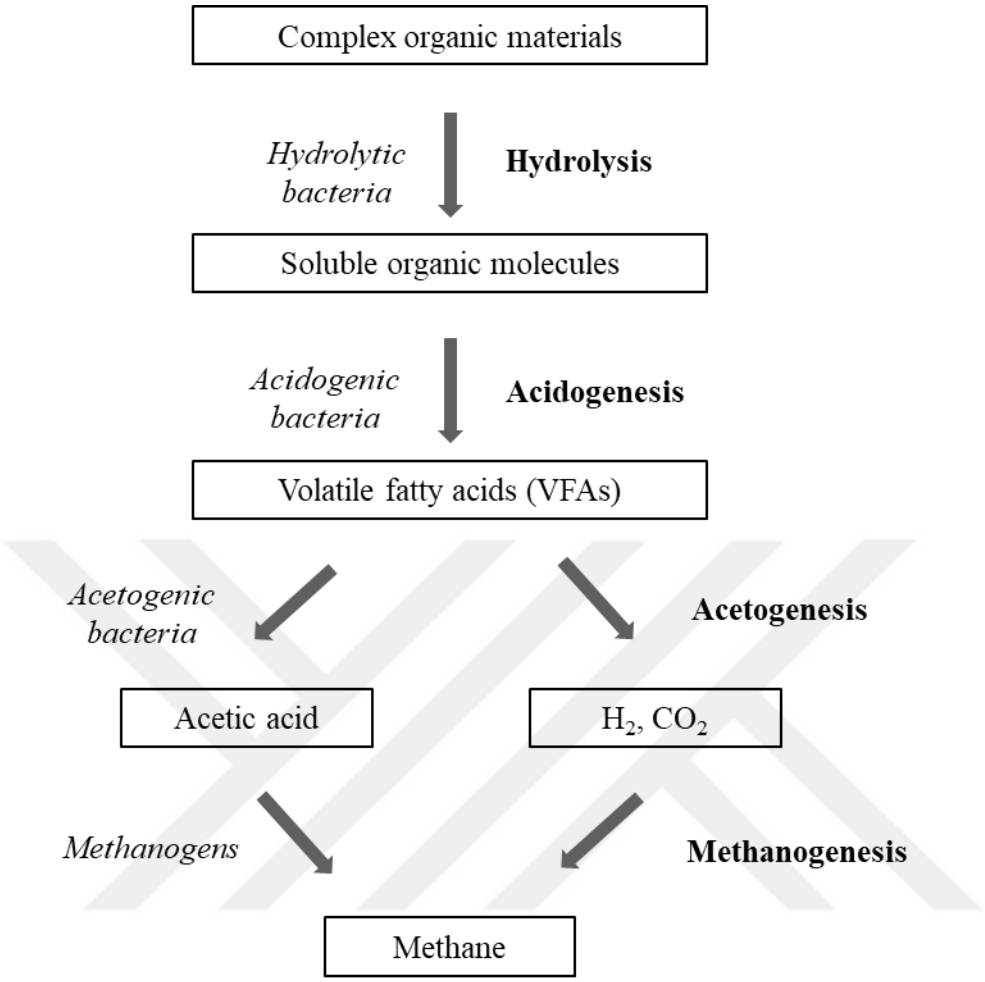

Figure 2.1. AD stages and the microorganisms responsible for each stage (Adopted from Y. Liu et al., 2021)

The first stage of AD (hydrolysis) is where the conversion of organic polymers (carbohydrates, proteins, fats) into their monomers (sugars, amino acids, lipids) within the presence of water takes place (Uçkun Kiran et al., 2016a). In this stage, hydrolytic bacteria excrete their extracellular enzymes for this conversion. With the help of extracellular enzymes, organic materials are broken, and they are transferred through the cell membrane. During the second stage named acidogenesis, acidogenic bacteria convert soluble organic compounds produced in hydrolysis into dicarboxylic acids, VFAs, carbon dioxide and hydrogen (Meegoda et al., 2018; Uçkun Kiran et al., 2016). For the production of VFA, pH is an important parameter. When pH is greater than 5, VFA production is enhanced (Anukam et al., 2019). Due

to rapid growth of acidogenic bacteria, pH decreased as a result of acid accumulation and the performance of AD in terms of methane production is inhibited if the acids produced in acidogenesis are not degraded effectively in acetogenesis (Uçkun Kiran et al., 2016a). In acetogenesis, acetogenic bacteria converts VFAs produced in acidogenesis into acetate, carbon dioxide and hydrogen (Meegoda et al. 2018). In this stage, the balance between the production and consumption of hydrogen is important, because higher than 10^{-4} atm partial pressure of hydrogen as a result of lower consumption can inhibit the activity of acetogenic bacteria and the overall process can be harmed. In the final step of AD, methanogenesis, methanogens which are strictly anaerobic microorganisms take place for the production of methane from acetate and hydrogen produced in acetogenesis (Anukam et al., 2019). Methanogens can be divided into two groups, acetate consumer methanogens, called acetoclastic methanogens, and hydrogen consumer methanogens, called hydrogenotrophic methanogens. Acetoclastic methanogens consume acetate to produce methane, while hydrogenotrophic methanogens utilize hydrogen for methane production. In general, methanogens among other consortium microorganisms are the most sensitive group as they are mostly obligate anaerobes and slow-growing microorganisms, and hence highly sensitive to environmental changes and operational parameters.

2.1.2 Important Parameters Affecting AD Performance

For an effective AD performance, some operational and environmental parameters should be satisfied. Since there are many groups of microorganisms take a role in AD stages, providing a suitable operational and environmental conditions is very significant. Among many operational and environmental parameters for an effective AD performance, temperature, pH, F/M ratio, the availability of nutrients and reactor mixing are discussed in the following subtitles.

Temperature

Temperature is a significant parameter for the effective AD performance, because microbial growth rate, thermodynamic equilibrium and the kinetics of the reactions occurring during the stages, reactor stability and microbial community are highly dependent on temperature of the operation (Panigrahi & Dubey, 2019). There are three temperature ranges under which AD can take place: (i) psychrophilic, (ii) mesophilic, and (iii) thermophilic (Sudiartha et al., 2022). Temperature of less than 25 ^{0}C refers psychrophilic temperature range, and between 25-40 ^{0}C of temperature with an optimum value of 35 ^{0}C is accepted as mesophilic operation (Sudiartha et al., 2022). Operational temperatures above 40 ^{0}C can be defined as thermophilic temperature range (Jain et al., 2015; J. H. Park et al., 2020a). Although thermophilic operation has the advantages of higher biogas production rate, relatively lower hydraulic retention time (HRT) and higher growth rate of microorganisms, the high energy needs for heating the reactor and the instability problems due to higher sensitivity to change in temperature as compared to mesophilic operation are the drawbacks of thermophilic operation (Panigrahi & Dubey, 2019). The decrease in outside weather temperature due to seasonal changes, hence an increased energy demand for heating as compared to psychrophilic operation are important considerations for mesophilic operation.

pH

Effective AD performance is highly dependent on pH. Since there are different microorganisms responsible for each stage of AD, they prefer different pH levels for optimum activity. Mostly, neutral pH level is and optimum for overall AD performance. For methanogenic activity, the range of 6.0 - 8.5 should be satisfied and the optimum condition is between 7.0 and 8.0 (Uçkun Kiran et al., 2016a). When pH is decreased below 6.0 or increased above 8.5, AD is strongly inhibited. As a result of the accumulation of the products during the hydrolysis, significant changes in pH can occur. This can result in VFA accumulation due to inefficient consumption, and this can have negative impacts on overall methanogenic activity (Jain et al., 2015).

Food to Microorganism (F/M) Ratio

The amount of organic material fed to the reactor per unit of time implies the organic loading. For continuous systems, organic loading per unit volume is used as organic loading rate. On the other hand, food to microorganism (F/M) ratio is applied for batch systems. F/M ratio is a crucial parameter for AD performance. Very low F/M ratios can prevent the production and activity of enzymes which are crucial for biodegradation (Prashanth et al., 2006). On the other hand, high F/M ratio can cause an imbalance between the activities of acetogens and methanogens, lead to the accumulation of acids and ultimately process failure (Jain et al., 2015). Higher F/M ratios can also result in shock effects on microorganisms (Panigrahi & Dubey, 2019). On the other hand, the application of higher F/M ratio can provide a decrease in the footprint of the digester since it may enable the degradation of higher organic material per unit time. This benefit from the reactor size can decrease the cost of the digester; therefore, it is important to be able to operate an AD reactor at the highest possible loading rate without disturbing the process.

Nutrients

Adequate supplementation of macro- and micro-nutrients are very important for effective AD performance. Microbial growth and activity are strongly dependent on macro and micro-nutrients. Macro-nutrients such as phosphorus, nitrogen and sulphur are important nutrients especially for buffering capacity of the operation (Panigrahi & Dubey, 2019). On the other hand, micro-nutrients such as selenium, iron, cobalt and nickel should be supplied as cofactor in enzymatic activities. Additionally, nutrients can enhance methanogenic activity, which are specifically affected by the presence of iron, cobalt and nickel (Speece, 1996). Typically, in batch tests a cocktail containing macro nutrients and micro-nutrients along with buffer and reducing agents are prepared to test the impact on the AD.

Reactor Mixing

Mixing is an important operational parameter for AD performance since the homogeneity in the reactor in terms of temperature and organic content and enhanced mass transfer between microorganism and organic material can be provided via mixing (Kim et al., 2017). For an effective biodegradation of organic material and methane production, it is crucial for microorganisms to reach organic material as their food via mixing. Also, it was stated that the excessive mixing during anaerobic digestion can harm microbial communities, and this results in decrease in the performance of the digestion (Lindmark et al., 2014).

Oxidation – reduction Potential (ORP)

Oxidation-reduction potential (ORP) is another important parameter for the effective anaerobic digestion performance. It can be used as indicator to control the system since it measures the net values of oxidation and reduction reactions which are sensitive to the presence of oxygen and in the aqueous system (Nghiem et al., 2014). The optimum range of ORP is -200 to -400 mV for effective methanogenic activity (Hirano et al., 2013). In order to create an environment with low ORP values, reducing agents are used such as sodium sulfide (Salvador et al., 2017).

2.1.3 Variety of Feedstocks in AD

There are many carbon sources that can be used as substrate during AD. The highly complex organic materials that are used in AD can be mainly classified as municipal solid waste, industrial waste and agricultural waste (Nwokolo et al., 2020). Municipal solid waste is the wastes generated by household activities, industrial activities and commercials. Food waste, kitchen waste and organic fraction of municipal solid waste can be exemplified as municipal solid waste suitable for AD. Especially due to their high organic content and huge amount of production, municipal solid wastes are commonly used as feed in AD. Xiao et al., (2019) investigated AD of food waste and paper waste, and 460 mL CH_4/g volatile solid

(VS) of methane yield was obtained from food waste digestion at thermophilic temperature. Similarly, in another study, AD of organic fraction of municipal solid waste was studied and methane yield of organic fraction of municipal solid waste was enhanced via co-digestion (Ghosh et al., 2020). Industrial wastes are the end product of industrial activities such as pulp and paper industry, food industry, petrochemical refinery industry and textile industry. Since highly toxic and chemical wastes are generated as result of these industrial activities, their application on AD as carbon source should be carefully managed. Lin et al., (2017) obtained a methane yield of 429 mL CH_4/g VS from AD of pulp and paper mill sludge at mesophilic temperature. It was also investigated that 200 and 400 mL CH_4/g VS from AD of untreated and treated textile product were observed, respectively (Jeihanipour et al., 2013). Agricultural waste consists of lignocellulosic biomass and animal waste. Lignocellulosic biomass has highly cellulose, hemicellulose and lignin contents, and the amount of lignin affect its biodegradability as that is a recalcitrant component of biomass (N. Xu et al., 2019). Animal wastes is an important alternative as carbon source to be used in AD. In addition to its high organic content, animal waste should be properly managed because it has a high nitrogen and phosphorus which can be contamination source for water bodies and soil (Nwokolo et al., 2020).

2.1.4 Electron Transfer Mechanisms in AD

The balance and syntrophic interactions between bacteria carrying out hydrolysis, acidogenesis and acetogenesis and archaea carrying out methanogenesis are essential for AD process to be operated successfully (Martins et al., 2018). The syntrophic interactions between bacteria and archaea depend on the electron transfer of these microorganisms (Table 1).

Table 2.1. Acetogenic and methanogenic reactions possible during AD process.

Pathway	**Reaction**	**Microorganism**	**Reaction no.**
Aceticlastic methanogenesis	$CH_3COOH \rightarrow CH_4 + CO_2$	Aceticlastic methanogens	1
Syntrophic acetate oxidation	$CH_3COOH + 2H_2O \rightarrow 2CO_2 + 4\ H_2$	Syntrophic acetate oxidizing bacteria	2
Hydrogenotrophic methanogenesis	$CO_2 + 4H_2 \rightarrow CH_4 + 2\ H_2O$	Hydrogenotrophic methanogens	3

During AD process, electron transfer can be carried out by indirect or mediated interspecies electron transfer (MIET), in which microorganisms use molecules such as hydrogen as electron shuttle. As given in Reaction 2 of Table 1, during acetate oxidation by bacteria, hydrogen is produced and is then consumed by hydrogenotrophic methanogens (Reaction 3) in Table 1. This is illustrated in Figure 2.2a (Mostafa et al., 2020). For the further categorization of MIET, it can occur through hydrogen molecules named as interspecies hydrogen transfer, IHT or formate molecules named as interspecies formate transfer, IFT. In both cases there is an intermediate product. MIET could also take place via extracellular soluble compounds such as flavin and quinones (Figure 2.2b). In addition to MIET, DIET carried out by cellular structures such as conductive pili or cytochrome rather than using hydrogen or formate is an alternative route and shown in Figure 2.2c and Figure 2.2d, respectively (W. Wang & Lee, 2021).

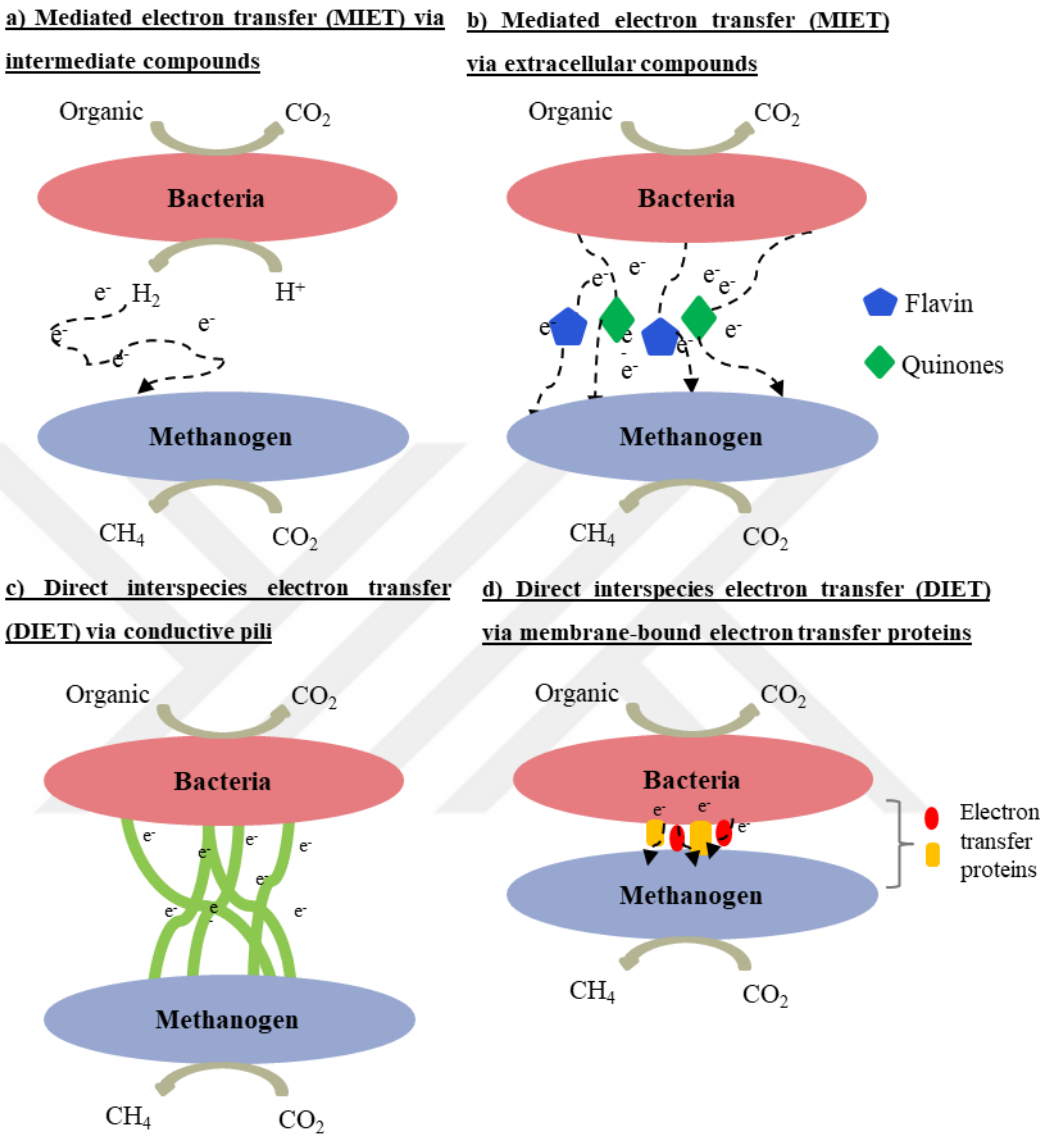

Figure 2.2. Electron transfer mechanism during AD process; a) MIET via hydrogen, b) MIET via extracellular soluble compounds, and c) DIET via conductive pili d) DIET via electron transfer proteins. (Modified from Lovley, 2017; Stams et al., 2006)

2.1.5 Limitations of AD

Although AD is a well-known technology, it has some limitations. During AD, inefficient synthesis of fermentative intermediates such as propionate decreases the performance of AD because the production of these intermediates limit electron transfer between different microorganisms (Namal, 2020). Also, low efficient degradation of these intermediates is another limitation for AD (J. Liu et al., 2020). Due to slow reactions during AD, long acclimation time is needed for effective AD performance (Park, Kang, et al., 2018). In addition to these, in terms of AD performance, low methane yield and methane content and inhibition due to high organic loading are drawback of AD process (W. Wang & Lee, 2021).

2.1.6 Methods used for AD Performance Enhancement and its widespread Application

Although AD is a well-known technology and widely used for bioenergy production and organic decomposition, its effectiveness should be improved due to process instabilities and the reasons mentioned above. For an effective AD performance, the syntrophic interactions between different microorganisms are the key factor. In order to prevent process stability and enhance syntrophic interactions between microorganisms, different strategies for the improvement of AD performance have been examined and evaluated.

AD Feed Pre-Treatment

Some pre-treatment methods of organic wastes can be applied in order to improve the hydrolysis of these organic wastes (González et al., 2018). The reason for feed pretreatment is to enable fast and higher degree hydrolysis of complex wastes, which makes the activity of hydrolytic microorganisms more effective. Some widely applied pre-treatment methods are:

- Chemical

- Thermal
- Mechanical
- Mechanical-chemical
- Thermo-chemical
- Thermo-mechanical

As mentioned in the literature, the application of thermal pre-treatment of activated sludge improved the biogas yield 50% as compared to untreated activated sludge (Bougrier et al., 2006). As another example, ultrasound pre-treatment of activated sludge increased the biogas yield 30% (Martínez et al., 2015). Although the application of pre-treatment of organic wastes seems beneficial, the energy demand of this approach should be carefully evaluated. Biological, physiochemical, and chemical pre-treatment method have been widely applied to cattle manure (Orlando & Borja, 2020). As an example of chemical pre-treatment, the application of pre-treated cattle manure with calcium oxide resulted in 26% increase in methane yield (Ramos-Suárez et al., 2017). For physiochemical pre-treatment, the incubated cattle manure at 68 ^{0}C enhanced the yield 56% with respect to cattle manure without any pre-treatment (Nielsen et al., 2004).

AD Effluent Post-Treatment

The effluent of AD named as digestate contains materials with different biological and chemical characteristics (Issah et al., 2020). The operational parameters such as pH, temperature, organic loading and microbial community results in this variety. The digestate generally have low carbon content because it was consumed during AD, and pH of it is in the neutral range (Issah et al., 2020). On the other hand, nitrogen (N) and phosphorus (P) are not removed from the digestate during AD. For the sake of widespread application of AD, the removal of these nutrients should be evaluated. Otherwise, AD becomes an alternative approach for methane production but not for nutrient removal because it contains high amount of N and P which makes the digestate available as fertilizer. Although the digestate is suitable for the use as fertilizer, the amount of production of the digestate from the industries could not be

used totally as fertilizer. Struvite precipitation can be a good option as effluent treatment for AD to remove residual nutrients (Palominos et al., 2021). Struvite is a crystal which combines magnesium (Mg), N and P at high pH values, and it can be used as fertilizer (Palominos et al., 2021). Although struvite precipitation will not affect the system performance in terms of methane production yield, methane production rate, lag time etc., it is an alternative approach for the effluent of AD. (Cerrillo et al., 2015) observed that the precipitation of struvite from the effluent of AD of pig slurry is beneficial and this struvite can be used as fertilizer due to its high nutrient content.

The Integration of Bioelectrochemical Systems (BESs) with AD

BESs are the systems where electrochemistry is combined with biological degradation and involves electrodes for the reactions (W. Wang et al., 2022). In these systems, organic oxidation releasing electrons, protons and carbon dioxide takes place in the anodic compartment. Electrons are then transferred by microorganisms to anode via extracellular electron transfer (EET). These anodes associated microorganisms are named as exoelectrogens since they have the ability to transfer the electrons extracellularly to a solid state electron acceptor, *i.e.*, anode (Anukam et al., 2019). After the transfer of electron from anode to cathode, some products are generated via reduction reactions in cathodic compartment. The kind of products are different for each BES. In microbial electrolysis cells (MECs) methane can be produced if cathode is colonized by methanogens in a process named as electromethanogenesis (W. Wang et al., 2022) (Figure 2.3).

In the integrated AD-MEC systems, exoelectrogenic bacteria on anode for oxidation of organic matter participate in and hydrogenotrophic methanogenesis or electromethanogenesis take place in cathode (Baek et al., 2021). Similar to AD, in hydrogenotrophic methanogenesis H_2 is converted to methane by hydrogenotrophic methanogens. Different from AD systems, with the application of external voltage, H^+ and electrons produced methane via CO_2 reduction (Baek et al., 2021). There are recent studies that combined AD and MEC systems for the enhancement of methane

production. J. Park, Lee, et al. (2018) obtained 70% higher methane yield from the digestion of food waste in the integrated AD-MEC system as compared to AD system with the application of copper, nickel and iron coated graphite cathode at an external voltage of 0.3 V. 47% increase in methane yield was observed in the integrated AD-MEC system at an external voltage of 1.2 V with stainless-steel mech cathode when wastewater sludge was used as substrate (Asztalos & Kim, 2015).

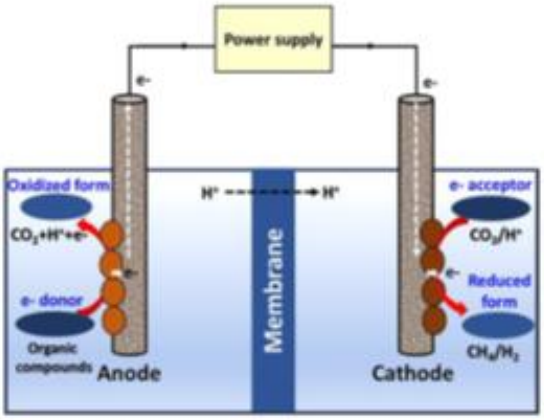

Figure 2.3. Microbial electrolysis cell (MECs) as an example of bioelectrochemical systems (BESs) (W. Wang et al., 2022)

The stimulation of DIET via Amendment of Conductive Materials to AD Reactors

Normally, electrons are transferred in AD systems via the pathways given in Figure 2.2; i) intermediate products such as H_2 or acetate, ii) extracellular compounds, iii) conductive pili and iiii) membrane-bound electron transfer proteins. In these transfers, MIET (i and ii) and DIET (iii and iiii) mechanisms are observed. As more feasible and faster electron transfer mechanism, DIET vi CoM, was observed without the need of the production intermediate products, the addition of extracellular compounds and the ability of conductive pili (Figure 2.4). Kato et al., (2012) reported that methane production was observed in the co-cultures of Geobacter and Methanosaeta species within the presence of CoM. They also suggested that the methane production in this environment is because of electrical connections between Geobacter and Methanosaeta created by CoM. After these findings, it was observed that Geobacter metallireducens and Methanosaeta barkeri species could produce

methane from ethanol degradation within the presence of CoM (Liu et al., 2012). They did not observe any methane when conductive material was not amended. After these reports on the enhancement of methane production between co-cultures with the presence of CoM, the effect of conductive material amendment on AD of organic wastes was studied. In terms of methane yield, methane production rate and lag time, CoMs enhanced AD performance. It was observed that the amendment of biochar as CoM to AD of dairy manure enhanced methane yield 25% over AD control (Jang et al., 2018), and this enhancement via biochar is associated with DIET mechanism. In another study, it was observed that the amendment of graphite to AD reactor enhanced the methane production rate 36% over AD control when commercial dog food was used as organic source and based on microbial community analysis they also suggest that DIET mechanism takes play in the improvement of system perfromance (Dang et al., 2016a). These studies show that DIET mechanism without intermediate products, extracellular compounds and conductive pili can occur via the amendment of CoMs.

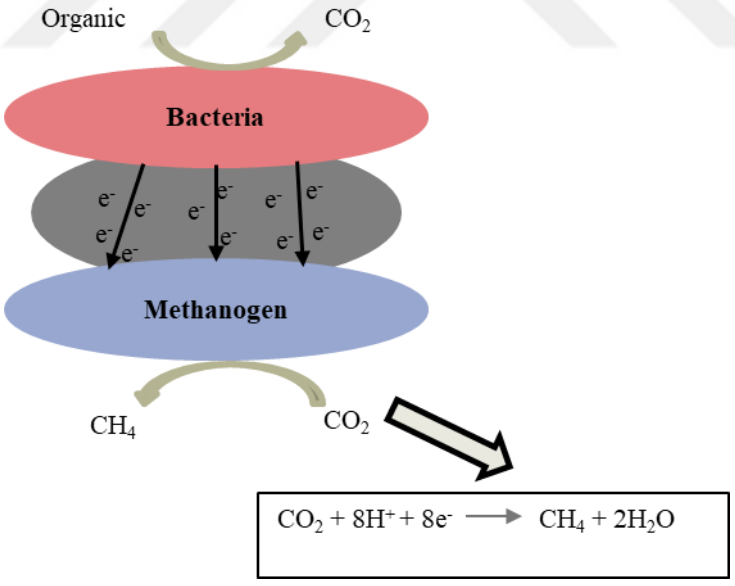

Figure 2.4. DIET via CoM (Modified from Park, Park, et al., 2018)

2.2 The impact of Conductive Material Amendment on AD Process

2.2.1 Impacts of CoMs on AD

Enhanced methane production via CoM amendment to AD

In the literature, it was strongly suggested that the amendment of CoM enhanced methane yield and methane production rate as compared to AD system. He et al. (2021) observed that the addition of different carbon-based CoMs (GAC, carbon cloth, nanoparticle of GAC) increased methane yield from mesophilic AD of co-digestion of fat, oil, grease and wastewater sludge as compared to AD control. Although the result of this study has been also evaluated based on electrical conductivity of CoMs, the surface area for microbial attachment and interactions provided by GAC and carbon cloth was suggested as an important factor for the enhancement (He et al., 2021). In another study, the amendment of graphene as CoM enhanced methane yield 25% and methane production rate 20% as a result of ethanol degradation at mesophilic temperature under batch operation (Y. Lin et al., 2017b). They suggested that the high electrical conductivity and surface area provided by graphene addition plays an important role in this improvement, and they also provide supportive evidence by the fact that there were microbial nanowires on cell surfaces within the presence of graphene which can make electron transfer easier (Lin et al. 2017). J. H. Park et al., 2020a) studied the impact of the amendment of GAC as CoM on AD of wastewater sludge under batch operation at psychrophilic and mesophilic operation temperature. Their results showed that although methane yield was not improved at mesophilic temperature, 20% enhancement was observed at psychrophilic temperature (J. H. Park et al., 2020a). Based on microbial community analysis, they suggested that the main reason behind this improvement comes from the predominantly presence of DIET-related microbial communities and hydrogenotrophic methanogens over AD control (J. H. Park et al., 2020a).

Decrease in lag time via CoMs

Different from methane yield and methane production rate, based on literature survey, it was observed that the addition of CoM decreased lag time over AD control. Similar to methane production rate, J. H. Park et al. 2020a observed that the addition of GAC on wastewater sludge digestion decreased lag time at mesophilic temperature over AD control. 8% decrease in lag time via GAC amendment was obtained in this study, and this improvement can be attributed to DIET-related microorganisms as explained in previous subtitle (J. H. Park et al., 2020a). Z. Yang et al. (2016) obtained that the addition of magnetite (Fe_3O_4) as CoM at mesophilic range decreased lag time over AD control when mixed VFA was used as substrate. They emphasized that the addition of magnetite improved methanogenesis at the early stage of the digestion (Z. Yang et al., 2016). In other words, the reactions occurring during the digestion started earlier which results in earlier electron transfer between microorganisms than AD control.

Mitigation of inhibitory compounds via CoMs

In addition to enhancement of methane yield and methane production rate and decrease in lag time, successive consumption of VFA, tolerance of ammonium, pH and high organic loading are other improvements via CoM addition to AD systems. Although the enhancement in methane production can be seen due to surface area provided by biochar, they stated that the buffering capacity which prevents VFA accumulation is the main reason behind the improvement (Jang et al., 2018). Yin et al. (2020) stated that the accumulation of VFA due to high organic loading results in the failure of AD system. They mentioned that the addition of CoM can prevent the failure of the system performance due to VFA accumulation and high organic loading since the organic decomposition and electron transfer between microorganisms can fasten with CoM. (W. Wang & Lee, 2021) also stated that the amendment of CoM can alleviate the impact of high organic loading and VFA accumulation. In another study, (Yan et al., 2020) evaluated the impact of different CoMs (zero-valent iron, magnetite nanoparticles and powdered activated carbon)

under ammonium -stressed condition. They observed that the addition of zero-valent iron and magnetite nanoparticles could prevent ammonium inhibition and the methane production did not fail (Yan et al., 2020)). In terms of the mitigation of ammonium inhibition via CoM amendment (J. H. Park, Kang, et al., 2018) stated that the adsorption of ammonium on CoM surface can decrease ammonium concentration in bulk solution and create a more favorable environment for AD.

2.2.2 Types of CoMs

Carbon-based CoMs

Carbon-based CoMs used for the stimulation of DIET mechanism includes GAC, powdered activated carbon, PAC, graphene, biochar, carbon fibers, carbon cloth, graphite, graphite felt, carbon felt and carbon nanotubes (Park, Kang, et al., 2018; Kutlar et al., 2022). Their high conductivity, large surface area and resistance against corrosion are main characteristics for the preference as CoMs in methanogenic environments. GAC with different size and dosage has been applied for the stimulation of DIET mechanism.

The application of carbon-based CoMs to AD reactors

In order to enhance the degradation of kitchen waste, 8-20 mesh size of GAC was used with GAC dosage of 13 g/L (J. Zhang et al., 2020). Namal, (2020) used 15-75 μm of GAC with 1 g/L of dosage for glucose oxidation. Higher dosage of GAC was also evaluated on AD. 50 g/L of GAC was applied to AD of dry organic fraction of municipal solid waste (Dang et al., 2017a). The powdered structure of activated carbon in addition to granular structure, GAC was also used as CoM for degradation of synthetic brewery wastewater and food waste with the dosages of 5 g/L and 15 g/L (S. Xu et al., 2015; L. Zhang et al., 2018) Similar to GAC, with the porous structure, biochar was also widely used for the degradation of organic waste and the production methane. Herrmann et al., (2021) added 50 g/L of biochar produced from agricultural residues for AD of piggery waste. Also, Tiwari et al., (2021) investigated

the effect of different dosages of biochar (0.6, 1.2, 1.8, 2.4 and 3 g/L) on AD of the co-digestion of sewage sludge and wheat. Graphene and carbon felt were also used as CoMs on oxidation of ethanol and degradation of dog foot, respectively. (Dang et al., 2016b; R. Lin et al., 2018). Zhao et al., (2015) used 12 graphite rods for the enhancement of the oxidation of ethanol. Carbon nanotube as carbon based CoM have been also applied for improved acetate oxidation by (Shen et al., 2020)

Metal-based CoMs

Other than carbon-based CoMs, non-carbon based CoMs have been also used for the stimulation of DIET. Metal-based CoMs include magnetite, hematite (Fe2O3) and stainless-steel. Based on physical and electrical characteristics, these materials can be also used as CoMs to AD reactors for the enhancement of system performance.

The application of metal-based CoMs to AD reactors

Zhou et al., (2014) investigated the comparison of two iron-based CoM, hematite and magnetite. The effect of different hematite dosages (12.5, 187.5, 375, and 875 mM Fe) on the degradation of swine manure was studied by Lu et al., (2019) For the enhancement of butyrate degradation, nanosized magnetite was used with a particle size of 30 nm (H. Li et al., 2015). In addition to iron-based CoMs, stainless steel has been also used as CoM for the enhancement of AD performance (Y. Li et al., 2017)). T. Wang et al., (2016) used two different metal-based CoMs, magnesium oxide and silver nanoparticles with a particle size of less than 0.05 μm and 0.1 μm for sludge digestion, respectively.

2.2.3 Electrochemical Analysis of Microbial Electron Transfer: Cyclic Voltammetry (CV)

Electroactive microbial biofilms and microbial community in these biofilms for BESs have been studied for a long time since they effect the performance of the system and they play an important role in the system (Harnisch & Freguia, 2012). Cyclic voltammetry (CV) analysis is one of the most-widely used electrochemical

technique that can be used for the detection and evaluation of the biofilms in BESs (Harnisch & Freguia, 2012). The analysis consists of working electrode, counter electrode and reference electrode. For BESs, if the working electrode is anode, the oxidation reaction and oxidation peak on voltammogram are analyzed (Harnisch & Freguia, 2012). On the other hand, the reduction reactions and reduction peaks are analyzed when the working electrode becomes cathode (Harnisch & Freguia, 2012). For the demonstration of potential biofilm formation, electrochemical activities and the determination of electron uptake patterns, CV analysis can be also applied to AD systems (An et al., 2020; Rowe et al., 2019).

Lee et al., (2016) investigated CV analysis for AD of synthetic wastewater within the presence of GAC as CoM. The disappearance of reduction peak on the voltammogram of GAC biomass on without GAC biomass indicated that the reduction peak was obtained as a result of biofilm formation on GAC because when this biofilm was removed from GAC, the reduction peak was disappeared. Also, it was implied that the location of the reduction peak on the voltammogram of GAC biomass indicates biological methane production via potential DIET mechanism. In another study, the location of the reduction peak was also appeared with implication of methanogenesis (-0.44 V vs Ag/AgCl) (Y. Li et al., 2017). An et al., (2020) also suggested that the absence of reduction peak in the control reactor implies very limited DIET mechanism in conventional AD operation. On the other hand, they obtained significant reduction potential on the voltammogram of the reactor with a conductive electrode at -0.53 V (vs. Ag/AgCl) (An et al., 2020).

2.2.4 Microbial Communities of CoM amended AD Reactors

It was strongly suggested that electron transfer via DIET mechanism takes place between fermentative bacteria and methanogenic archaea within the presence of CoM, which makes the identification of involved bacterial and archaeal species important. Once such species are identified, the information gathered may be used for providing conditions for higher enrichment of such species in the bioreactors. In

the pioneer work of DIET stimulation, Summers et al., (2010) observed the co-culture of *G. metallireducens* as exoelectrogen and Geobacter sulfurreducens exhibited DIET. For the bacterial community, it was stated that Geobacter species as exoelectrogens were mostly enriched in the studies investigating the amendment of CoM on AD process (Kutlar et al., 2022; Park, Kang, et al., 2018). Apart from Geobacter species, Syntrophomonas was mostly enriched on the surface of GAC (J. Zhang et al., 2020). Similarly, Lei et al. (2016) observed that the most abundant bacterial specie in the system with the amendment of carbon cloth as conductive material is Syntrophomonas. In addition to bacterial species, Kutlar et al. (2022) stated that Methanosarcina and Methanosaeta species are the most enriched archaeal species in DIET systems. J. Zhang et al. (2020) observed that the most enriched archaeal specie is Methanosarcina within the presence of GAC as CoM. On the other hand, Park, Park, et al. (2018) stated that the abundance of Methanosarcina decreased after the amendment of GAC while the abundance of Methanosaeta increased. For a comprehensive examination of DIET and the species participating in DIET, microbial community analysis should be assessed.

CHAPTER 3

MATERIALS AND METHODS

3.1 Waste and Inoculum Characteristics

In this thesis, CM was used as feed in the AD reactors. It was taken from the inlet of a full-scale CM fed biogas plant, Polres in Polatlı. CM samples was blended for 1 hour for homogenization and no other pre-treatment was applied. For characterization of CM, total solids (TS), volatile solids (VS), total chemical oxygen demand (COD), soluble chemical oxygen demand (sCOD), total phosphorus, total ammonium and alkalinity analysis have been conducted. Different experimental sets were performed at different times throughout this thesis work, and since different CM samples were collected from time-to-time characterization of the waste has been repeated before each set. The characteristics of CM and inoculum used in Set 1 are given in Table 3.1. The inoculum used in the experimental sets was taken from the anaerobic digester of Eskisehir Municipal Wastewater Treatment Plant (ESKİ) and was also characterized as described. Inoculum characteristic of each set is also given in the corresponding tables along with CM.

Table 3.1. The characteristics of CM and inoculum used in Set 1

Parameter	CM	Inoculum
Density (g/mL)	0.997	0.997
pH	7.8	7.6
TS (%)	12.2 ± 0.1	4.7 ± 0.0
VS (%)	9.2 ± 0.1	1.8 ± 0.0
VS/TS (%)	76.0 ± 0.7	39 ± 0.5
COD (mg/L)	88,000 ± 11,000	30,500 ± 1,050
sCOD (mg/L)	18,700 ± 1,100	nd
Ammonium (mg NH_4-N/L)	4,380 ± 390	nd
Alkalinity (mg $CaCO_3$/L)	18,200 ± 430	nd

nd: not determined

After characterization experiments were conducted, CM sample was kept in the refrigerator at -20^{0}C to prevent the loss of organic content. The results of characterization experiments for Set 2 are given in Table 3.2.

Table 3.2. The characteristics of CM and inoculum used in Set 2

Parameter	CM	Inoculum
Density (g/mL)	0.881	0.974
pH	7.8	7.5
TS (%)	12.2 ± 0.1	3.3 ± 0.0
VS (%)	9.5 ± 0.1	1.8 ± 0.0
VS/TS (%)	77.6 ± 0.0	52.7 ± 0.4
COD (mg/L)	151,743 ± 6,446	30,027 ± 61
Phosphorus (mg PO_4-P/L)	35.3 ± 1.6	nd
Ammonium (mg NH_4-N/L)	1,897 ± 116.8	nd

nd: not determined

The characteristics of CM and inoculum used in Set 3 are given in Table 3.3.

Table 3.3. The characteristics of CM and inoculum used in Set 3

Parameter	CM	Inoculum
Density (g/mL)	0.921	0.929
pH	7.7	7.5
TS (%)	12.2 ± 0.1	3.9 ± 0.0
VS (%)	9.5 ± 0.1	2.1 ± 0.0
VS/TS (%)	78.1 ± 0.2	54.6 ± 0.2
COD (mg/L)	140,000 ± 5,185	35,716 ± 963
Phosphorus (mg PO_4-P/L)	42.8 ± 2.6	nd
Ammonium (mg NH_4-N/L)	945 ± 58.1	nd

nd: not determined

CM and inoculum characteristics for in Set 4 are given in Table 3.4.

Table 3.4. The characteristics of CM and inoculum used in Set 4

Parameter	CM	Inoculum
Density (g/mL)	0.887	0.998
pH	7.7	7.6
TS (%)	11.5 ± 0.1	2.5 ± 0.0
VS (%)	8.7 ± 0.1	1.4 ± 0.0
VS/TS (%)	75.6 ± 0.3	56.8 ± 0.5
COD (mg/L)	131,800 ± 1,918	21,068 ± 321
Phosphorus (mg PO_4-P/L)	62.5 ± 4.7	nd
Ammonium (mg NH_4-N/L)	1483 ± 83.4	nd

nd: not determined

For quality control purposes, characterization experiments were conducted in duplicate and for each parameter the coefficient of variation (CoV), which is the ratio of standard deviation to the average of the measurements was calculated. For the characterization experiments, 10% of CoV was determined as a cut-off value and when CoV value was higher than 10%, the analysis was repeated.

3.2 Basal medium

To provide optimum conditions during AD and investigate the impact of additives selected number of reactors were supplemented with a basal medium (BM) in Set 1. To this purpose, BM with the following constituents was prepared (concentrations are given in parenthesis as mg/L): NH_4Cl (1200), $MgSO_4.7H_2O$ (400), KCl (400), $Na_2S.9H_2O$ (300), $CaCl_2.2H_2O$ (50), $(NH_4)2HPO_4$ (80), $FeCl_2.4H_2O$ (40), $CoCl_2.6H_2O$ (10), KI (10), $MnCl_2.4H_2O$ (0.5), $CuCl_2.2H_2O$ (0.5), $ZnCl_2$ (0.5), $AlCl_3.6H_2O$ (0.5), $NaMoO_4.2H_2O$ (0.5), H_3BO_3 (0.5), $NiCl_2.6H_2O$ (0.5), $Na_2WO_4.2H_2O$ (0.54), Na_2SeO_3 (0.5), cysteine (10), $NaHCO_3$ (6000) (Demirer et al., 2000). In this cocktail cysteine acts as a reducing agent and bicarbonate works as a buffer, while the others provide the macro nutrients and micro nutrients.

3.3 Analytical Methods

3.3.1 Characterization experiments

For characterization experiments, TS, VS, COD, sCOD, total Kjeldahl nitrogen (TKN), phosphorus, ammonium and alkalinity analysis were conducted. For these experiments, the followed methods are presented in Table 3.5. For COD analysis of CM, since it had high solid content and it was hard to take samples homogenously, hence we followed the Method 5220 B (Open Reflux Method). For inoculum, COD was measured by following the Method 5220 C (Closed Reflux Colorimetric Method). sCOD was measured by filtering the sample through 0.45 µm pore size filters before applying to the standard method (Standard Methods for the Examination of Water and Wastewater, 1999).

pH of wastes and inoculum were measured with a pH meter (Starter300, OHAUS, USA) and pH probe (ST320, OHAUS).

ORP and electrical conductivity of the initial and final reactor content were measured using a multi-parameter ORP probe (Multi3320, WTW, USA) and a conductivity meter (Sension5, HACH, Germany), respectively.

Table 3.5. The methods used in the characterization experiments

Analysis	Followed method
TS	Method 2540 B (APHA, 1995)
VS	Method 2540 E (APHA, 1995)
Open Reflux Method for COD	Method 5220 B (APHA, 1995)
Closed Reflux Method for COD	Method 5220 C (APHA, 1995)
TKN	Method 4500N (APHA, 1995)
Alkalinity	Method 2320 B (APHA, 1995)
Phosphorus	Hach Method 8178
Ammonium	Hach Method 8038

3.3.2 Determination of Biogas Production and the Content of Biogas

Biogas of the reactors were measured periodically during the operation. In order to measure the total biogas production in each reactor during the operation, a water displacement device was used (Figure 3.1). For the elimination of dissolution of CO_2 and correct measurement, acidic waster (2% H_2SO_4) was used as displacement water (Tezel et al., 2007).

Figure 3.1. Water displacement device used for the measurement of total biogas production

The composition of biogas produced in the reactors were determined a gas chromatography device (Trace GC Ultra, Thermo Scientific) equipped with a thermal conductivity detector (TCD) and columns connected series in (CP-Moliseve 5A and CP-Porabond Q). The temperature of oven, injector and detector were 35 ^{0}C, 50 ^{0}C and 80 ^{0}C, respectively. The carrier gas was helium at constant pressure of 75 kPa.

Daily produced methane was calculated from methane content and total produced biogas (Filer et al., 2019)with the following Equation (3.1):

$$V_{(CH4)} = \left(\frac{\%\,CH4,t}{100} * Vbiogas + \frac{\%CH4,t - \%CH4,t-1}{100}\right) * Vheadspace \quad (3.1)$$

where V_{CH4}, V_{biogas} and $V_{headspace}$ represent daily produced methane volume (mL), daily produced total gas (mL) and volume of reactor headspace (mL), respectively. $\%CH_4$, t and $\%CH_4$, t-1 are the methane percent of total biogas production in the corresponding day and the previous day, respectively.

In order to have correct values for the composition of biogas and methane production, gas chromatography was calibrated with a calibration gas (50% H_2, 10% N_2, 10% CH_4 and 30% CO_2) for methane and carbon-dioxide before each set. The equation obtained from the calibration curve was used to calculate methane production in each reactor. Calibration was repeated periodically during this thesis work and an example of calibration curve for methane and carbon-dioxide is shown in Figure 3.2. To check the calibration validity a mid-point standard was injected periodically.

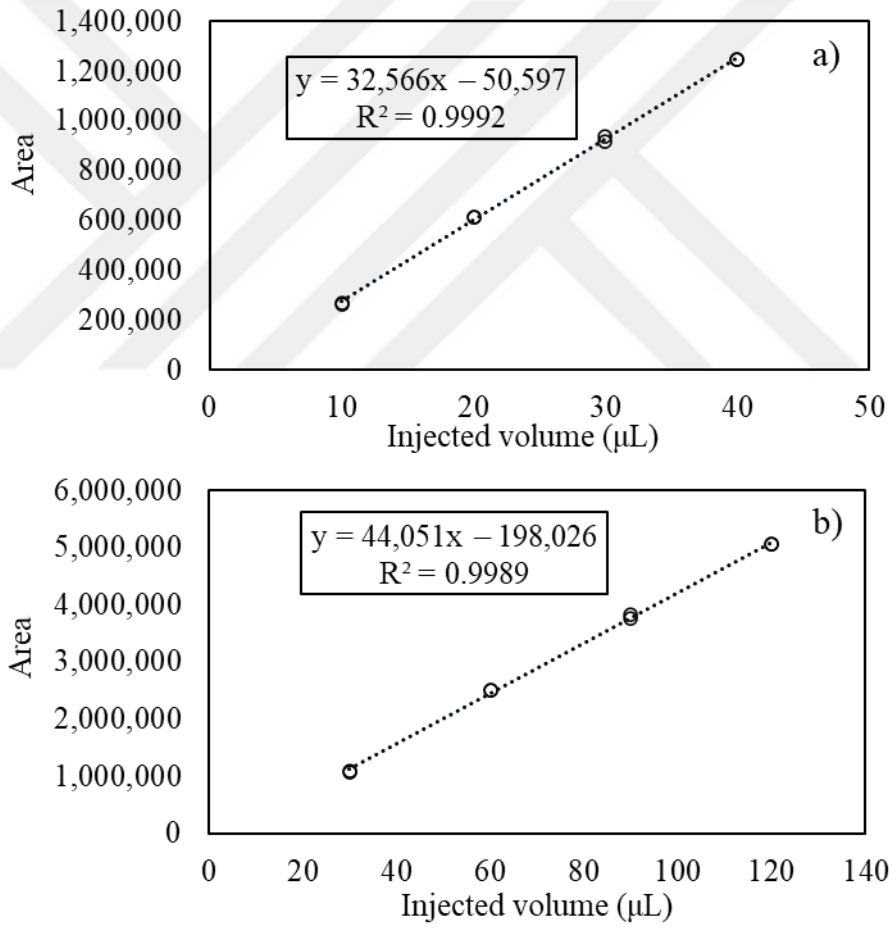

Figure 3.2. An example of calibration curves a) for methane and b) for carbon dioxide

3.3.3 Determination of Volatile Fatty Acid (VFA) Concentrations

Since volatile fatty acids (VFAs) are intermediate products produced in acidogenesis and converted during acetogenesis and methanogenesis during AD, their concentration and accumulation significantly affect the performance of AD. In Set 3 and Set 4, we monitored the concentration of acetic acid, butyric acid and propionic acid periodically in order to see VFA profiles of our reactor in terms of possible acid accumulation. For VFA measurements a gas chromatography (Trace GC Ultra, Thermo Scientific) with flame ionization detector (FID) that is equipped with a carboxylic acid measurement column (Nukol-Model 25326, 15 m * 0.53 mm, Supelco) was used. The carrier gas was helium with a flow rate of 6 mL/mins dry air. The detector and the inlet temperatures were 280 ^{0}C and 250 ^{0}C, respectively. The temperature of oven was initially set 100 ^{0}C then increased up to 200 ^{0}C with the ramp of 8 ^{0}C/min. VFA measurement was performed per week for Set 3 and Set 4. Each week, after GC measurement for biogas production, 2 mL of suspended sludge was taken from the reactors in the glovebox in order to prevent any oxygen entrance to the reactors. After taking the sample in the glovebox, the reactors were purged with mix gas to remove any oxygen in the headspace of the reactors. Before the measurement of VFAs, samples were firstly filtered through 0.22 µm filters, and they were acidified with formic acid (98%) to decrease pH of samples below 2.5 in order to convert them in their free forms.

Similar to the practice followed during biogas composition analysis, we also calibrated the gas chromatography for acetic, propionic and butyric acids with the calibration standard of 1 mM, 2.5 mM, 5 mM and 10 mM VFA. An example of calibration curves for acetic, propionic and butyric acids is given in Figure 3.3.

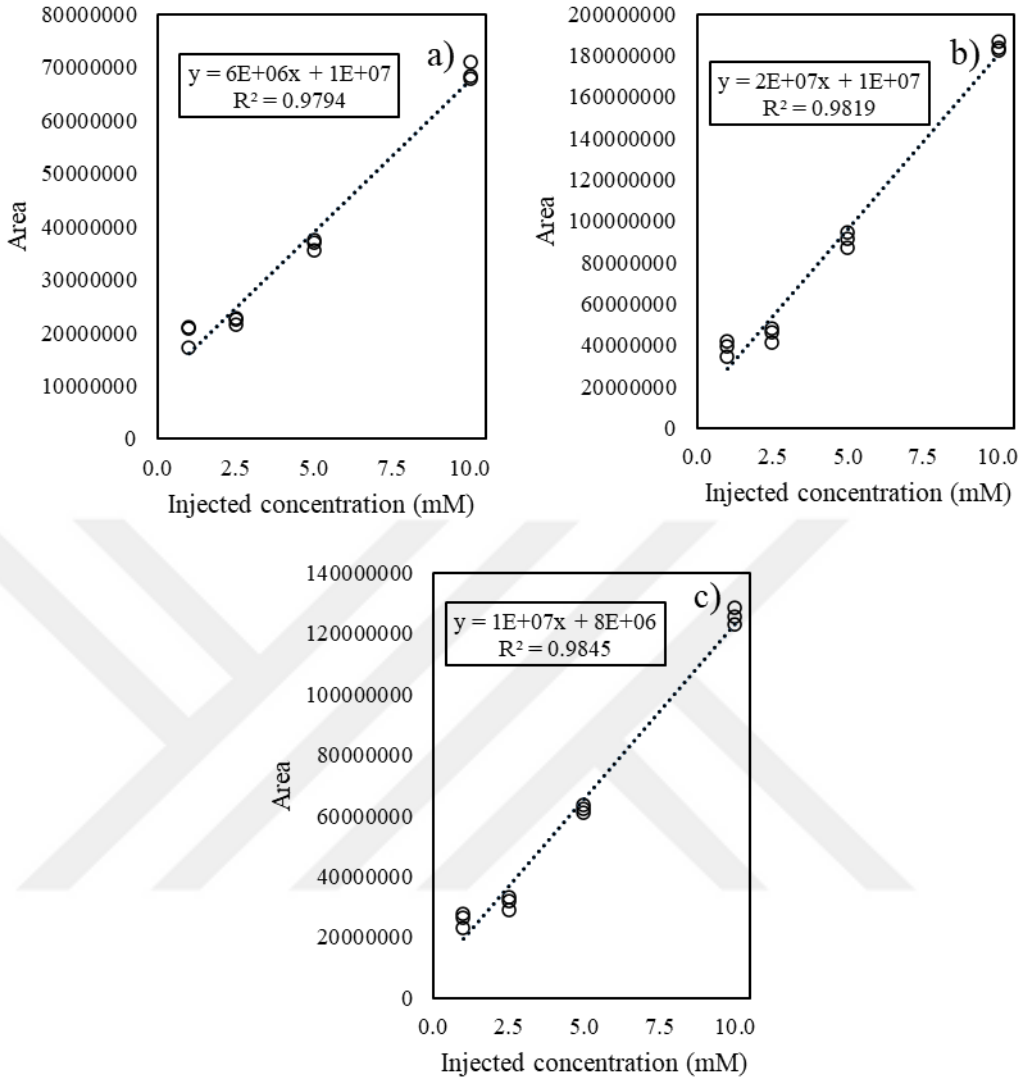

Figure 3.3. An example calibration curve for a) acetic acid, b) butyric acid, and c) propionic acid

3.4 BioMethane Production Data Analysis

To provide a comparative analysis of methane production within a set or between different sets the cumulative methane production data was fit using the modified Gompertz model (Zwietering et al., 1990). The kinetic parameters such as specific methane production potential (mL, B_t), maximum methane production potential (mL, B_0), methane production rate (mL CH_4/day, R_m) and lag time for the reactor

(day, λ) were determined using the modified Gompertz model provided in Equation (3.2):

$$B_{(t)} = B0 * \exp\{[\frac{Rm*e}{B0} * (\lambda - t) + 1]\}, t \geq 0 \quad (3.2)$$

where t is incubation time (day) e is 2.718

3.5 Experimental Sets and Procedures

In this study, four experimental sets were conducted as shown in the schematic representation (Figure 3.4). The details of these sets will be explained separately in the following sections.

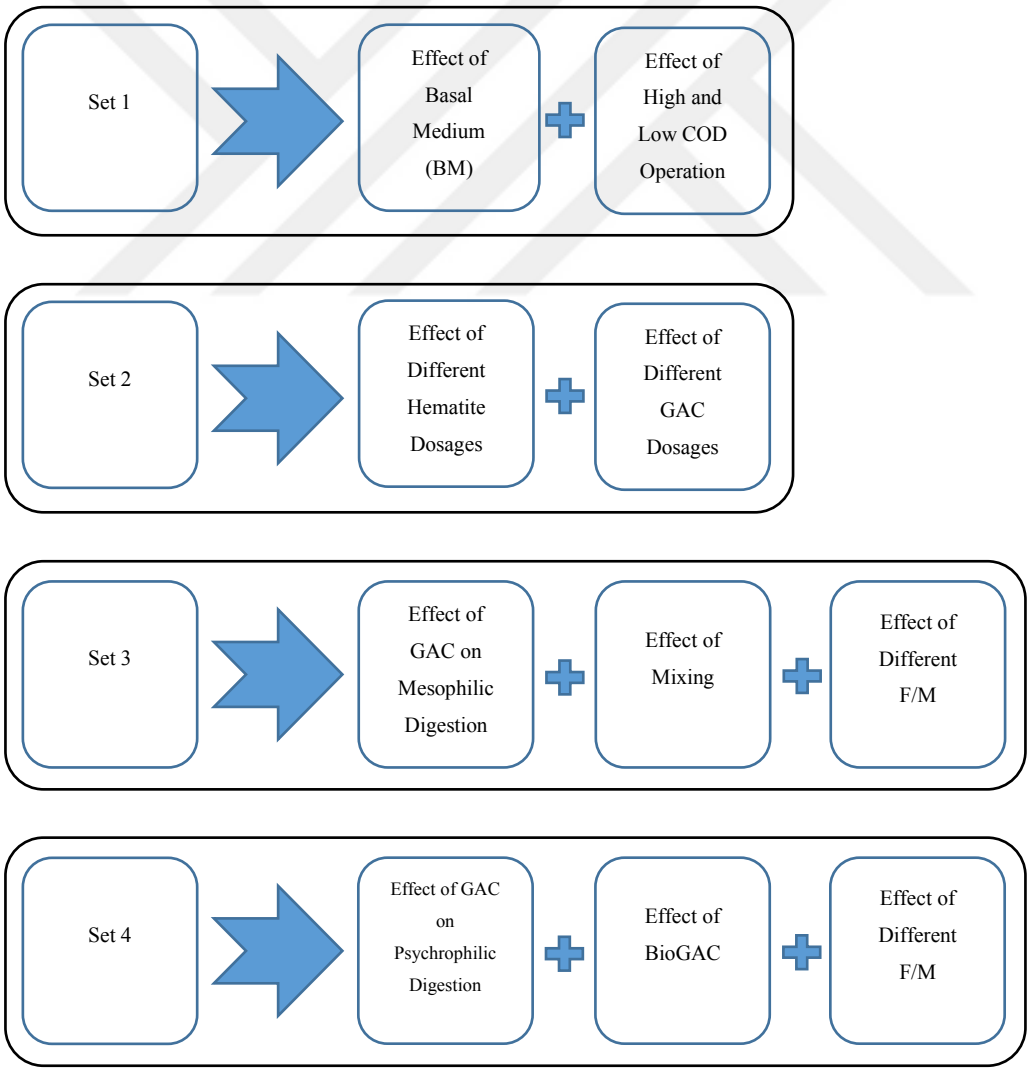

Figure 3.4. Schematic representation of the experimental sets

3.5.1 The reactor configuration

In this work, there are two types of reactors in the sets. For Set 1, the serum bottles with total volume of 100 mL and active volume of 60 mL were used as reactors (Figure 3.5).

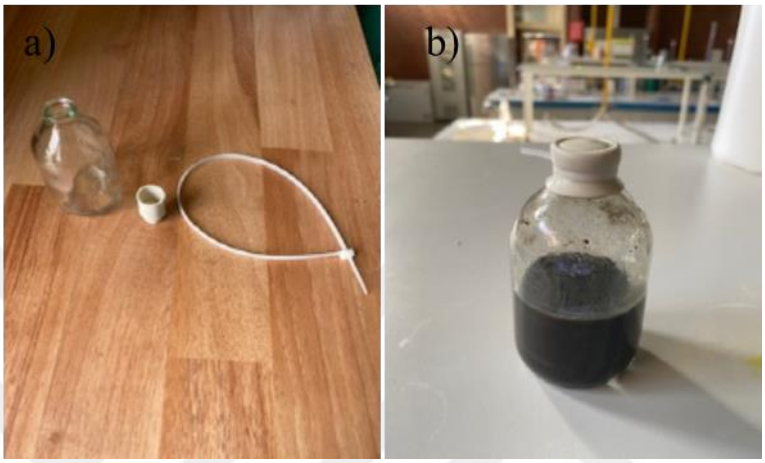

Figure 3.5. a) The serum bottle, stopper and clamp and b) the reactor filled with inoculum and cattle manure for Set 1

For Set 2, Set3 and Set 4, the serum bottles with total volume of 300 mL and active volume of 150 mL were as reactors (Figure 3.6).

Figure 3.6. The serum bottle, cap and stopper used in Set 2, Set 3 and Set 4

3.5.2 Set 1: The impact of Basal Medium on Mesophilic Anaerobic Digestion of Cattle Manure

In this set, our objectives were two-fold: to determine (i) the impact of BM on the anaerobic digestibility of CM, and (ii) the effect of initial COD (as higher and lower COD) on AD performance. Two different initial COD concentrations representing higher (~ 30,000 mg/L) and lower COD (~20,000 mg/L) were adjusted. After setting up the reactors initial CODs were measured and in the reactors with higher COD, the COD concentrations ranged between 30,240 mg COD/L and 31,240 mg COD/L and in the reactors with lower COD, the initial COD concentrations ranged between 21,760 mg COD/L and 22,240 mg COD/L.

Set 1 experiments were conducted in 110 mL serum bottles with an active volume of 60 mL (Figure 3.7). All reactors were inoculated with 30 mL of AD seed. Then, 20 mL of CM was added to the reactors. These additions established different F/M ratios (in mg/L VS basis) in the reactors. F/M ratios of higher COD (HCOD) reactors were around 1.9 and lower COD (LCOD) reactors were around 1. The experimental design for Set 1 is shown in Table 3.6.

When needed, 10 mL of BM was added into the reactors according to the experimental design to determine the effect of BM on AD performance. Blank reactors having only inoculum in the absence of BM (B1) and in the presence of BM (B2) were also operated to find out the background methane production from the inoculum.

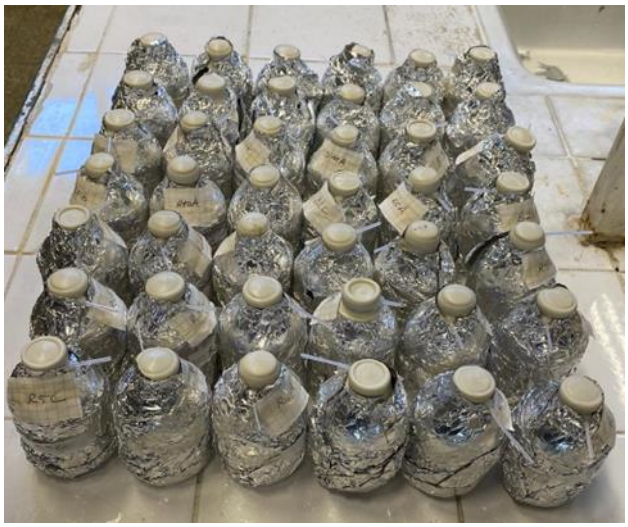

Figure 3.7. The reactor filled with inoculum and cattle manure wrapped with aluminum foil in Set 1

Table 3.6. The experimental design for Set 1

Reactor	Inoculum	CM	BM	Initial COD (mg /L)	Initial VS (mg /L)	F/M ratio
B1 w/o BM	+	-	-	-	-	-
B2 w/ BM	+	-	+	-	-	-
AD1, HCOD w/o BM	+	+	-	30,240 ± 1,020	21,950 ± 317	1.9
AD2, HCOD w/ BM	+	+	+	31,200 ± 880	23,650 ± 450	1.9
AD3, LCOD w/o BM	+	+	-	21,760 ± 640	16,500 ± 167	1.0
AD4, LCOD w/ BM	+	+	+	22,240 ± 720	17,067 ± 567	1.0

HCOD: higher COD; LCOD: lower COD; BM: basal medium

In this set, reactors were operated in triplicate without mixing. When all reactors were filled according to the experimental design before the incubation, all 21 reactors were sparged with 70% N_2 and 30% CO_2 for 3 mins to maintain anaerobic conditions in the reactors. After sparging, the reactors were immediately sealed with rubber stoppers that are tied with plastic cable. For the removal of oxygen in the headspace and providing an anaerobic environment, the headspaces of the reactors were purged with the same gas for 2 mins. After sparging and purging, the reactors were covered

with aluminum foil in order to prevent phototrophic metabolism. Then, the reactors were incubated in a temperature-controlled room (35 ± 1 ^{0}C) at 150 rpm of mixing.

During the incubation period, produced biogas amount and its composition was monitored periodically. When cumulative methane production as compared to previous measurement was less than 10% for two times in a row, the operation of the reactors was stopped. After the completion of the batch test, all reactors were stored at 4 ^{0}C until the final analysis of composition was complete. TS, VS and COD analysis for the reactor effluents were conducted. For the comparison of the reactor performances, cumulative methane productions, methane yields (based on amount of added VS) and organic removals were calculated. Additionally, modified Gompertz fitting to cumulative methane production data was conducted for each reactor.

3.5.3 Set 2: Enhancement of CM Digestion via Amendment of Conductive Materials: Hematite vs. Granular Activated Carbon

In Set 2, the impact of the amendment of two different CoMs on the performance of CM digestion in terms of methane yield, methane production rate and lag time was studied under mesophilic conditions. In this set, two different CMs were tested: (i) a carbon-based CoM, GAC (Merck, Germany) with 2.5 mm particle size and (ii) a metal-based CoM, hematite (Polres, Turkey) (particle size distribution of hematite is given in Figure 3.6). The particle size distribution of hematite was performed in our lab with the help of sieves with different sizes. GAC and hematite were chosen as CoMs to be used to provide a comparative analysis (Figure 3.7). In the experiments different dosages of these CoMs s were used with the aim of choosing the better CoMs in terms of performance enhancement.

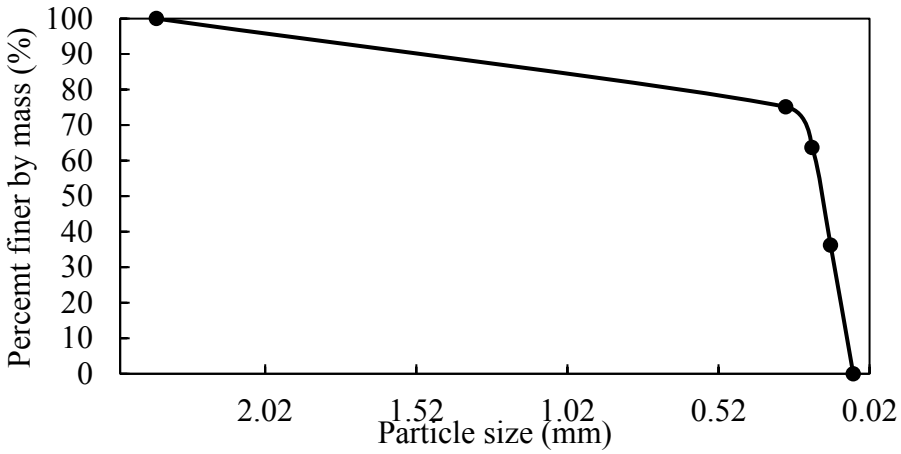

Figure 3.8. Particle size distribution for hematite

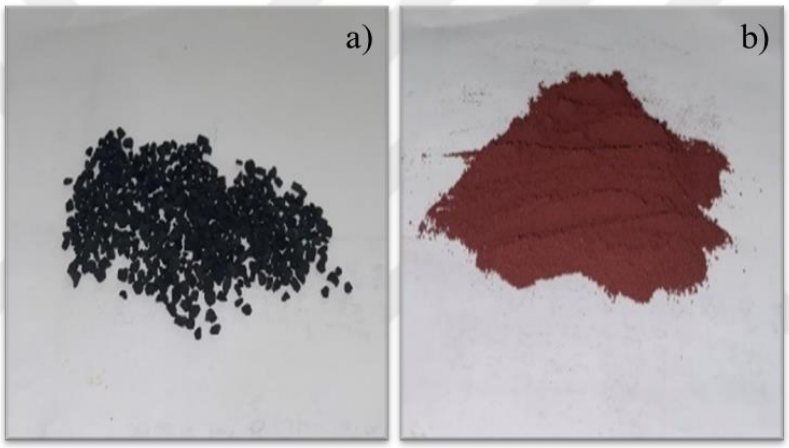

Figure 3.9. a) GAC and b) hematite used as CoM in Set 2

In the scope of characteristics of GAC and hematite, TS and VS results are given in Table 3.7.

Table 3.7. TS and VS results for GAC and hematite

CoM	TS (%)	VS (%)	VS/TS (%)
GAC	88.2 ± 1.2	3.9 ± 0.0	4.4 ± 0.0
Hematite	99.2 ± 0.0	0.4 ± 0.0	0.4 ± 0.0

Based on literature survey, for GAC application, three different dosages 20 g/L (GAC20), 40 g/L (GAC40) and 60 g/L (GAC60), and for hematite application, two

different dosages of hematite; 20 mM Fe containing hematite (Fe20) and 50 mM Fe containing hematite (Fe50) were used in the experiments. For the reactors having GAC, the dosages can be indicated as 0.6 g GAC/g VS_{added} for GAC20, 1.3 g GAC/g VS_{added} for GAC40 and 2.0 g GAC/g VS_{added} for GAC60. But based on literature survey and for clear comparison, we indicated GAC dosages as the amount of GAC addition per active volume in the thesis.

The experimental design of Set 2 is given in Table 3.8. For the determination of the performance of AD of CM and compare it with the amendment of CoMs, we set the control (AD) without any CM. Also, we set a blank reactor (B) having only inoculum as another control to determine the methane production coming from only inoculum.

Table 3.8. The experimental design for Set 2

Reactor	Inoculum	CM	Initial COD (mg/L)	Initial VS (mg/L)	F/M ratio	Dosage of CM
Blank	+	-	-	-	-	-
Control	+	+	52,400 ± 640	32,066 ± 505	1.2	-
GAC20	+	+	51,600± 860	31,961 ± 350	1.2	20 g/L of GAC
GAC40	+	+	50,800 ± 820	30,852 ± 279	1.1	40 g/L of GAC
GAC60	+	+	48,800 ± 1200	30,777 ± 751	1.1	60 g/L of GAC
Fe20	+	+	49,200 ± 940	31,964 ± 209	1.2	20 mM Fe (hematite)
Fe50	+	+	48,400 ± 820	31,580 ± 104	1.1	50 mM Fe (hematite)

In Set 2, the reactor volumes were increased slightly in comparison to Set 1. In this set, 300 mL serum borosilicate bottles were used with a working volume of 150 mL (Figure 3.8a). Before setting up the reactors, GAC was washed with deionized water for several times to remove fine particles, and dried in an oven set to 80 ^{0}C overnight (Ryue et al. 2019). The initial COD of the reactors were aimed to be around 50 g/L and initial COD measurements ranged between 48400-52400 mg COD/L with an F/M ratio of approximately 1.

As explained in Set 1, similarly before starting the operation all reactors were sparged with a mixture gas of 70% N_2 and 30% CO_2 for 3 mins and purged with the same gas mixture for 2 mins to rem maintain anaerobic conditions. All reactors were then covered with aluminum foil and incubated at 35±1 ^{0}C in the temperature-controlled room with mixing at 150 rpm with the help of a shaker (Figure 3.8b). Mixing was applied during the operation in order to prevent the settlement of CoMs. All reactors were operated in triplicate.

Figure 3.10. a) The reactors filled with inoculum and cattle manure and b) the reactors on the shaker in Set 2

During the reactor operation, total produced biogas was measured via water displacement device and the composition was determined using gas chromatography. When cumulative methane production between consecutive measurements was less than 10% for three times, the operation of the reactors was completed. After the reactor operation, pH, electrical conductivity and ORP measurement of the effluents were conducted. Also, final phosphorus and ammonium concentrations of the effluents were analyzed. For the comparison of the application of different CMs with different dosages on AD of CM, the reactors were examined in terms of cumulative methane production, methane yields (based on amount of added VS and COD) and organic removals. Also, the reactor

performances were compared in regard to kinetic parameters (methane production rate and lag time) calculated via modified Gompertz modeling.

3.5.4 Set 3: The Impact of GAC Amendment on Mesophilic AD of CM under Different Organic Loads and the Impact of Mixing on the Performance

Based on the results of Set 2 experiments, in Set 3 the experiments were designed to determine the impact of GAC amendment on the performance of CM digestion at varying operational conditions. The studied operational conditions were (i) mixing, (ii) F/M ratio. In Set 3, GAC dosage of 40 g/L was kept constant in all the reactors. Further, extra control reactors were operated by the amendment of a non-conductive material with the same particle size to GAC and at the same dosage to investigate the impact of providing extra surface area for microbial attachment on the reactor performance. The dosage of GAC and sand can be indicated as 1.3 g GAC/g VS_{added} and 1.3 g Sand/g VS_{added}. The objective here was to observe whether the reason of the enhancement of AD via GAC supplementation is only because of the extra surface area provided by GAC which can be used biomass attachment. To this purpose, as a non-conductive we used sand particles.

Set 3 experimental design is provided in Table 3.9. In this set, two groups of reactors, were operated. The reactors were arranged to have an F/M ratio of 1 and 3. In each group, there are the reactors having GAC as CoM, sand as a control. Further, conventional AD reactors without any amendment of GAC and sand were also operated as control. The reactors of each group were operated both under mixing and no-mixing condition (Figure 3.9). Also, blank reactors having only inoculum at both F/M ratios and under both mixing conditions were operated to determine the background methane production coming from only inoculum.

Before the reactors were set, GAC and sand particles were washed with deionized water for several times to remove fine particles and dried in an oven at 80 ^{0}C

overnight as described earlier. The initial COD of all reactors of ranged between 50,400-51,600 mg COD/L. F/M ratio of the reactors were aimed to be around 1 and 3, and they were 1.2 and 2.8.

Table 3.9. The experimental design for Set 3

Reactor*	Inoculum	CM	Initial COD (mg /L)	Initial VS (mg /L)	F/M ratio	Dosage of additive
B1	+	-	-	-	-	-
Control1	+	+	51,600 ± 880	32,863 ± 86	1.2	-
GAC1	+	+	51,200 ± 600	32,703 ± 460	1.2	40 g/L of GAC
Sand1	+	+	50,400 ± 640	32,941 ± 326	1.2	40 g/L of sand
B3	+	-	-	-	-	-
Control3	+	+	50,800 ± 940	31,991 ± 245	2.8	-
GAC3	+	+	50,800 ± 820	32,133 ± 415	2.8	40 g/L of GAC
Sand3	+	+	50,400 ± 920	31,632 ± 67	2.8	40 g/L of sand

*In Set 3, reactors were operated under two mixing conditions: mixing at 150 rpm, and no-mixing.

Similar to Set 2, 300 mL borosilicate serum bottles were used with an active volume of 150 mL. Water displacement device were used to monitor total biogas production. The quantification of produced biogas and VFA concentrations in the reactors were analyzed by gas chromatography. When cumulative methane production between consecutive measurements was less than 10% for three times, the operation of the reactors was stopped. pH, conductivity, ORP, final phosphorus and ammonium concentrations of the effluents were measured after the operation. For the determination of the impact of GAC and sand on CM digestion under different operational parameters, cumulative methane production, methane yields (based on added amount of VS and COD) and organic removal were examined. Kinetic parameters calculated from modified Gompertz modeling were also calculated for discussion of the results.

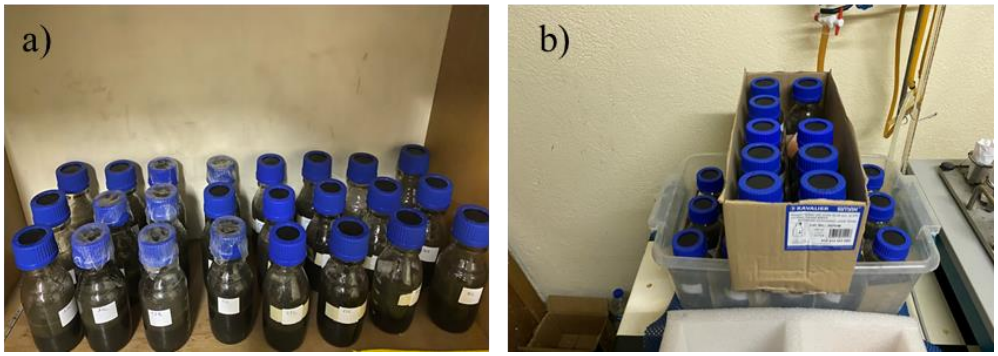

Figure 3.11. a) The reactors without mixing and b) the reactors with mixing on shaker

Apart from the routine performance analysis, in order to investigate the electrochemical activity and the potential of electroactive biofilm formation on GAC and sand particles and the controls, CV analysis was performed using three-electrodes system with a reference electrode as described in detail in Section 3.6.

At the end of the set the reactor effluents were used for struvite precipitation experiments with the purpose of investigating the nutrient recovery potential and to determine the impact of GAC on downstream processing of the effluent. To this purpose, the effluents of each group of triplicate reactors were combined in three groups, AD (the effluents from the controls), GAC (the effluents from GAC amended reactors) and sand (the effluents from sand amended reactors). Here the F/M ratios or mixing condition was disregarded. After we obtained these three groups based only on the presence of additives, struvite precipitation experiments were conducted as possible downstream treatment with the purpose of nitrogen and phosphorus recovery and to determine any potential impact of GAC application on downstream processing of the effluent. The protocols followed for struvite precipitation experiments are described in Section 3.7.

3.5.5 Set 4: The Impact of GAC Amendment on Psychrophilic Anaerobic Treatability of CM under Different Organic Loads

The objective of Set 4 experiments was to investigate the impact of the amendment of bare GAC on anaerobic treatability of CM at psychrophilic temperature under two different F/M ratios of 1 and 3. Similar to Set 3, GAC dosage was kept constant at 40 g/L.

There are two main stages before setting the reactors for this set. These stages are the acclimation of inoculum to psychrophilic temperature and the biofilm formation on GAC particles, which later was named as BioGAC. These stages will be explained in the following sections.

Acclimation of Inoculum to Psychrophilic Temperature

In Set 4, first we acclimated the inoculum taken from the full-scale mesophilic digester to psychrophilic operation temperature of ~18 °. For the acclimation stage, 5L of glass bottle connected to a water displacement device was used as shown in Figure 3.10. Inoculum was acclimated in a batch reactor with an active volume of 4 L by feeding with filtered CM (with a COD of 2000 mg/L) in fed-batch mode. The reactor was kept under mixing at 150 rpm.

Figure 3.12. The reactor set-up for acclimation of inoculum

Methane production of acclimation reactor was monitored as described earlier using a GC periodically. The operation of the acclimation lasted 3 cycles (total 37 days). Cycle implies the period of operation until less than 10% increase in cumulative methane production as compared to previous measurement is obtained for two times.

Biofilm Formation on GAC Particles

For comparison of bare GAC and BioGAC on psychrophilic AD of CM, we conducted a pre-step for biofilm formation on GAC particles. For this stage, 40 g/L of GAC were put into 6 identical serum bottles of 110 mL of total volume. For GAC dosage, it can be specified as 1.7 g GAC/g VS_{added}. The bottles with an active volume of 65 mL were inoculated and fed with filtered CM (with a COD of 2000 mg/L) at laboratory temperature (~18 ^{o}C). Methane production of the bottles were monitored periodically and when cumulative methane production as compared to previous measurement was less than 10% for two times, a new fed-batch cycle was started by feeding substrate again.

GAC particles collected from these reactors are named as BioGAC, referring to the biofilm attached GAC. Before setting up the reactors for Set 4, the bottles having BioGAC particles were put in the anaerobic glovebox for the transfer of the particles into the reactors used in Set 4. In anaerobic glovebox, the bottles having BioGAC particles were shaken by hand, and the content of it was poured into the reactor that will be operated in Set 4. After waiting for a while for the settlement of BioGAC particles in the reactor, suspended sludge was taken with a pipette, and only BioGAC particles was remained in the reactor without any suspended sludge from acclimation period. The experimental design of Set 4 is shown in Table 3.10. All reactors were mixed at 150 rpm.

Table 3.10. The experimental design for Set 4

Reactor	Inoculum	CM	Initial COD (mg/L)	Initial VS (mg/L)	F/M ratio	Dosage of additives
B1	+	-	-	-	-	-
Control1	+	+	35,500 ± 660	24,370 ± 156	1.1	-
GAC1	+	+	35,560 ± 540	24,507 ± 715	1.1	40 g/L of bare GAC
BioGAC1	+	+	36,400 ± 500	24,011 ± 485	1.1	40 g/L of BioGAC
B3	+	-	-	-	-	-
Control3	+	+	35,560 ± 820	23,347 ± 294	3.1	-
GAC3	+	+	36,400 ± 680	23,283 ± 375	3.1	40 g/L of bare GAC
BioGAC3	+	+	36,960 ± 760	23,640 ± 194	3.1	40 g/L of BioGAC

Similar to Set 3 reactors were run at two different F/M ratios. Blank reactors having only inoculum under both F/M ratios of 1 (B1) and 3 (B3) were also prepared to determine the methane production coming from only inoculum. During the operation of this set temperature was recorded with a data collector (RC-4, Elitech) for the whole duration.

Before starting to operate the reactors, similar to previous sets, all reactors were sparged and purged with a mixture gas of 70% N_2 and 30% CO_2 for 3 mins and 2 mins, respectively. to maintain the anaerobic conditions in the reactors.

Similar to other sets, total biogas production was measured with water displacement device. Methane content of produced biogas and VFA concentrations of the reactors were determined by gas chromatography. When cumulative methane production between consecutive measurements was less than 5% for three times, the operation of the reactors was stopped. pH, conductivity, ORP, final ammonium and phosphorus concentrations of the reactors were analyzed at the end of the operations. For the investigation of the impact of bare and BioGAC under different F/M ratios

under psychrophilic conditions, cumulative methane productions, methane yields (based on both added VS and COD) organic removal were calculated. Modified Gompertz equation was also applied for more informative comparison of the reactor performances.

Similar to Set 3, in Set 4 for the investigation of electrochemical biofilm formation on GAC particles and for the control, CV analysis was also conducted. Further, a techno-economic analysis was conducted to compare the performances of GAC amendment at psychrophilic temperature and conventional mesophilic AD of CM under different organic loadings. Lastly, microbial community analysis was performed for the determination of key microorganisms on GAC biofilm and provide a comparison with the suspended culture present in the reactors. The details of microbial community analysis are provided in Section 3.9.

3.6 Cyclic Voltammetry (CV) Analysis

In order to investigate the electrochemical activity and to demonstrate the presence of electroactive biofilm formation for Set 3 and Set 4, CV analysis was performed using three-electrodes system with a potentiostat (Interface 1010B, Gamry). CV analysis was performed at the end of the batch reactor operation. In summary, two graphite plates (2.5*2.5*0.3 cm) connected with a titanium wire were located in the reactors to be used anode and cathode (Figure 3.11). As a reference electrode an Ag/AgCl electrode (3 M NaCl, MODEL re-5b, BASi).) was used. The reactors were fed with filtered CM and this mixture was incubated for 3 days. Then, CV analysis was conducted for each set. During the analysis, the voltage ranges were ranged between -0.7 to 0 and scan rate was kept at 1 mV/S.

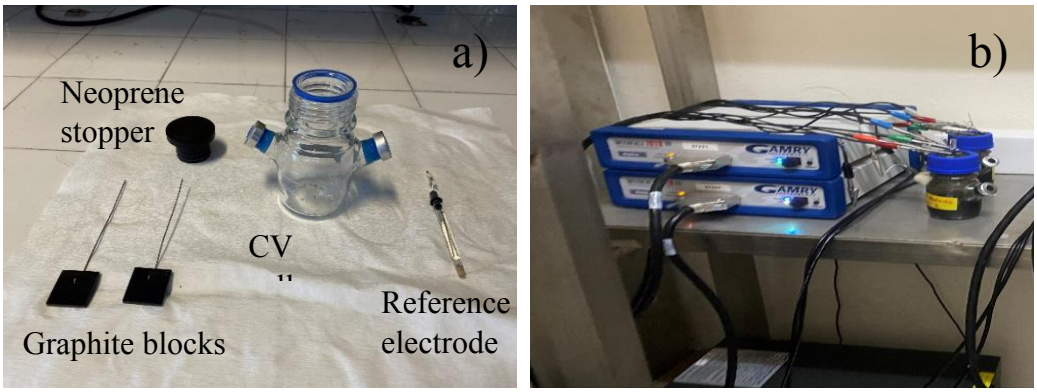

Figure 3.13. a) Neoprene stopper, graphite blocks, reference electrode and CV cell used in the analysis and b) during CV analysis reactors connected to a potentiostat

3.7 Struvite Precipitation Experiments and Product Analysis

The effluents of the reactors in Set 3 were used for struvite precipitation experiments. The effluents collected after operation were combined in three separate groups: (1) control group, having the effluent of all controls (Control1-mix, Control1-no mix, Control3-mix and Control3-no mix, (2) sand group, having the effluent of all sand amended reactor (Sand1-mix, Sand1-no mix, Sand3-mix and Sand3-no mix, and (3) GAC group, having the effluent of all GAC amended reactor (GAC1-mix, GAC1-no mix, GAC3-mix and GAC3-no mix. For the precipitation of struvite from the effluents, the steps followed are: (i) chemical addition to adjust the molar ratio to desired level, (ii) pH adjustment, (iii) mixing, (iv) settling and (v) filtration. From each group of the samples (AD, GAC and Sand), 40 mL of sample was put into the beakers. Then, Mg and P sources were added into the reactors with calculated amount in order to have molar concentration ratio of the ions Mg:P:N of 1.5:1.2:1 as this was an optimum molar ratio determined in a previous study from BioERG (Kutlar & Yilmazel, 2022). Waste magnesite dust (WMD) and bone meal were used as Mg and P sources, respectively (Kutlar & Yilmazel, 2022). Then pH of the mixture was adjusted to 8.5 using 10% NaOH (v/v) solution. Following the pH adjustment, the solution was mixed for 30 min with a stirrer at 200 rpm. Finally, for settling we have waited for 60 mins. After settling down, the content of the beaker

was filtered through coarse filter and N and P analysis of the filtrate were conducted. Filter paper was waited at 35 ± 1 ^{0}C to be dried in the temperature-controlled room. After drying period, the precipitate was scratched from the paper and stored at room temperature (Figure 3.12) till X-ray analysis for the confirmation of the presence of struvite.

XRD analysis was conducted in METU Central Laboratory (Merkezi Laboratuvar) at Middle East Technical University (METU) using Rigaku Ultima-IV X-ray diffractometer. For data collection 2Theta method was used, where the scan range and sampling step were 5 – 70 ^{0} and 0.02^0, respectively. Duration time was set to 1^0/min. Data analysis for the precipitate dentification were also conducted at the Central Laboratory.

Figure 3.14. Precipitate scratched from the filter paper to be analyzed with XRD

3.8 Cost-Revenue analysis

Within the scope of the application of GAC and BioGAC at psychrophilic temperature as compared to conventional AD operation at mesophilic temperature, the calculation of the difference between cost and revenue was carried out for AD1-mix (mesophilic AD), GAC1 and BioGAC1 (psychrophilic AD with GAC amendment).

For cost-revenue ratio, similarly, the costs of additive (c) were calculated with the unit (per kg) prices of hematite and GAC as mentioned (not per added amount of VS at this time). Revenue from methane production rate was calculated using the following Equation (3.4) (Lu et al., 2020):

$$E_{methane} = s_{CH4}*(R_R-R_C)* L_{heat}*ή \quad (3.4)$$

Where

$E_{methane}$: revenue from methane production rate (dollars/day)

R_R: methane production rate of the reactor with GAC

R_C: methane production rate of the control

L_{heat}: lower heating value for methane (35800 kj/m^3)

ή: energy conversion efficiency (90%)

s_{CH4}: sale price of methane as electricity (0.033 dollars/kWh) (https://www.epdk.gov.tr/, 2022)

For the cost of heating for mesophilic temperature AD (Set 3), the following Equation (3.5) was used (Yasemin Dilsad Yilmazel, 2014):

$$E_{heat} = ((C_P * F * (T_d-T_r)) + (U*A*(T_d-T_r) * 86{,}400)) * P_{electricity} \quad (3.5)$$

where

E_{heat}: input energy for heating of anaerobic reactor (kj/d)

C_P: specific heat capacity of manure (kj/kg ^{0}C)

F: feed (kg/d)

U: overall coefficient of heat transfer (W/m^2 ^{0}C)

A: surface area of reactor walls through which heat loss occurs (m^2)

T_d: temperature of mesophilic AD operation (35 ^{0}C)

T_r: temperature of psychrophilic AD operation (18 ^{0}C)

$P_{electricity}$: price of electricity consumption for industrial zones (0.13 dollars/kWh) (https://www.epdk.gov.tr/, 2022)

In this calculation, C_p was calculated based on following Eqaution (3.6) (Yasemin Dilsad Yilmazel, 2014):

$$C_p = 1.44 + 2.75 * Mc \quad (3.6)$$

where Mc is moisture content of cattle manure which is approximately 88% for cattle manure which we used in our study.

Also, U was calculated by summing up U_{wall} (0.68 W/m^2 ^{0}C), U_{floor} (0.85 W/m^2 ^{0}C) and U_{roof} (0.91 W/m^2 ^{0}C).

After the calculation of all costs (GAC cost and heating cost) and revenue (from methane production rate), the differences between cost and revenue for GAC application at psychrophilic temperature (GAC1 and BioGAC1 in Set 4) and conventional AD at mesophilic temperature (AD1-mix in Set 3) were calculated.

For the cost of GAC, 2.5 dollars per kilogram (Ceyka Chemical Industry and Trade Limited Company, Turkey) was used.

3.9 Microbial Community Analysis

Microbial community analysis was carried out for Set 4 only as there are less studies conducted under psychrophilic conditions and our results will fill a gap in the literature. In total 10 samples were prepared to compare the microbial community distribution with each other. DNA isolation was performed mainly from two types of samples i) suspended culture, for this liquid sample collected directly from the reactor content was used, ii) GAC biofilm, for this GAC particles collected from the reactors were used as a sample for DNA isolation. The suspended culture of the

following reactors was sampled: Control1, GAC1, BioGAC1, Control3, GAC3 and BioGAC3. For the GAC particles samples from the following reactors were sampled: GAC1, BioGAC1, GAC3 and BioGAC3 (Table 3.10 shows the Set 4 experimental design). The DNA from the collected samples were isolated using PowerSoil DNA Isolation Kit (MoBio laboratories, CA) according to the manufacturer's protocol. For microbial community analysis of GAC particles, prior to the manufacturer's protocol, the buffer in the bead tube of the manufacturer was poured in 15 mL falcon tube having sterile glass beads. The falcon tubes were centrifuged and vortexed for 5 mins at 12,000 g and 10 mins at maximum speed, respectively in order to rupture microbial biofilm samples on GAC particles into liquid samples. Then the isolation kit protocol was followed without any changes. DNA concentration and the purity of DNA samples were determined via gel electrophoresis and nanodrop (NanoPhotometer P-Class, Implen), respectively. Isolated DNA samples were sent to BM Laboratory Systems Company (Ankara, Turkey) for metagenomics analysis, in which V3-V4 variable region of bacterial and archaeal 16 rRNA genes were used. The polymerase chain reaction (PCR) program includes 28 PCR cycles. Each cycle with the steps of 95 °C for 3 min, then 28 cycles of 95 °C for 30 s, 55 °C for 3 min and 72 °C for 3 min followed by a final elongation at 72 °C for 5 min. Both PCR positive and negative controls were analyzed. For a second PCR with Illumina sequencing adapters and dual-index barcodes to the target using KAPA HiFi HotStart Ready-mix PCR Kit (Kapa Biosystems, USA) and Nextera XT index kit (Illumina, USA) in according to the manufacturer's protocol. The second PCR program includes the steps at 95 °C for 3 min followed by 8 cycles at 95 °C for 30 s, 55 °C for 30 s and 72 °C for 30 s followed by a final elongation at 72 °C for 5 min.

CHAPTER 4

RESULTS AND DISCUSSIONS

4.1 Set 1: The Impact of Basal Medium on Mesophilic Anaerobic Digestion of Cattle Manure

Reactors were operated with two different initial COD concentrations labeled as higher and lower COD (See Table 3.6 for Experimental Design). Cumulative methane production, organic removal (based on VS and COD) and methane yields (based on added amount of VS and COD) of the higher COD and lower COD reactors are depicted in Figure 4.1.

In terms of cumulative methane production, the highest production was observed in AD1 w/o BM (141 ± 5 mL CH_4) which is 25% higher than the production in AD2 w/ BM (113 ± 6 mL CH_4) among HCOD reactors (Figure 4.1a). Similarly, for LCOD reactors, AD3 w/o BM (79 ± 8 mL CH_4) produced 39% higher cumulative methane than AD4 w/ BM (57 ± 4 mL CH_4). From the point of view of higher and lower COD application, AD1 and AD2 with higher COD increased cumulative methane production 78% and 98% as compared to AD3 and AD4 with lower COD, respectively. In terms of percent methane, when BM was not added into the reactors, AD1 and AD3 had 62.3 ± 0.5% methane and 66.1 ± 2.8% methane, respectively. On the other hand, BM addition decreased the percent methane in total biogas in AD2 and AD4. 55.6 ± 2.1% methane and 58.3 ± 1.1% methane were obtained in AD2 and AD4, respectively.

The reactor performances in terms of VS removal were similar. VS removals were 34% and 37% for HCOD and LCOD reactors, respectively, without showing any significant change due to BM addition (Figure 4.1b). Among HCOD reactors, COD removals were 44% and 40% in AD1 and AD2, respectively. For the reactors with

LCOD, the removal of COD did not change with the addition of BM, and it was 36% for AD3 and AD4.

Methane yields were also evaluated based on the added amount of VS and COD (Figure 4.1c). HCOD reactors, AD1 (107 ± 4 mL CH_4/g VS_{added}) showed 35% higher yield as compared to AD2 (79 ± 4 mL CH_4/g VS_{added}). Similarly, for LCOD, the absence of BM in AD3 (79 mL ± 8 CH_4/g VS_{added}) resulted in 41% increase in methane yield over AD4 (56 ± 4 mL CH_4/g VS_{added}) with BM addition. In addition to this, the application of HCOD resulted in higher methane yield in AD1 and AD2 as compared to AD3 and AD4. 35% higher methane yield was observed in AD1 that was operated at HCOD over AD3 that was operated at LCOD within the absence of BM. When BM was present in the reactor, 43% higher methane yield was obtained in AD2 as compared to AD4. Methane yields based on added COD had also similar trends. The absence of BM increased the yield 30% in AD1 (78 mL ± 3 CH_4/g COD_{added}) over AD2 (60 ± 3 mL CH_4/g COD_{added}) for higher COD reactors and 40% enhancement was observed in AD3 (60 ± 6 mL CH_4/g COD_{added}) without BM addition as compared to AD4 (43 ± 3 mL CH_4/g COD_{added}) with BM among LCOD reactors.

In addition to cumulative methane production, organic removal and methane yield, the comparison of kinetic parameters for each reactor was conducted using modified Gompertz modeling. The kinetic parameters (P, specific methane production potential, R_m, methane production rate and λ, reactor lag time) calculated using the model were given in Table 4.1. Sample calculations for both models are given in Appendix A.

As given in Table 4.1, the R^2 values were ranging 0.9811-0.9938 which indicates that the experimental data is well fitted to the model data calculated from the modified Gompertz equation. The cumulative methane production graphs showing experimental data and the model data are shown in Appendix B. In terms of methane production rate, among HCOD reactors, there was a higher methane production rate without BM; in AD1 w/o BM, the rate (12.0 ± 0.6 mL CH_4/day) was 103% higher

than the rate of AD2 w/ BM (5.9 ± 0.6 mL CH_4/day). Same applies to LCOD reactors, in the absence of BM methane production rate was 19% higher than the reactor with BM addition. Further, higher COD reactors showed higher methane production rate in comparison to lower COD reactors; AD1 HCOD w/o BM reactors showed 40% higher rate than AD3 LCOD w/o BM.

Additionally lag time of reactors were increased when there was BM supplementation, showing its adverse impact.

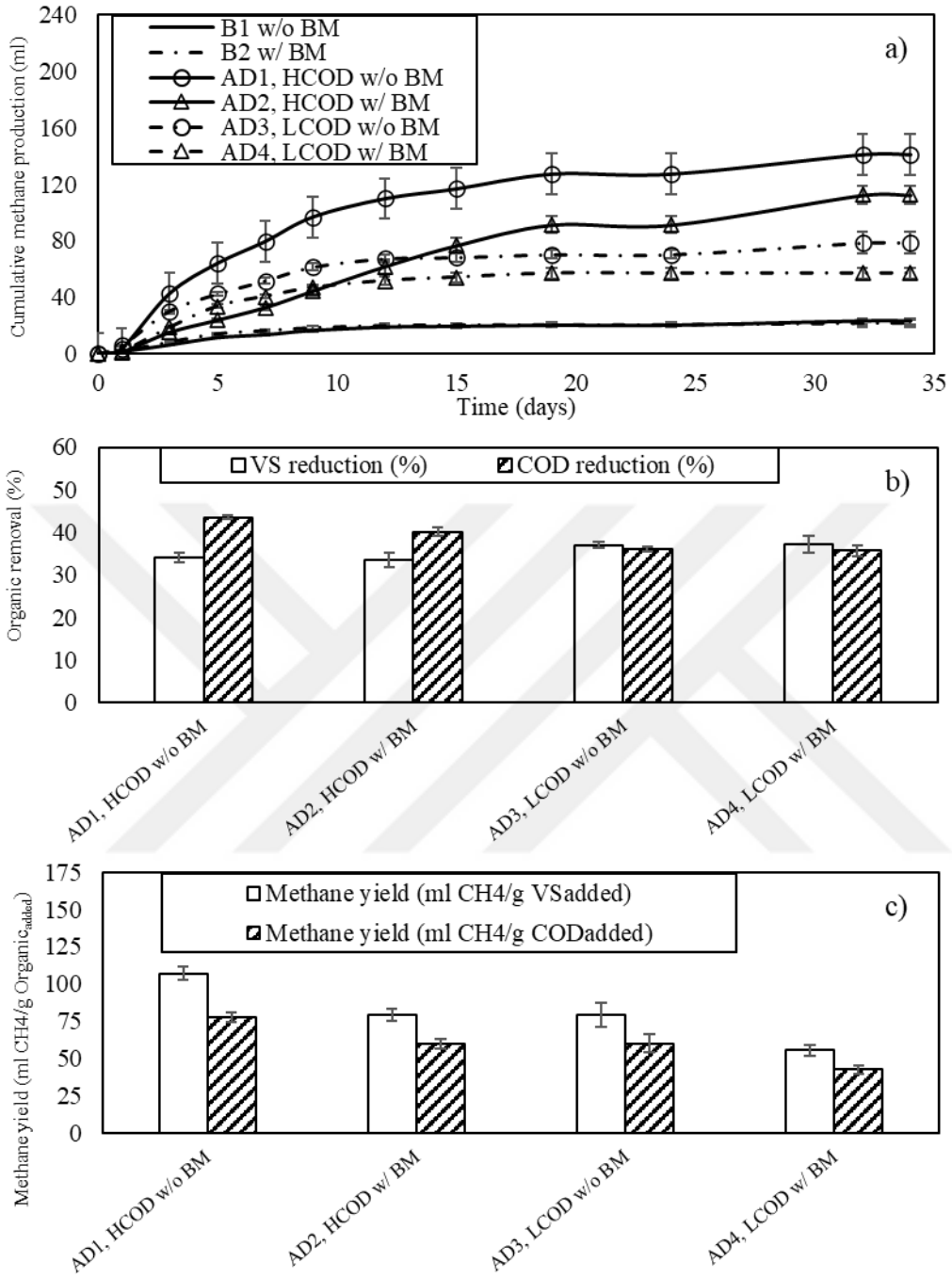

Figure 4.1. a) Cumulative methane production, b) organic removal and c) methane yield for Set 1

Table 4.1. The results of kinetic parameters calculated from the Modified Gompertz modeling for the reactors in Set 1

Reactor	P (mL)	R_m (mL CH_4/day)	λ (day)	R^2
AD1, HCOD w/o BM	133.8 ± 6.2	12.0 ± 0.6	0.2 ± 0.1	0.9822
AD2, HCOD w/ BM	113.1 ± 5.9	5.9 ± 0.6	1.5 ± 0.2	0.9914
AD3, LCOD w/o BM	73.6 ± 5.8	8.6 ± 0.7	0.1 ± 0.2	0.9811
AD4, LCOD w/ BM	56.1 ± 4.2	7.2 ± 0.1	0.7 ± 0.0	0.9938

To summarize, in both COD conditions the presence of BM showed negative impact on methane production rate and yield. Further, HCOD reactors showed a higher performance in terms of methane yield and organic removal as compared to LCOD reactors. In Table 4.2, methane yields of different studies in which CM was used as carbon source are given. As given in Table 4.2, a wide range (89-266 mL CH_4/g VS_{added}) in terms of methane yield of CM digestion was observed in the literature. The methane yield attained in HCOD reactors of this study are within this range. There can be several reasons for obtaining different methane yield in different studies, such as the lignin content of manure used, the initial organic loading, F/M ratio and VS amount of wastes and the use of different inoculums.

Table 4.2. Methane yields of similar studies when CM was used as feed

Inoculum	Temperature (^{0}C)	Operation mode	Organic loading	Methane yield (mL CH_4/g VS_{added})*	Reference
AD sludge from WWTP	36	Batch	32904 mg /L initial COD	265.6	(Huang et al., 2016)
Sludge from a laboratory-scale anaerobic digester	37	Batch	Initial 6% TS	88.9	(Zheng et al., 2015)
AD sludge from CM biogas plant	37	Batch	Initial 8% TS	150	(Song & Zhang, 2015)
Mixed anaerobic cultures	35	Batch	a) 12000 mg /L initial COD b) 53500 mg /L initial COD	a) 155* b) 195*	(Güngör-Demirci & Demirer, 2004)
Sludge from a dairy farm	35	Batch	Initial 7% TS	124	(Rosenberg & Kornelius, 2017)
Sludge from a laboratory-scale anaerobic digester	35	Batch	Initial 15 g VS/L	231	(Wei et al., 2019)
Digested slurry	35	Batch	Initial 15 g TS/L	251 210*	(Li et al., 2011)
AD sludge from WWTP	35	Batch	a) 22,000 mg /L initial COD l b) 30,720 mg /L initial COD	a) 79, 60* b) 107, 78*	This study

* Methane yield based on added amount of COD: **mL CH_4/g COD_{added}**

From the results of methane yields suggested that the presence of BM on AD of CM causes an inhibition under both lower and higher COD operations. Additionally, the presence of BM decreased methane production rate under both operations. Also, it causes an increase in lag time (in AD2 and AD4) as compared to no BM addition (AD1 and AD3). This can be attributed to nutrient content of CM. Similarly, it is reported that the nutrient in CM is already sufficient for anaerobic microbial growth without the need an extra addition and in fact BM addition resulted in lower performance in terms of methane production (Güngör-Demirci & Demirer, 2004). In other words, since nutrient in CM is sufficient for AD, the digestion is inhibited with the extra nutrient addition via BM. In terms of the amount of organic loading, the reactors with higher COD showed higher methane productions and methane yields than the reactors with lower COD, and this can be resulted from an amount of higher available carbon source for microbial growth and methane production.

The results of Set 1 show that for biomethane recovery from CM there is no need for BM addition. This may be due to its complex content. Additionally, as mentioned above, organic loading is an important factor for AD process, and under higher COD operation (AD1 and AD2), reactors showed a better performance than lower COD operation in terms of methane yield and organic removal. Based on the results of Set 1, we decided to continue the rest of the experimental studies without BM addition under higher COD loads.

4.2 Set 2: Enhancement of Mesophilic AD of CM via Amendment of Conductive Materials (CoMs): Hematite vs. GAC

In Set 2, the impact of the amendment of GAC and hematite as different CoMs with different dosages were investigated. Reactors were set according to the experimental design given in Table 3.8. Cumulative methane production, organic removal (based on VS and COD) and methane yields (based on added amount of VS and COD) of the reactors are depicted in Figure 4.2.

The impact of additives on biomethane production and organic removal

In the case of GAC amendment an increase in cumulative methane production was observed for all three dosages in comparison to the control reactor. All GAC amended reactors produced similar amounts of biomethane in 28 days of operation; GAC20 reactor produced a total of 752 ± 10 mL of CH_4, GAC40 reactor produced a total of 754 ± 14 mL of CH_4 and GAC60 reactor produced 750 ± 14 mL of CH_4 (Figure 4.2a). However, the control reactor produced only 583 ± 2 mL of CH_4 during 28 days of reactor operation. At an average 29% increase in the cumulative methane production was observed in the GAC amended reactors when compared to the control reactor, regardless of the dosage added. In terms of percent methane in total produced biogas, the values were ranged between 50.9 ± 0.7% - 54.7 ± 0.4% methane among the reactors amended with GAC. For hematite reactors, Fe20 and Fe50 had 58.1 ± 1.1% methane and 59.1 ± 0.2% methane in total produced biogas, respectively.

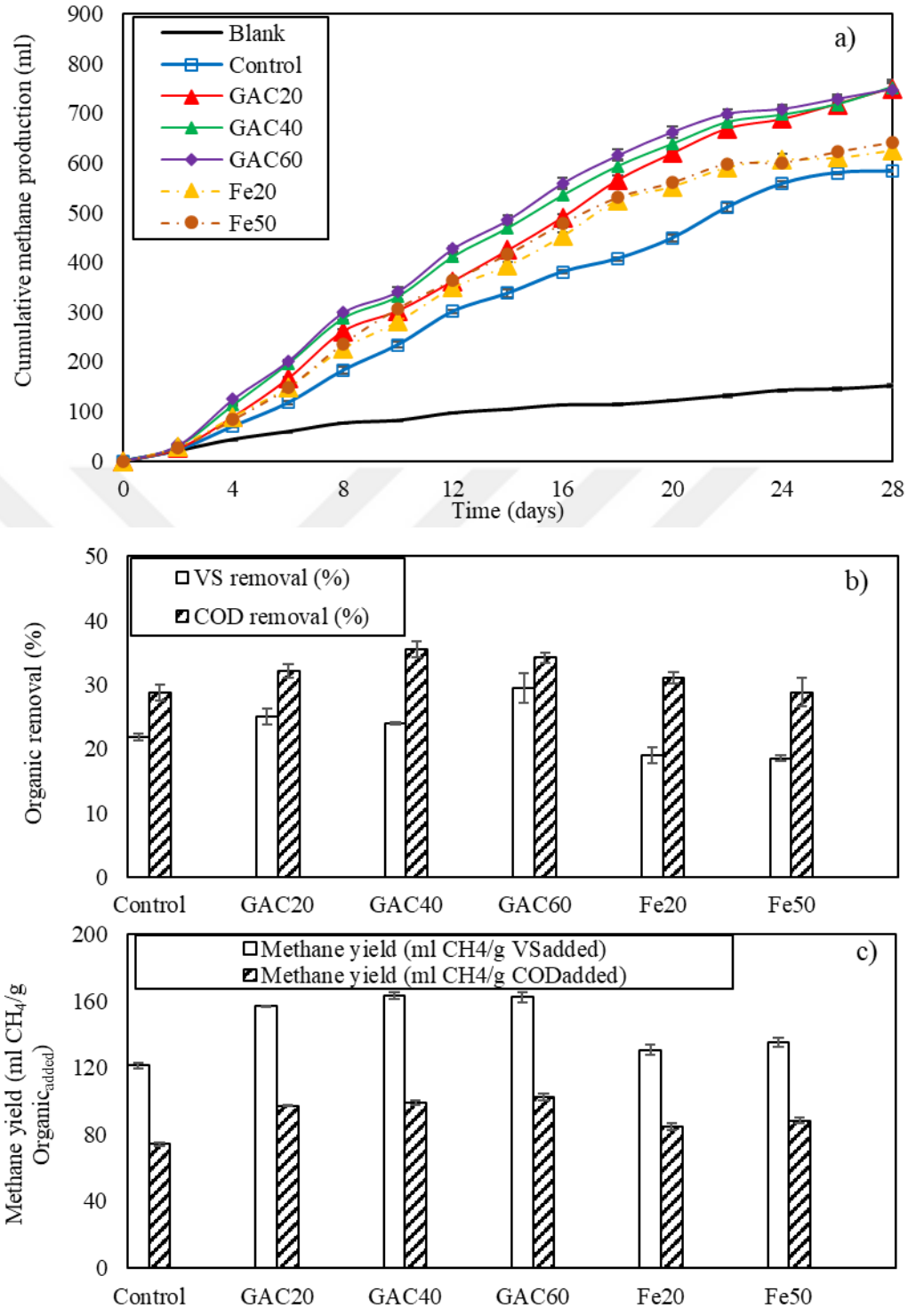

Figure 4.2. a) Cumulative methane production , b) organic removal and c) methane yields for the reactors in Set 2

In the scope of literature survey, we observed that the amendment of GAC on AD of CM digestion has not been studied extensively although swine manure and chicken manure were used as substrate. This situation is also an important motivation for this study. In Table 4.3, the studies using GAC for the enhancement of conventional AD are presented. Generally, in these studies, WAS and simple substrates such as acetate have been used as carbon sources. For example, in a study conducted with dewatered activated sludge as substrate, GAC amendment enhanced cumulative methane production 17% over the control (Y. Yang et al., 2017). Similarly, in another study, cumulative methane production was enhanced via GAC 31% as compared to the control when acetate was used as carbon source (J. H. Park, Park, et al., 2018).

In our study, the increase in dosage of GAC did not enhance cumulative methane production further. He et al., (2021) even reported a decrease in methane production when the dosage of GAC was increased from 10 g/L to 15 g/L during the co-digestion of fat, oil, grease and activated sludge. They observed that 13% increase in cumulative methane production via 10 g/L of GAC amendment decreased to 7% when GAC dosage was increased to 15 g/L.

Table 4.3. Comparison of results from different studies using GAC amendment in AD

GAC dosage (g/L)	Operation mode	Seed	Substrate	Improvements	References
50	Batch	Sludge form WWTP	Municipal solid waste (initial COD of 220,000	%1800 times higher methane production	(Dang et al., 2017)
33	Batch	AD seed	Acetate	80% higher methane production rate	(Zhang et al., 2017)
5	Batch	AD seed	Dewatered activated sludge (initial COD of	17% higher methane production	(Yang et al., 2017)
10	Batch	Sludge from brewery treatment system	Co-digestion of activated sludge with fat, oil & grease	a) 13% higher methane production	(He et al., 2021)
6	Batch	AD seed	Acetate and ethanol	31% enhancement in methane production 72% enhancement in methane production rate	(Park et al., 2018)
25	Batch	AD seed	Food waste	100% enhancement in methane yield 26% enhancement in methane production rate	(Ryue et al., 2019)
15	Batch	Sludge from an up-flow anaerobic sludge blanket reactor	Swine manure	19% enhancement in methane yield 19% enhancement in lag time	(Romero et al., 2020)
40	Batch	AD seed	CM	34% enhancement in methane yield 30% enhancement in lag time	This study

The amendment of hematite also increased cumulative methane production in comparison to control reactor. Similar to the GAC amended reactors, there was a slight difference in the cumulative methane production of different dosage reactors (Fe20 and Fe50). Fe20 reactors produced a total of 626 ± 13 mL of CH_4 and Fe50 reactors produced 641 ± 1 mL of CH_4 corresponding to 7% and 10% increase over control reactor, respectively (Figure 4.2). The studies using hematite for the enhancement of conventional AD are summarized in Table 4.4. There was only one study conducted with animal manure and the authors reported 11% increase in methane yield via hematite addition to AD reactors fed with swine manure (Lu et al.,2019). Similar to GAC higher enhancements with hematite has also been observed with simple substrates such as acetate (Table 4.4).

Table 4.4. Comparison of results from different studies using hematite amendment in AD

Hematite dosage (mM Fe)	Operation mode	Seed	Substrate	Improvements	References
20	Batch	Paddy soil	Acetate	Stimulated methanogenesis Shortened start-up	Kato et al 2011
25	Batch	Paddy soil	Acetate	110% enhancement in cumulative methane production	Zhou et al 2013
25	Batch	Paddy soil	Benzoate	25% enhancement in methane production rate	Zhuang et al 2015
187.5,	Batch	Inoculum from swine farm	Swine manure	11.1% enhancement in methane yield	Lu et al 2019
250	Batch	Sludge from a laboratory-scale upflow anaerobic sludge blanket reactor	Activated sludge	36% enhancement in methane yield	Ye et al. 2018
20,	Batch	AD seed	CM	8% enhancement in methane yield 26% increase in methane production rate	This study
50				12% enhancement in methane yield 34% increase in methane production rate	

When compared to the increase over control in GAC reactors (~29%) in the cumulative amount of methane, the increase in hematite amended reactors (max of

10%) was significantly lower. Methane production yield is clearly a better parameter for comparison of the reactor performances. Therefore, methane yield per gram organic matter added is calculated for each reactor in Set 2 (Figure 4.2c). Upon GAC amendment methane production yields are increased by approximately 30% in the case of GAC20 reactor (157 mL ± 2 CH_4/g VS_{added}) and around 34% in the case of GAC40 (163 ± 3 mL CH_4/g VS_{added}) and GAC60 (162 ± 3 mL CH_4/g VS_{added}) reactors in comparison to the control (121 ± 0.4 mL CH_4/g VS_{added}). The results show that even though there was a slight increase in the yield when dosage was increased from 20 to 40 in dosage of GAC further from 40 to 60 g/L did not change the yield. When the yields were represented in terms of COD similar results were obtained. The increase in the methane yield per COD basis ranged between 31% - 38% when compared to control. Similarly, He et al., (2021) observed that the addition of GAC enhanced methane yield 13% as compared to the control on the co-digestion of fat, oil, grease and activated sludge. In another similar study, it was observed that the addition of GAC enhanced methane yield based on added COD, by 19% with swine manure as the feed (Romero et al., 2020).

In the case of hematite amendment enhancement of methane production yield was lower in comparison to GAC amendment. Fe20 (131 ± 2.6 mL CH_4/g VS_{added}) and Fe50 (135 ± mL 0.2 CH_4/g VS_{added}) enhanced methane yield by 8% and 12% as compared to the control, respectively (Figure 4.2). In the literature, it was obtained that the addition of hematite improved the yield 7% from AD of swine manure (T. Lu et al., 2019). Similarly, Ye et al., (2018) observed 36% increase in methane yield via hematite application on AD of activated sludge. Although there is a 2.5 times difference in dosage values of Fe20 and Fe50, the enhancement in methane yield in Fe50 as compared to Fe20 is not as significant.

The application of GAC increased VS and COD removal as compared to the control. 25 ± 1 %, 24 ± 0 % and 30 ± 2 % VS removals were observed in GAC20, GAC40 and GAC60, respectively, which are all greater than the VS removal attained in the control (22± 1 %) (Figure 4.2). Similarly, 50% improvement in VS removal was

obtained via GAC amendment on AD of the dry organic fraction of municipal solid waste over the control (Dang et al., 2017a). In another study, GAC application on AD of waste fat, oil and grease enhanced VS removal 85% over the control (He et al., 2021). In addition to added amount of VS, the reactors having GAC enhanced COD removals 10%, 24% and 17% in GAC20 (32 ± 1 %), GAC40 (36 ± 1%) and GAC60 (34 ± 1%) as compared to the control (29 ± 1 %), respectively. Similarly, Romero et al., (2020) found that the application of GAC on AD of liquid fraction of swine manure enhanced COD removal 16% over the control. As discussed in the literature, the amendment of CoMs can improve organic removal as compared to the control (Y. Liu et al., 2021). It is stated that GAC can accelerate the decomposition of organic and can tolerate the adverse shocks during AD. As a result of this acceleration in organic decomposition and recovery of the shocks, enhanced methane production can be obtained.

Among the reactors with hematite, there was no significant change in VS or COD removal as compared to the control was not observed (Figure 4.2). Although the enhancement in cumulative methane production and methane yields was observed in the reactors with hematite (Fe20 and Fe50) as compared to the control, there was no enhancement in organic removal. As reported in the literature, the amendment of hematite did not enhance the organic removal in AD of swine manure (T. Lu et al., 2019). Similar trend was observed with the application of another iron-based CoM, magnetite (Fe_3O_4) (Yin et al. 2016). They also reported that there is no significant change in organic removal via magnetite application over the control.

The results of modified Gompertz modeling are given in Table 4.5 in terms of methane production potential (P), lag time (λ) and methane production rate (Rm). For all the reactors, the R^2 values were ranging between 0.9939-0.9982 indicating a well-fit of experimental data to the model data. The cumulative methane production graphs showing experimental data and the model data for Set 2 are shown in Appendix C. Methane production rates are 37.6 ± 0.6 mL CH_4/day, 40.3 ± 1.0 mL

CH_4/day and 42.4 ± 1.2 mL CH_4/day in GAC20, GAC40 and GAC60, respectively which are higher than the control (28.5 ± 0.5 mL CH_4/day).

Table 4.5. Kinetic parameters calculated from the fitting with the modified Gompertz model in Set 2

Reactor	P (mL)	R_m (mL CH_4/day)	λ (day)	R^2
Control	674.9 ± 6.8	28.5 ± 0.5	2.2 ± 0.1	0.9939
GAC20	836.7 ± 16.7	37.6 ± 0.6 (32%)	2.1 ± 0.1 (5%)	0.9958
GAC40	797.1 ± 16.9	40.3 ± 1.0 (41%)	1.6 ± 0.1 (27%)	0.9964
GAC60	793.1 ± 8.2	42.4 ± 1.2 (49%)	1.7 ± 0.1 (23%)	0.9964
Fe20	674.2 ± 14.1	35.9 ± 0.7 (26%)	2.1 ± 0.1 (5%)	0.9973
Fe50	666.3 ± 4.3	38.2 ± 0.6 (34%)	2.2 ± 0.1 (-)	0.9982

The number in the parenthesis indicates the enhancement in methane production rate and decrease in lag time as compared to the control.

Similarly, it was observed that the addition of GAC enhanced methane production rate 26% over the control on AD of food waste (Ryue et al., 2019). In another study, Park et al., (2018) found 72% increase in methane production rate via GAC application when the carbon source was acetate. As given in Table 4.4, the amendment of GAC enhanced both simple substrate degradation such as acetate and complex substrate degradation such as food waste in terms of methane production rate. Zhang et al., (2017) and Park et al., (2018) observed 80% and 72% improvement in methane production rate when acetate was carbon source, while the improvement via GAC over the control was 26% in food waste digestion (Ryue et al., 2019). This

higher enhancement in simple substrate degradation can be attributed to its more simplicity than complex substrates.

In terms of lag time, there is a slight improvement in GAC20 (2.1 ± 0.1 day) as compared to the control (2.2 ± 0.1 day). On the other hand, when GAC dosage was increased, a significant decrease in lag time was observe; GAC40 (1.6 ± 0.1 day) and GAC60 (1.7 ± 0.2 day) decreased lag time 27% and 23% over the control, respectively. (Xie et al., 2020). Others have also reported similar results. GAC amendment decreased the lag time 31% on AD of activated sludge (Xie et al., 2020).

The application of hematite was also enhanced methane production in terms of methane production rate as given in Table 4.3. Fe20 (35.9 ± 0.7 mL CH_4/day) and Fe50 (38.2 ± 0.6 mL CH_4/day) improved the rate 26% and 34% over the control, respectively. Similarly, it was reported that the application of hematite enhanced methane production rate by 34% on AD of swine manure (T. Lu et al., 2019). On the other hand, there was no significant improvement in lag time with the application of hematite over the control.

The impact of additives on nutrient concentrations

ammonium concentration is an important parameter for AD performance since the release of ammonium during protein degradation can cause inhibition on methanogenic activity (Rasapoor et al., 2020). Final ammonium concentration for each reactor is depicted in Figure 4.3.

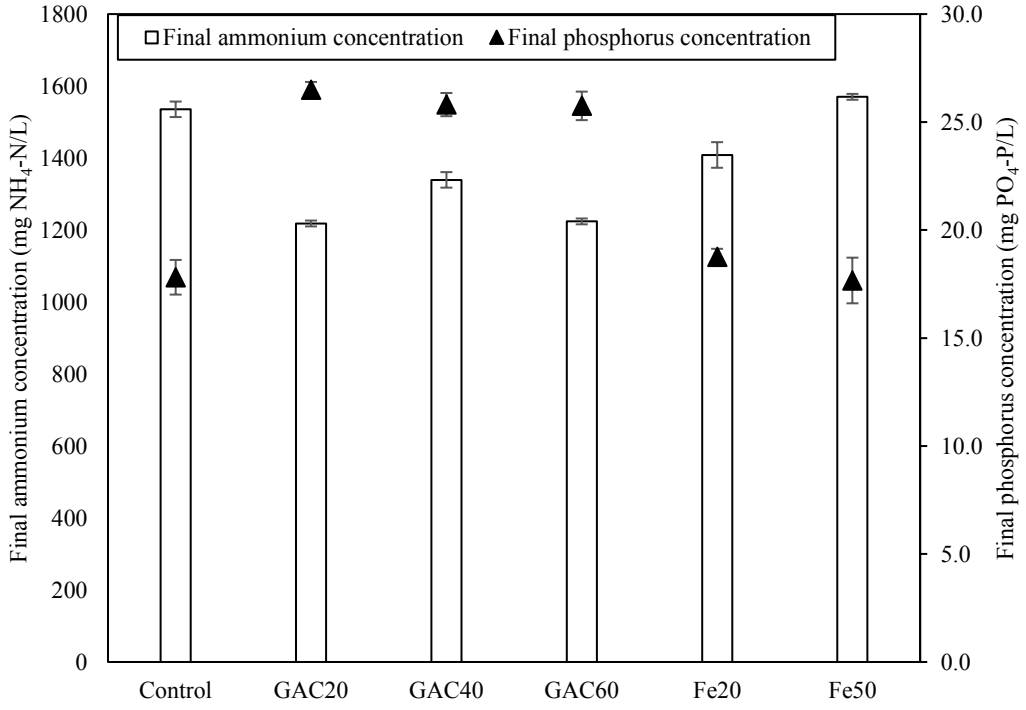

Figure 4.3. Final ammonium and phosphorus concentrations in Set 2

The addition of GAC decreased the final ammonium concentration as compared to the control. GAC20 (1218 ± 8 mg NH_4-N/L), GAC40 (1339 ± 2 mg NH_4-N/L) and GAC60 (1224 ± 8 mg NH_4-N/L) decreased final ammonium concentration 21%, 13% and 20% over the control (1536 ± 22 mg NH_4-N/L), respectively. Similar result was found by another study (He et al., 2021). It was observed that the addition of GAC on the co-digestion of fat, oil, grease and activated sludge decreased final ammonium concentration 37% as compared to the control. The decrease may stem from the adsorption of ammonium on GAC particles, and lower concentration of ammonium may create more suitable environment for methanogens for their activity (He et al., 2021). As stated in the literature, ammonium concentrations for the reactors having GAC are below the inhibition level that is approximately 2800 mg NH_4-N/L (Krakat et al., 2017). Also, based on another study, ammonium concentrations are less than the inhibition level that was stated as 1500 mg NH_4-N/L (Chen et al., 2016). On the other hand, final orthophosphate concentrations in

GAC20 (27 ± 0.4 mg PO_4-P/L), GAC40 (26 mg ± 0.5 PO_4-P/L) and GAC60 (26 ± 0.7 mg PO_4-P/L) were slightly higher than the control (18 ± 0.8 mg PO_4-P/L) as shown in Figure 4.3 yet were all comparatively small to cause any inhibition.

The amendment of hematite did not significantly change final ammonium concentration over the control (Figure 4.3). Only 8% decrease in Fe20 (1409 ± 36 mg NH_4-N/L) was observed as compared to the control. On the other hand, Fe50 (1570 ± 8 mg NH_4-N/L) caused a slight increase (~2%) over the control. For final phosphorus concentration, Fe20 (19 ± 0.4 mg PO_4-P/L) and Fe50 (18 ± 1 mg PO_4-P/L) had values close to the control without any significant change. Due to its high ammonium content of CM, ammonium concentration is an important factor on the performance of AD. Also, it affects pH of the system, eventually methane production. As shown in Figure 4.3, ammonium concentrations ranged between 1200 - 1600 mg NH_4-N/L which is less than the inhibition level mentioned as 3000 mg NH_4-N/L (Krakat et al., 2017).

The impact of additives on pH, ORP and electrical conductivity

The effects of GAC and hematite amendment on AD performance in terms of pH, ORP and electrical conductivity were also assessed. pH, ORP and electrical conductivity of the reactor effluents are given in Figure 4.4.

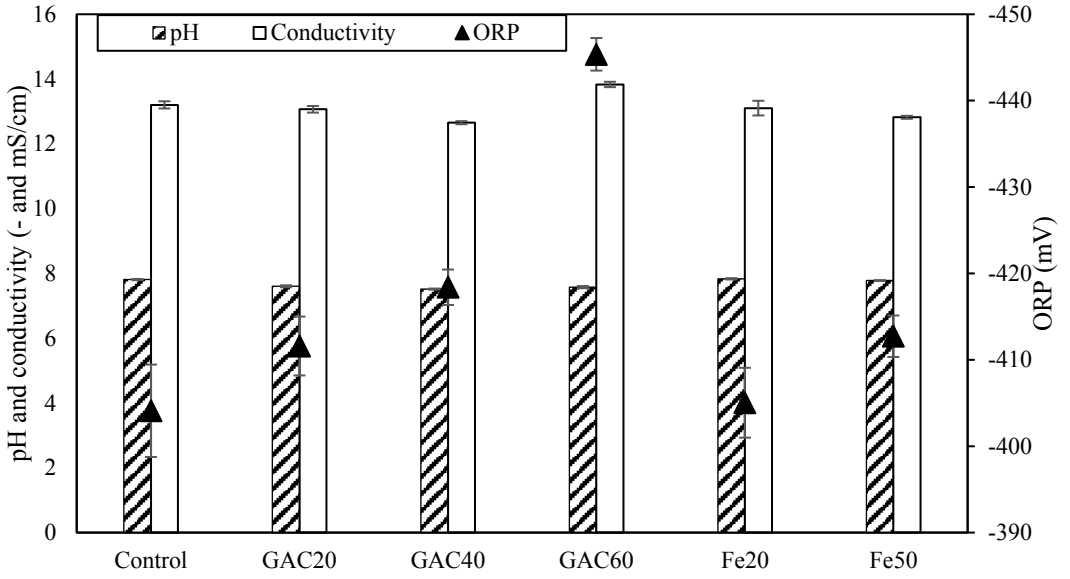

Figure 4.4. Final pH, electrical conductivity and ORP values in Set 2

pH which is an important operational parameter for AD was measured after the incubation of the reactors and the final pH level of each reactor is depicted in Figure 4.4. Final pH values ranged between 7.5-7.8, which is approximately neutral pH range indicating no significant acid accumulation. As reported in the literature, these pH values are between the optimum pH range which is 7.0-8.0 (Uçkun Kiran et al., 2016).

Electrical conductivity has also been measured in the reactor effluents (empty bars, Figure 4.4). The addition of GAC and hematite did not significantly change electrical conductivity values as compared to the control. Similarly, the addition of GAC did not change electrical conductivity in the reactors with GAC as compared to the control reactor when co-digestion of brewery waste activated sludge and food waste was performed (Johnravindar et al., 2020).

We also conducted final ORP measurement, which is an important parameter for the microbial activity of methanogens, and the results are depicted in Figure 4.4 (triangles). ORP values of GAC20, GAC40 and GAC60 are -412 ± 2 mV, -418 ± 2 mV and -445 ± 4 mV, respectively, which are slightly higher than ORP value of the

control (-404 ± 3 mV). Methanogenesis ideally occurs at ORP range of -200 mV to -400 mV (Martins et al., 2018). ORP values of the control and GAC reactors are not out of the range and only in the case of GAC60, ORP value was lowered considerably with respect to other reactors. Since more negative values of ORP is correlated with more effective methanogenesis as reported in the literature, GAC addition is presented as an applicable approach for more effective methanogenesis as it results in relatively lower ORP (Martins et al., 2018). It can be suggested that the addition of GAC on CM digestion creates only a slightly more suitable environment than conventional system based on ORP reduction; hence other impacts should be more significant. ORP values in the reactors having hematite are -405 ± 2 mV and -413± 2 mV in Fe20 and Fe50, respectively, which are very close to ORP value in the control. Since hematite is a metal-based CoM, it was expected that it may decrease ORP value to more negative values as occurred in GAC application, but it did not significantly change ORP values over the control.

Comparison of GAC and Hematite

The results of methane yields and kinetic parameters showed that the performance of AD of CM can be improved via GAC and hematite. Although there is an improvement in both GAC and hematite application, GAC showed a higher enhancement than hematite in both methane yield, methane production rate and decreasing the lag time of the process. For the amendment of GAC, the enhancement in methane production in general can be attributed to the supplementation of available surface are via GAC for microbial growth, the adsorption of toxic compounds which are inhibitory compounds for methanogens and provide an opportunity for DIET between microorganisms, which enables a faster and more effective electron transfer in the reactor (Johnravindar et al., 2020). In addition to these improvements in AD performance, it was also suggested that to elucidate the mechanisms of enhancement relevant controls with amendment of same size non-conductive materials is important (Martins et al., 2018).

For the application of hematite, it was mentioned that DIET mechanism for electron transfer between bacteria and methanogen can be a major reason for the enhancement in methane production with hematite application (Zhuang et al., 2015). Lu et al., (2019)explained that although iron can be used as trace element for metabolic activities, since the release of soluble iron was not observed, and it did not affect microbial communities. Within the presence of hematite, improvement in the secretion of extracellular polymeric substances (EPSs) can promote DIET (T. Lu et al., 2019). Also, they found that based on the analyses of functional genes, the addition of hematite improved methanogenesis rather than acetogenesis (Lu et al., 2019). It can be concluded that the application of hematite as CoM on AD of CM is another feasible way to improve AD performance. Since BM used in Set 1 contains $FeCl_2.4H_2O$, there is a Fe source for the system. Based on the calculation, due to BM addition in Set 1, 0.03 mM Fe was added to the reactors having BM in Set 1, but this is a considerable low concentration as compared to Fe concentrations of 20 mM and 50 mM due to hematite addition in Set 2. Therefore, it was suggested that this concentration due to BM did not have a significant impact on AD performance.

Among all reactors, it is obvious that the reactors amended with GAC improved AD performance at a higher rate than the reactor amended with hematite in terms of methane yield, organic removal, methane production rate and reduction in lag time. Among the reactors with GAC, GAC40 and GAC60 performed better than GAC20 in terms of methane yield, methane production rate and lag time. When GAC dosage was increased from 20 g/L to 40 g/L, methane yield was enhanced 4%, and the application of 20 g/L of GAC did not improve lag time. There was no significant difference between GAC40 and GAC60 in terms of methane yields but GAC40 decreased lag time of the control with a significant difference as compared to GAC60. Therefore, we continued the rest of the investigations with GAC at a dosage of 40 g/L.

4.3 Set 3: Enhancement of CM Digestion via GAC under Different Organic Loads and Mixing

In Set 3, the impact of the amendment of GAC under different organic loads were investigated within the presence and absence of mixing. Also, the reactors amended with sand were operated as a control to determine the impact of providing extra surface area for microbial attachment on the reactor performance in terms of methane production. Based on the results of Set 2, 40 g/L of dosage was used both for GAC and sand. Reactors were set according to the experimental design given in Table 3.9.

The impact on biomethane production

Cumulative methane production, organic removal (based on VS and COD) and methane yields (based on added amount of VS and COD) of reactors with F/M ratio of 1 and 3 reactors are depicted in Figure 4.5. Among the reactors with F/M ratio of 1 without mixing, the application of GAC increased cumulative methane production 12% and 42% in GAC1-no mix (611 ± 34 mL CH_4) over Control1-no mix (546 ± 6 mL CH_4) and Sand1-no mix (431 ± 14 mL CH_4), respectively (Figure 4.5a). Similarly, when mixing was applied, cumulative methane production in GAC1-mix reactor (682 ± 33 mL CH_4) was enhanced over Control1-mix (539 ± 12 mL CH_4). As opposed to no mixing, in the case of mixing Sand1-mix (571 ± 15 mL CH_4) reactor also produced 6% higher than control reactor (Figure 4.5a). In terms of percent methane in total produced biogas, for the reactors without mixing at F/M ratio of 1, the values are 38.3 ± 1.5%, 42.8 ± 3.0% and 52.4 ± 2.6% methane in AD1-no mix, GAC1-no mix and Sand1-no mix, respectively. When mixing was applied, the values for AD1-mix, GAC1-mix and Sand1-mix are 38.0 ± 0.6%, 42.8 ± 2.1% and 38.2 ± 0.8% methane, respectively. For the reactor at F/M ratio of 3, AD3-no mix, GAC3-no mix and Sand3-no mix had 36.9 ± 1.4%, 41.1 ± 0.9% and 45.3 ± 1.4% methane, respectively. When mixing was applied, the percent methane values in AD3-mix, GAC3-mix and Sand3-mix are 34.5 ± 0.7%, 35.7 ± 2.4% and 31.0 ± 0.5% methane, respectively.

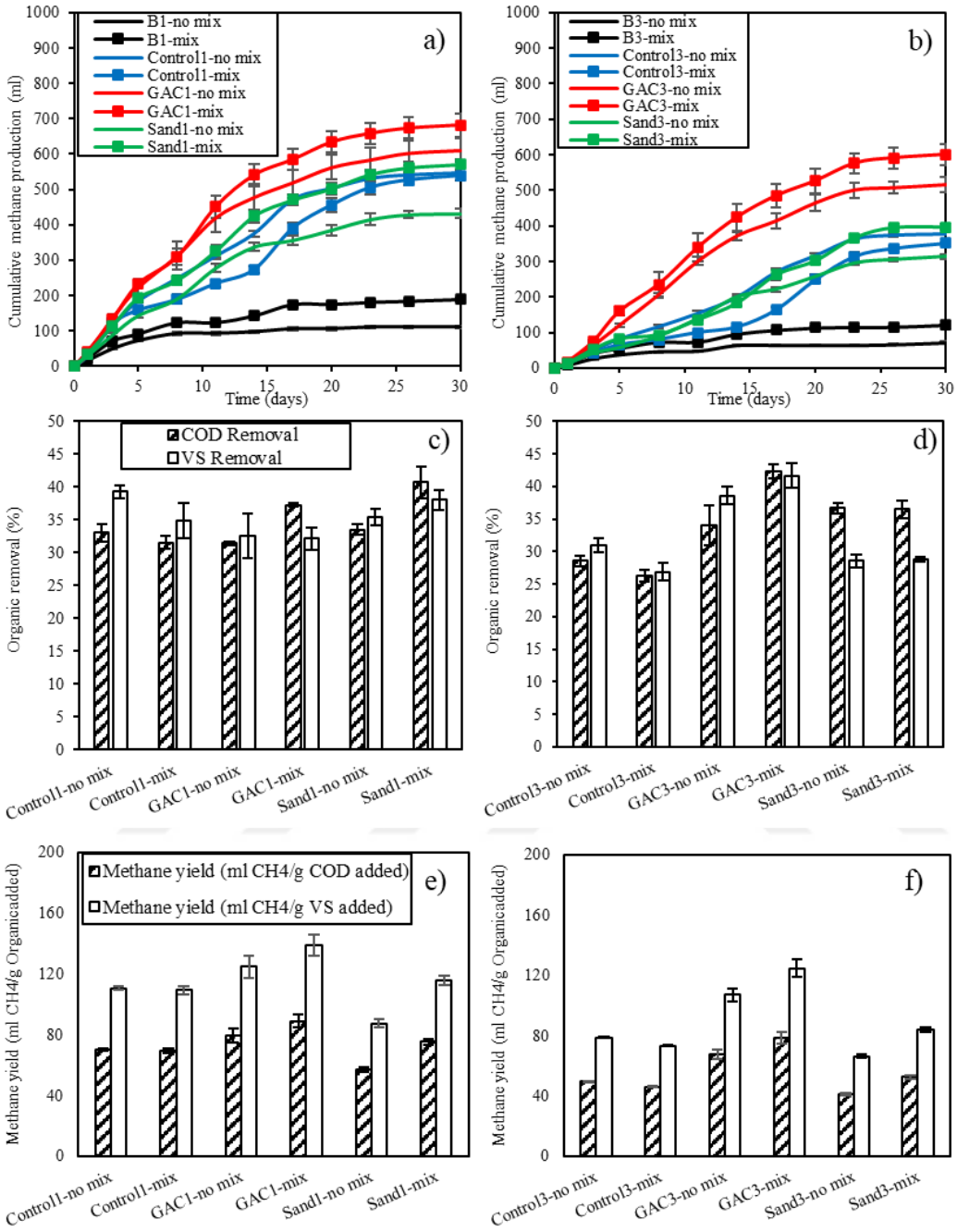

Figure 4.5. a)-b) Cumulative methane production for F/M of 1 and 3 reactors, c)-d) organic removal for F/M of 1 and 3 reactors and e)-f) methane yields for F/M of 1 and 3 reactors in Set 3

Similar to the reactors with F/M ratio of 1, GAC3-no mix (515 ± 22 mL CH_4) showed 36% higher methane than Control3-no mix (378 ± 1 mL CH_4) and 64% higher

methane than Sand3-no mix (314 ± 6 mL CH_4) (Figure 4.5b). Similar to F/M ratio of 1 when mixing was not applied; the application of sand caused a decrease in cumulative methane production. Cumulative methane production in GAC3-mix (601 ± 29 mL CH_4) reactor was 70% higher than Control3-mix (352 ± 2 mL CH_4) and 51% higher than Sand3-mix (397 ± 8 mL CH_4).

In terms of methane yields based on added VS for the reactor with F/M ratio of 1, the application of GAC increased the yield by 13% and 44% in GAC1-no mix (125 ± 7 mL CH_4/g VS_{added}) as compared to Control1-no mix (111 ± 1 mL CH_4/g VS_{added}) and Sand1-no mix (87 ± 3 mL CH_4/g VS_{added}), respectively (Figure 4.5e). Sand application decreased the yield in this case. With Sand1-mix around 6% increase in the yield (based on VS) was observed in comparison to control and in GAC1-mix around 28% increase in the yield was obtained over Control1-mix (109 ± 2 mL CH_4/g VS_{added}).

Among the reactors with F/M ratio of 3, the improvement in the yields is higher in the reactors with GAC compared to their corresponding controls as compared to the reactors with F/M ratio of 1 (Figure 4.5f). Methane yield based on added VS was increased by 35% in GAC3-no mix (107 ± 5 mL CH_4/g VS_{added}), but the yields decreased by 16% in Sand3-no mix (66 ± 1 mL CH_4/g VS_{added}) as compared to Control3-no mix (79 ± 0 mL CH_4/g VS_{added}). In GAC3-mix reactor methane yield was recorded as 125 ± 6 mL CH_4/g VS_{added}. This yield is 71% higher than Control3-mix (73 ± 0 mL CH_4/g VS_{added}) and 49% higher than Sand3-mix (84 ± 2 mL CH_4/g VS_{added}).

Among the reactors with F/M ratio of 1, in terms of VS removal, the removals are ranging 32%-39% with the highest removal was recorded in GAC1-mix and the lowest removal was recorded in Sand1-mix reactors (Figure 4.5c).

For the reactor with F/M ratio of 3, VS removals are ranging 29%-42% with the highest VS removal in GAC3-mix. A similar finding was observed by the fact that the addition of magnetite as CoM enhanced COD removal as compared the addition

of silica as non-conductive material especially at higher organic loadings (Wang et al., 2020).

Among the reactors with F/M ratio of 1, R^2 values are ranging 0.9781-0.9948 implying that the experimental data are well fitted to the model data (Table 4.6). The cumulative methane production graphs showing experimental data and the model data are shown in Appendix D. GAC amendment enhanced the methane production rate in GAC1-no mix by 33% when compared to Control1-no mix. When mixing was applied, the addition of GAC improved the rate in GAC1-mix by 96% in comparison to the control. Further, Sand1-mix reactor also showed around 42% increased methane production rate in comparison to control. In terms of lag time, there was no difference among the reactors as F/M ratio of 1.

Table 4.6. The results of kinetic parameters calculated from Gompertz modeling for the reactors in Set 3

	P (mL)	R_m (mL CH_4/day)	λ (d)	R^2
Control1-no mix	571.2 ± 5.6	31.2 ± 0.5	0.2 ± 0.1	0.9893
Control1-mix	651.9 ± 9.1	23.0 ± 0.8	0.1 ± 0.1	0.9781
GAC1-no mix	608.1 ± 27.5	41.6 ± 4.8 (33%)	0.3 ± 0.0 (-)	0.9939
GAC1-mix	690.4 ± 28.1	45.1 ± 4.0 (96%)	0.6 ± 0.2 (-)	0.9948
Sand1-no mix	438.0 ± 13.7	26.8 ± 1.2 (-)	0.3 ± 0.1 (-)	0.9932
Sand1-mix	588.5 ± 12.4	32.6 ± 2.0 (42%)	0.2 ± 0.2 (-)	0.9818
Control3-no mix	441.4 ± 2.7	18.6 ± 0.8	2.1 ± 0.5	0.9907
Control3-mix	577.9 ± 29.4	15.3 ± 0.4	4.6 ± 0.5	0.9732
GAC3-no mix	529.5 ± 21.4	32.4 ± 1.5 (74%)	1.7 ± 0.1 (19%)	0.9979
GAC3-mix	621.1 ±19.1	36.2 ± 4.3 (137%)	1.4 ± 0.1 (70%)	0.9969
Sand3-no mix	344.1 ± 10.0	16.3 ± 0.2 (-)	2.2 ± 0.2 (-)	0.9953
Sand3-mix	507.7 ± 15.8	18.1 ± 0.5 (18%)	2.8 ± 0.3 (39%)	0.9877

The number in the parenthesis indicates the enhancement in methane production rate and decrease in lag time as compared to the corresponding control.

For the reactors with F/M ratio of 3, R^2 values are ranging from 0.9732 to 0.9979 indicating that there is a good correlation between experimental data and the model data (Table 4.6). At F/M of 3, GAC increased methane production rate by 137% under mixing condition in GAC3-mix and by 74% under no mixing condition in GAC3-no mix. Again, only in mixed reactors surface area provided an increase in methane production rate but it was limited to 18%, showing that most of the contribution to increased methane production rate can be attributed to the presence

of GAC and not only due to providing extra surface area. In terms of lag time, similar trends observed in methane production rate were obtained. GAC decreased the lag time 19% in GAC3-no mix compared to Control3-no mix. The highest decrease was attained by 70% in GAC3-mix reactor in comparison to the Control3-mix.

Comparison of amendment of non-conductive particles and GAC particles

In each condition in terms of performance parameters, the improvement in the reactor with GAC was higher than the reactor amended with sand. Similar finding was observed in another work, where GAC amendment increased methane production rate to a higher extent than non-conductive ceramic particles addition during ethanol oxidation by *Geobacter* (Mei et al., 2018). In another study, the enhancement in GAC application on dog food digestion was higher than the enhancement in polyester cloth as non-CoM (Lei et al., 2016). Similarly, (S. Zhang et al., 2017) investigated the effect of GAC as CoM and zeolite as non-CoM on acetate oxidation and found that methane production was enhanced more via GAC than zeolite application. Additionally, it was found that the addition of high-density polyethylene (HDPE) as non-CoM on acetate oxidation did not improve the methane yields as much as modified graphite improved (J. Liu et al., 2020).

As mentioned, the application of GAC and sand had different impacts on AD of CM for both F/M ratios (Table 4.5). For the reactors with F/M ratio of 1, the application of GAC provided 55% and 38% higher improvement for methane production rate in GAC1-no mix and GAC1-mix as compared to Sand1-no mix and Sand1-mix, respectively. The improvement in the rate via GAC was also higher than sand addition among the reactors with F/M ratio of 3. GAC resulted in 99% and 100% higher increase in the rate than sand application under both no mixing and mixing conditions, respectively. Although biomass formation on GAC and sand particles may attribute to the enhancement over conventional AD, the significant difference between GAC and sand may not only be explained by biomass formation. Faster methane production via GAC amendment can be attributed to more effective interspecies electron transfer with DIET mechanism. Since there is no need for the

production of intermediate products such as H_2 or acetate as in MIET, DIET via GAC may provide faster and more effective electron transfer between syntrophic bacteria and methanogens. As a result of this phenomenon, electrons can be transferred faster between microorganisms and higher methane production is observed per unit time. Similar finding was observed by (J. Liu et al., 2020). They found that methane production rate was enhanced more with the application of graphite as CoM as compared to the enhancement via HDPE as CoM over the control. Other mechanisms of improvement in AD performance via GAC amendment may be adsorption of inhibitory compounds and further reduction in ORP (J. H. Park, Kang, et al., 2018). The former point is hard to elucidate, to this purpose we have measured ammonium concentrations as it is a common inhibitory product during AD of animal wastes. To investigate the latter we have analyzed ORP in each reactor as discussed later.

From the point of the lag time, the enhancements via GAC were higher than sand application as compared to the controls (Table 4.5). Although there is no lag time therefore no improvement among the reactors with F/M ratio of 1, the lag time was decreased via GAC application more than sand addition for the reactors with F/M ratio of 3 under mixing condition. 100% increase in decrease of the lag time was obtained via GAC in GAC3-mix as compared to Sand3-mix. These results suggest that electron transfer via DIET mechanism within the presence of GAC as CoM is faster than MIET mechanism via H_2 and acetate (Namal, 2020). Zhang et al., (2017) was also found that the addition of GAC showed shorter lag time than sand application for acetate oxidation. Similarly, the addition of GAC as CoM shortened the lag time of the reactor more than the amendment of polyester cloth as non-CoM on AD of dry organic fraction of municipal solid waste (Dang et al., 2017).

These results indicate that the improvement in methane production on AD of CM can be attributed to the enrichment of electro active microorganisms with GAC. In GAC amended reactors it may behave as an electron conduit between bacteria and methanogen, providing an opportunity for DIET. Although the surface area provided by GAC particles is not the only reason behind the improvement, the porous structure

of GAC may provide larger specific areas for biomass attachment than sand particles, and it can also contribute the improvement in methane production.

Effect of different F/M ratios

Organic loading is an important parameter for AD. For batch systems, F/M ratio is used to mimic organic loading. In Set 3 mostly the reactors with F/M ratio of 1 had higher methane yields than the corresponding reactor with F/M ratio of 3. The interesting part of our finding is that the addition of GAC with F/M ratio of 3 under mixing condition (GAC3-mix) compensated the decrease in methane yield from Control1-mix to Control3-mix. When F/M ratio was increased from 1 to 3, methane yield in Control1-mix (109 ± 2 mL CH_4/g VS_{added}) decreased to 73 ± 0 mL CH_4/g VS_{added} in Control3-mix because of slower methanogenic activity as compared to organic decomposition. With the addition of GAC at F/M ratio of 3 under mixing condition, GAC3-mix showed methane yield of 125 ± 6 mL CH_4/g VS_{added} which is in fact 15% higher than Control1-mix. This result indicate that more waste can be processed in the same reactor set-up without any reduction in the yield via amendment of GAC to a conventional AD reactor. Eventually, operation with the same methane yield but at a higher F/M ratio may translate into a significant saving in large scale application with shorter hydraulic retention time. For the reactors under no mixing condition, this compensation was not observed. Similarly, Xu et al., (2015) indicated that the addition of GAC enhanced methane production from AD of synthetic brewery wastewater as compared to control reactor when organic loading was increased from 2.9 g COD/L/d to 5.8 g COD/L/d in lab scale upflow anaerobic digesters. In another study, it was found that the application of carbon cloth as CoM on AD of leachate from municipal solid waste plant maintained the methane production with increasing organic loading (from 36.8 g COD/L/d to 49.4 g COD/L/d) although methane production rate was decreased in the control (Lei et al., 2016). Similar finding was stated by Zhao et al., (2015). They observed that the enhancement via GAC in methane production rate was increased when organic loading rate was increased from 4 to 12 kg COD/m^3/day on ethanol degradation as compared to the control.

Although the addition of GAC and sand enhanced methane production rate under both mixing and no mixing conditions, GAC application among the reactors with F/M ratio of 3 increased the rate more than GAC application for the reactor with F/M ratio of 1.

From our results and the literature, it can be implied that the addition of GAC as CoM can help the reactor to resist high organic loadings for the process performance. With the applicability of high organic loading, it can be also possible to have small footprints of the reactors without any decrease or inhibition during AD of CM via GAC amendment.

Effect of mixing

Mixing is another important parameter for an effective AD performance since it affects the contact between microorganisms and substrates and stability of microorganisms (Shekhar Bose et al., 2021). Mixing in AD controls did not change the methane yields; similar methane yields were attained in Control1-no mix and Control1-mix at F/M ratio of 1 and Control3-no mix an Control3-mix at F/M ratio of 3. On the other hand, the application of mixing increased methane yield in GAC added reactors. Among the reactors with F/M ratio of 1, mixing enhanced methane yield 11% for GAC application as compared to no mixing condition, respectively. Similarly, at F/M ratio of 3, 17% improvement in methane yield were observed in GAC3-mix as compared to GAC3-no mix. This can be attributed to continuous motion of biofilm on GAC particles to reach carbon source easily with mixing. Our results suggest that the application of mixing is an effective approach to enhance methane yield from AD of CM with the presence of GAC as CoM.

In terms of methane production rate, the mixing had also different impacts on AD of CM for the control and the reactor with GAC. The application of mixing caused 26% and 18% decrease in methane production rate of the control in Control1-mix and Control3-mix as compared to Control1-no mix and Control3-mix, respectively. This can be attributed to the morphological deterioration of microorganisms, especially for some methanogens. On the other hand, mixing was increased the rates for the

reactor having GAC. For the reactors with F/M ratio of 1, methane production rates were increased 8% in GAC1-mix over GAC1-no mix. Conformably, the rate was enhanced 12% in GAC3-mix over GAC3-no mix with the application of mixing for the reactor with F/M ratio of 3.

For the lag time of the reactors, since there is no lag time observation for F/M ratio of 1 operation, we did not see any effect of mixing on lag time for the reactors with F/M ratio of 1. On the other hand, the application of mixing shortened the lag time 18% in GAC3-mix over GAC3-no mix, although it did not further decrease the lag time in the control at F/M ratio of 3.

The impact on electro-active biofilm formation

The results of CV analysis for each set of the reactors are given in Figure 4.6. Among the reactors with F/M ratio of 1 under no mixing condition, the application of GAC and sand (GAC1-no mix and Sand1-no mix) showed similar reduction peaks which are bigger than the reduction peak observed in CV curve of Control1-no mix (Figure 4.6a). The difference between the peak heights were even more visible under mixing, which may be interpreted as an indication of higher activity of electro-active microorganisms present in these reactors (Figure 4.6b). The first derivative is calculated to find the reduction peak which is observed around -0.5 V vs. Ag/AgCl. This reduction peak point in CV voltammograms is in the range of carbon dioxide reduction to methane (Y. Li et al., 2017); which may be possible via DIET (Kutlar et al., 2022).

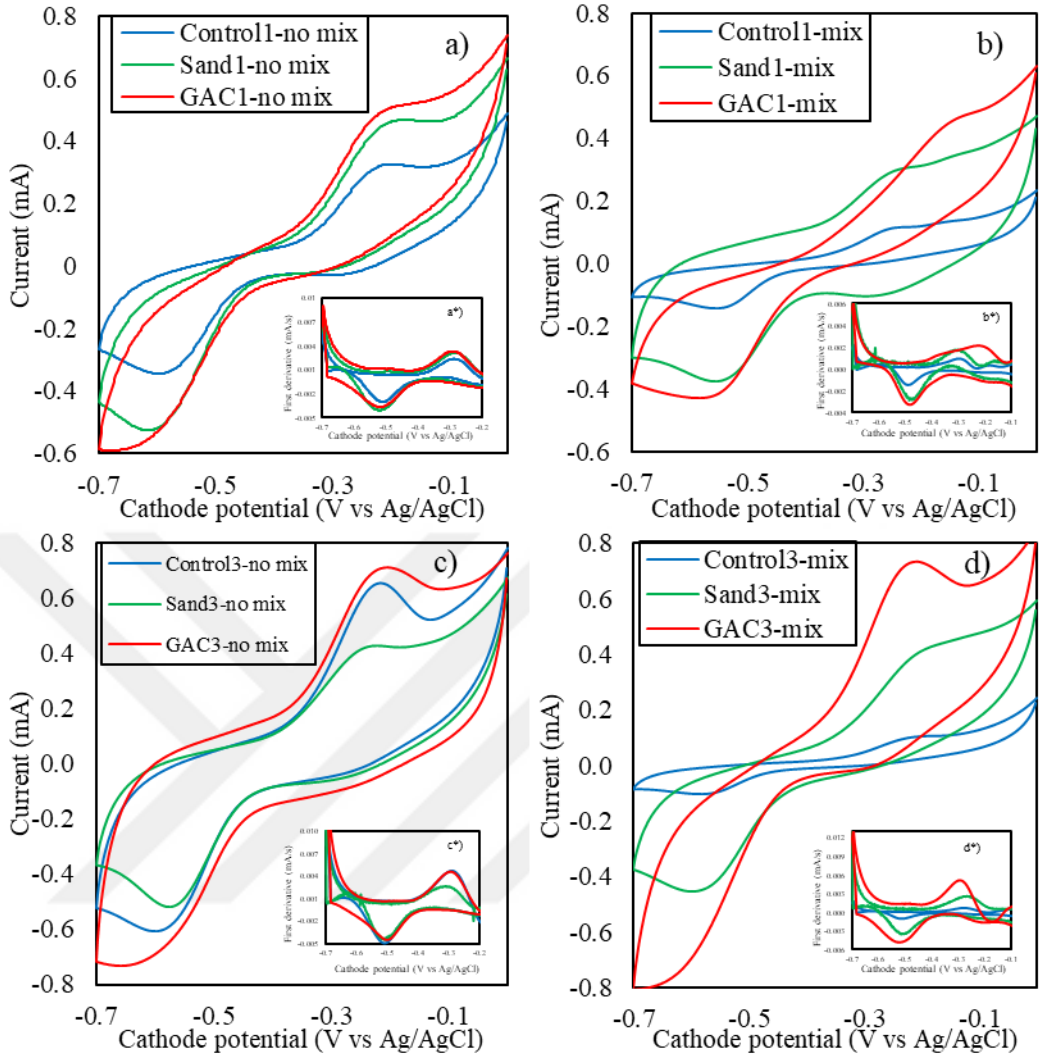

Figure 4.6. Cyclic voltammetry analysis of F/M 1 reactors under a) no mixing and b) mixing and F/M 3 reactors under c) no mixing and d) mixing (inset 1st derivative of CV results)

For the reactor with F/M ratio of 3, under no mixing GAC added and sand added reactors showed higher reduction and oxidation peaks over Control (Figure 4.6c). Under mixing condition at F/M ratio of 3, the reduction and oxidation peaks in GAC3-mix are clearly bigger than Control3-mix and Sand3-mix (Figure 4.6d). Also, sand application showed clear improvement over the control (Control3-mix) in terms of the reduction and oxidation peaks.

As mentioned in the literature, the redox peaks observed on CV suggest potential reduction of carbon dioxide to methane biologically via DIET mechanism (Lee et al., 2016). The results of CV analysis imply that GAC amendment on AD of CM significantly had impact on electro activity and electro active biofilm formation. GAC application on AD may promote more effective DIET mechanism for methane production than the control and sand application. Also, the application of sand showed an indication of DIET mechanism probably by providing a biofilm formation on sand particles. Similarly, as Li et al., (2017) stated the oxidation peaks observed in CV voltammograms of the reactors with GAC matched with the range of volatile organic acid oxidation by exoelectrogens such as *Geobacter* having the ability of giving electron outside the cell. Also, reduction peaks in CV voltammograms of the reactors with GAC fell into the range of carbon dioxide reduction to methane (Y. Li et al., 2017). The size of oxidation and reduction peaks imply the more oxidation and reduction substance to be used in the system (Sun et al., 2021). This indicates the amounts of reduction and oxidation active substances in the reactor with GAC are clearly more than the control and the reactors with sand. These results are clear indications for evidence of potential DIET mechanism provided by the amendment of GAC as CoM on AD of CM.

In addition to CV voltammograms, first derivatives of CV voltammograms were analyzed as shown in Figure 4.6. For the operation under mixing condition at both F/M ratios of 1 and 3, the application of GAC showed the highest peak for the first derivative than the control and the reactors with sand. For no mixing operation, the application of GAC and sand had the reduction peaks bigger than the controls. The location of the reduction peak in the first derivative of CV voltammograms (ca. approximately -0.5 V vs. Ag/AgCl) is an indication of biological methane production from carbon dioxide reduction (Fu et al., 2015).

VFA concentrations in Set 3 reactors

For the reactors with F/M ratio of 1 under no mixing condition, acetic acid concentration peaked in 2nd week in each set (Control1-no mix, Sand1-no mix and

GAC1-no mix) with the highest value of 1785 ± 159 mg/L in GAC1-no mix (Figure 4.7a). Although rapid degradation of acetic acid was observed in GAC1-no mix and Control1-no mix in 3rd week, Sand1-no mix showed significant acetic acid degradation in 4th week. It can be because of high propionic acid and butyric acid concentrations during 1st week in Sand1-no mix. Under mixing condition, Control1-mix had higher acetic acid concentrations in 1st and 2nd week over GAC1-mix and Sand1-mix. Although it was produced during 1st week and peaked, since it was not degraded properly probably higher propionic and butyric acid concentrations in Control1-mix, acetic acid concentration was still the highest in Control1-mix. GAC1-mix showed the peak concentration of acetic acid, butyric acid and propionic acid in 1st week, and they were degraded properly in the following weeks. VFA degradation was positively affected under mixing condition, especially in GAC1-mix. In GAC1-mix, all VFAs concentrations were peaked in 1st week, and they were degraded, but the time for reaching the peak concentration of all VFAs was retarded in GAC1-no mix. As stated in literature, the highest acetic acid concentration was 1785 ± 159 mg/L in GAC1-no mix that is less than 2000 mg/L mentioned as inhibitory level (Mawson et al., 1991). Beyond this concentration, propionic acid degradation can retard, and overall system performance can be affected due to propionic acid accumulation (Mawson et al., 1991).

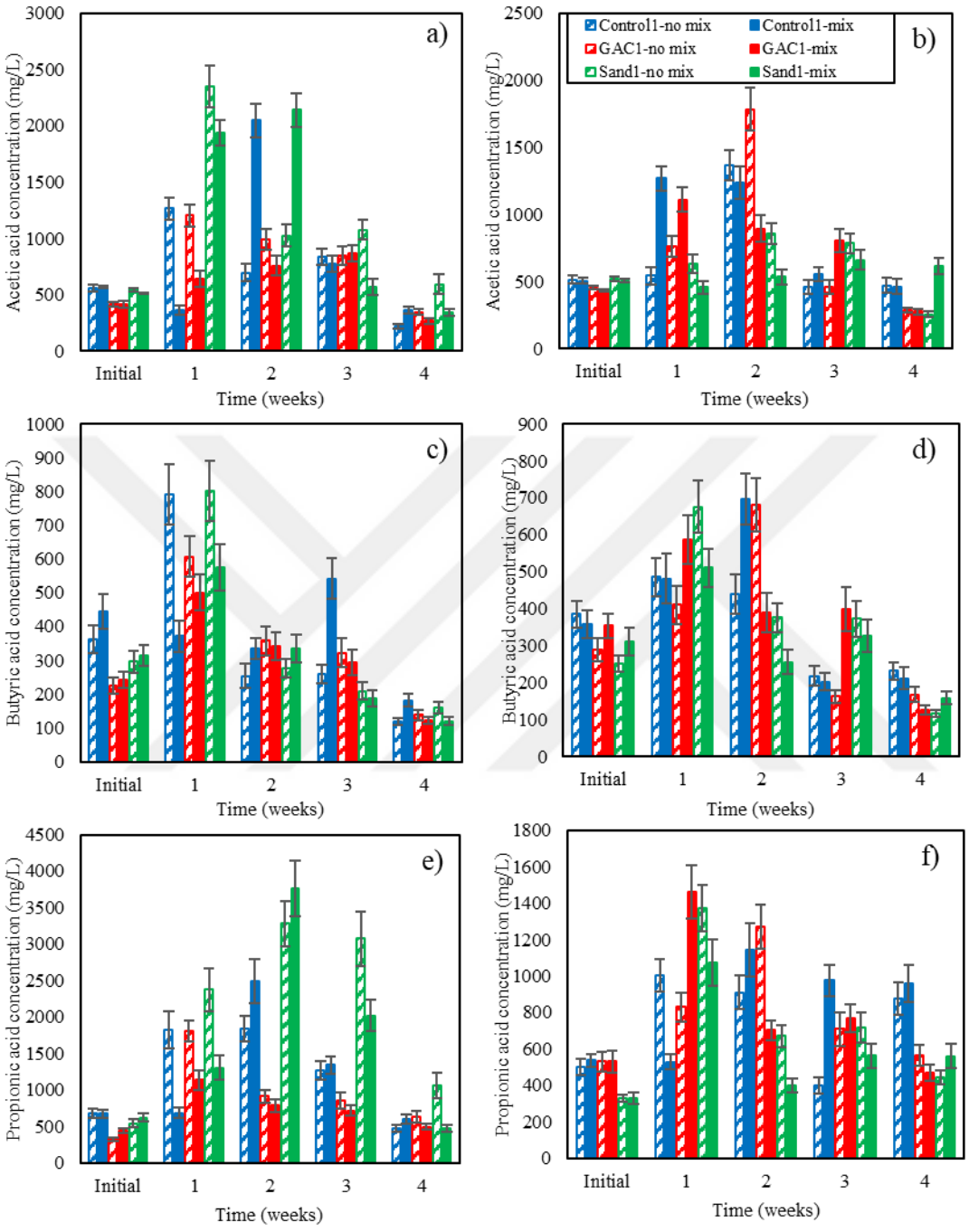

Figure 4.7. a)-b) acetic acid concentrations for F/M of 1 and 3 reactors, c)-d) butyric acid concentrations for F/M of 1 and 3 reactors and e)-f) propionic acid concentrations for F/M of 1 and 3 reactors in Set 3

Among the reactors with F/M ratio of 3 under no mixing condition, the peak concentrations of acetic acid and propionic acid in Control3-no mix, GAC3-no mix and Sand3-no in 1st week (Figure 4.7b). Although the degradation of VFAs was rapid in Control1-no mix and GAC1-no mix for the first 3 weeks, Sand3-no mix showed higher VFA concentrations in each week than Control3-no mix and GAC3-no mix. Under mixing condition, GAC3-mix showed lower VFA concentrations than Control3-mix and Sand-mix in each week. Although final acetic acid concentrations are not in the inhibitory level, in 1st and 2nd week, acetic acid concentrations were higher than 2000 mg/L which is inhibitory level in Sand3-no mix and Sand3-mix, respectively. As stated in the literature, this can cause the retard of propionic acid degradation, and it was observed by the fact that propionic acid concentrations were highest in Sand3-no mix and Sand3-mix in 1st and 2nd week, respectively (Mawson et al., 1991). Total VFA profiles for both reactors with F/M ratio of 1 and 3 are given in Figure 4.8.

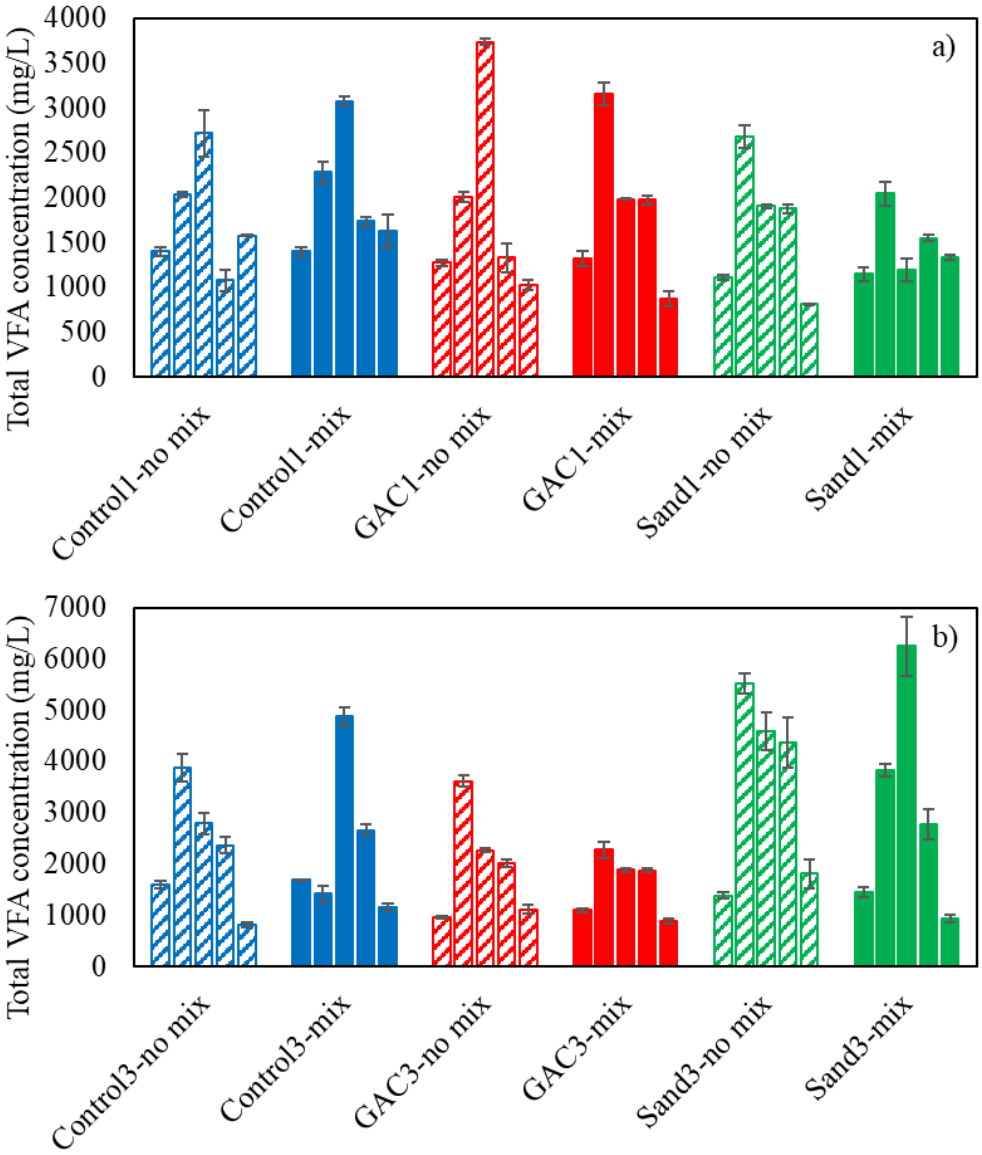

Figure 4.8. Total VFA profiles of the reactors with a) F/M 1 and b) F/M 3 in Set 3

The impact on pH, electrical conductivity and ORP results

After the operation of the reactors, pH of reactor effluents was measured, and the results are depicted in Figure 4.9. Among the reactors with F/M ratio of 1, pH values are ranging 7.3-7.5 which is between the suitable range of 7.0-8.0 for methanogenic activity as mentioned in the literature (Uçkun Kiran et al., 2016). For the reactors

with F/M ratio of 3, pH of 7.2 and 7.6 are the boundary values and these are also in the range of the safe zone as mentioned. Since the pH values of the reactors are not out of the neutral pH range and below 6.0, it can be suggested that there is no acid accumulation which can inhibit methanogenic activity.

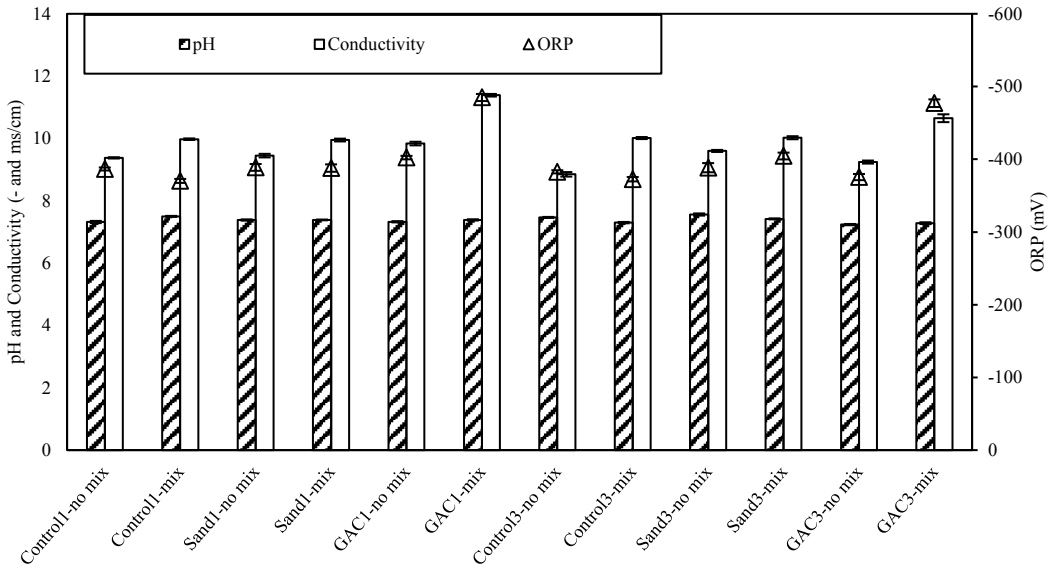

Figure 4.9. Final pH, electrical conductivity and ORP values in Set 3

In terms of electrical conductivity (Figure 4.9) there is no significant difference among the reactors with F/M ratio of 1. GAC1-mix had the highest electrical conductivity value of 11.4 ± 0.0 mS/cm. Among the reactors with F/M ratio of 3, the highest electrical conductivity value was observed in GAC3-mix (10.7 ± 0.1 mS/cm).

We also measured ORP for each reactor as one of the important parameters for methanogenic activity, and the results are given in Figure 4.9. Among the reactors with F/M ratio of 1, GAC1-mix showed the lowest ORP value with -485 ± 5 mV. Except from GAC1-mix, ORP values are ranging from -370 ± 3 mV to -402 ± 2 mV for the reactor with F/M ratio of 1. Among the reactors with F/M ratio of 3, ORP values are ranging from -373 ± 3 mV to -477 ± 5 mV, and the lowest values belongs to GAC3-mix. As mentioned before, more negative values represent more suitable environment for methanogenic activity. As stated in Martins et al. (2018), the

addition of CoM resulted in a more negative ORP values both for the reactor with F/M ratios of 1 and 3.

As shown in Figure 4.8, the highest ORP and electrical conductivity values are obtained in GAC1-mix at F/M ratio of 1 and GAC3-mix at F/M ratio of 3. Among the reactor at F/M ratio of 1, the average ORP and electrical conductivity values are -387 ± 10 mV and 9.7 ± 0.3 mS/cm except from GAC1-mix, and ORP and electrical conductivity values are -485 ± 5 mV and 11.4 ± 0.0 mS/cm GAC1-mix that is quite higher than others. Similarly for F/M ratio of 3, the average ORP and electrical conductivity values except from GAC3-mix are -385 ± 11 mV and 9.5 ± 0.5 mS/cm, but these values are -477 ± 5 mV and 10.7 ± 0.1 mS/cm in GAC3-mix. Among the reactors with F/M ratio of 1 and 3, the highest methane yields and methane production rates were obtained in GAC1-mix and GAC3-mix that is correlated with ORP and electrical conductivity values in these reactors.

The impact of additives on nutrient concentrations

Among the reactor with F/M ratio of 1, the highest ammonium concentration was observed in GAC1-mix with 1438 ± 42 mg NH_4-N/L which is 25% and 38% higher than Control1-mix (1149 ± 16 mg NH_4-N/L) and Sand1-mix (1045 ± 22 mg NH_4-N/L), respectively (Figure 4.10). For the reactors with F/M ratio of 3, final ammonium concentrations are ranging 936 ± 42 – 1074 ± 28 mg NH_4-N/L with small differences. Since, ammonium concentrations are not higher than the inhibition level that was stated as 3000 mg NH_4-N/L, ammonium inhibition was not observed in the reactors (Krakat et al., 2017).

For final phosphorus measurement, Control1-no mix (35 ± 0.6 mg PO_4-P/L) and Sand1-no mix (35 ± 1.9 mg PO_4-P/L) had the highest final phosphorus concentrations among the reactors with F/M ratio of 1 (Figure 4.10). Except from Control1-no mix and Sand1-no mix, final phosphorus concentrations ranged between 19-28 mg PO_4-P/L. Among the reactors F/M ratio of 3, Sand3-mix had the highest final phosphorus concentration with 36 mg PO_4-P/L, and the lowest value belongs to Control3-mix (14 ± 0.4 mg PO_4-P/L). Except from Sand3-mix and

Control3-mix, final phosphorus concentrations are ranging 21 ± 0.7 – 28 ± 0.9 mg PO_4-P/L for F/M ratio of 3. These levels are certainly below any inhibitory concentrations (R. Wang et al., 2015).

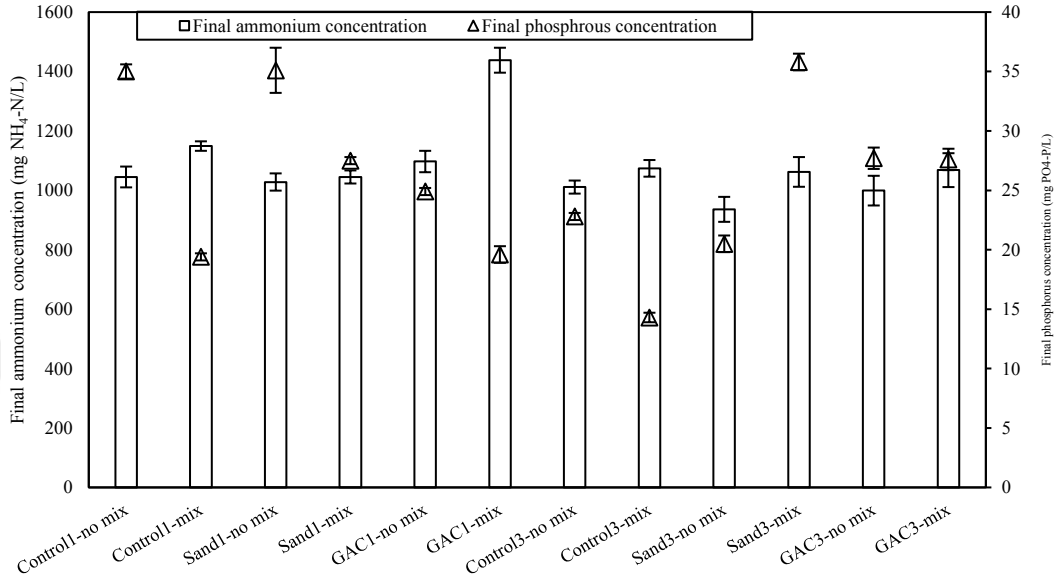

Figure 4.10. Final ammonium and phosphorus concentrations in Set 3

4.3.9 Struvite Precipitation from the Reactor Effluents (Set 3)

The results of struvite precipitation experiment are shown in Table 4.7 for each group (AD, GAC and Sand). The removal from the mixture of effluent sample (GAC, Sand and AD), WMD, and bone meal are given in Table 4.7. In terms of nutrient recovery, phosphorus removals are similar for each group. For ammonium removal, Sand group showed highest removal and AD group had the lowest ammonium removal.

Table 4.7. The results of struvite precipitation in terms of N&P removals and the amount of struvite precipitated in Set 3

Group	PO_4-P removal (%)	NH_4-N removal (%)	Product (g struvite/ml sample)
AD	97.4 ± 0.8	82.5 ± 0.4	0.036 ± 0.001
Sand	97.2 ± 0.5	92.0 ± 0.6	0.034 ± 0.002
GAC	96.6 ± 0.6	83.4 ± 0.3	0.027 ± 0.001

In order to be sure that the precipitates are struvite, they were analyzed with XRD technique as stated in Section 3.2. From the results of XRD analysis of the samples (Figure 4.11), the precipitates were determined as struvite. For clear comparison of the amount of struvite precipitation, the amount was normalized based on total volume of the sample (the mixture of effluent, waste magnesite dust and bone meal). GAC group had the lowest amount of precipitation. In AD and Sand groups, 33% and 26% more struvite than GAC group was precipitated, respectively. From the results it was strongly suggested that struvite precipitation as downstream treatment of wastes and nutrient recovery from reactor effluents can be an effective approach especially for AD operation, although the amendment of GAC caused a slight decrease in struvite precipitation.

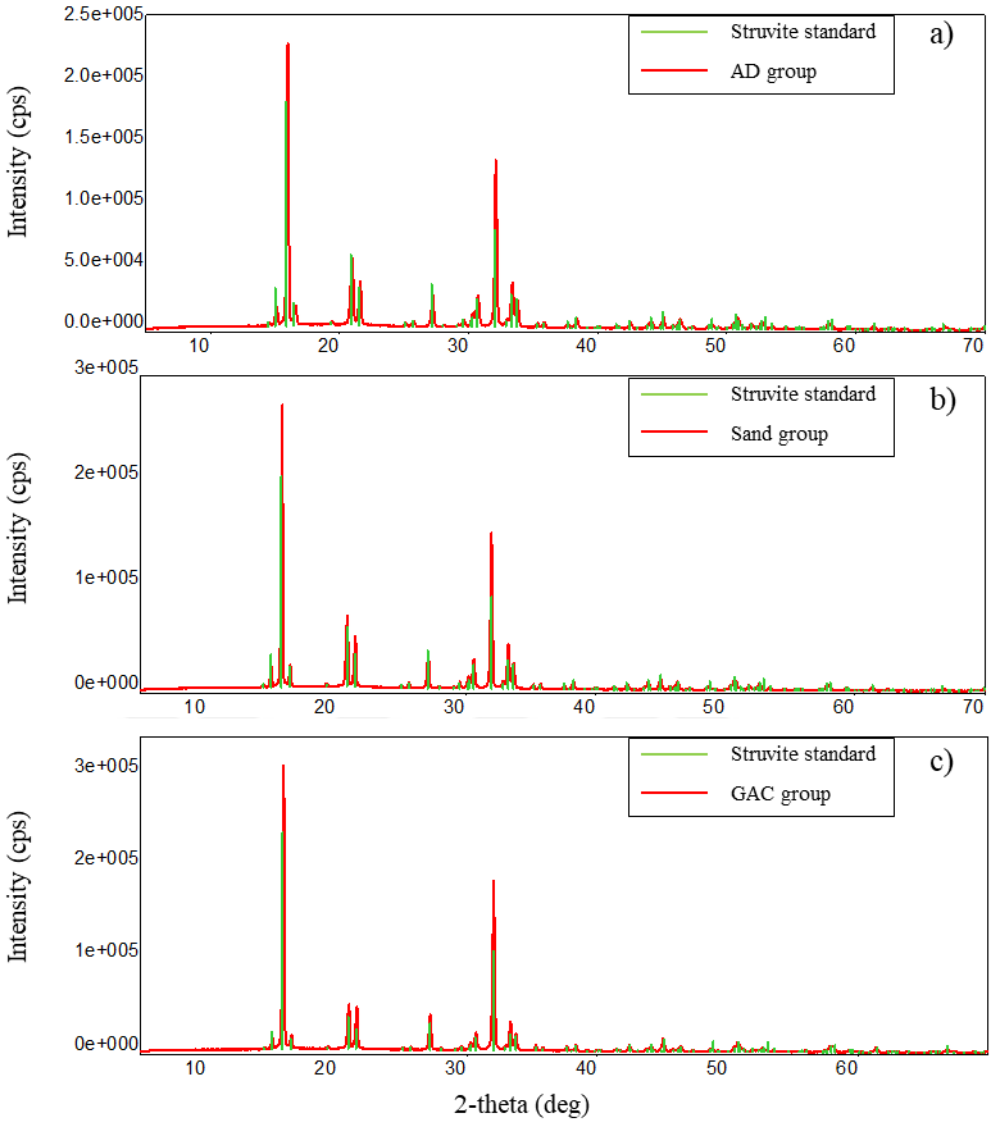

Figure 4.11. XRD analysis of the precipitate collected from the a) AD, b) Sand and c) GAC groups

4.4 Set 4: The Impact of GAC & BioGAC Amendment on Psychrophilic AD of CM under Different Organic Loads

In Set 4, the impact of the amendment of bare GAC and BioGAC on AD of CM at psychrophilic temperature two different F/M ratios of 1 and 3 was investigated. Similar to Set 3, 40 g/L of GAC were used. The experimental design for Set 4 is given in Table 3.10. Before setting the reactors for this set the stages of the acclimation of inoculum to psychrophilic temperature and the biofilm formation on GAC particles were conducted.

Acclimation of Inoculum to Psychrophilic Temperature

The inoculum from a mesophilic anaerobic digester in the WWTP was acclimated to psychrophilic temperature by feeding with filtered CM. During the acclimation period, methane production was monitored with GC, and a new cycle was started when cumulative methane production as compared to previous measurement was less than 10% for two times. The operation of the acclimation lasted three cycles (total 37 days), and cumulative methane production in each cycle was shown in Figure 4.12 After this stage, the inoculum was accepted as ready to be used for Set 4.

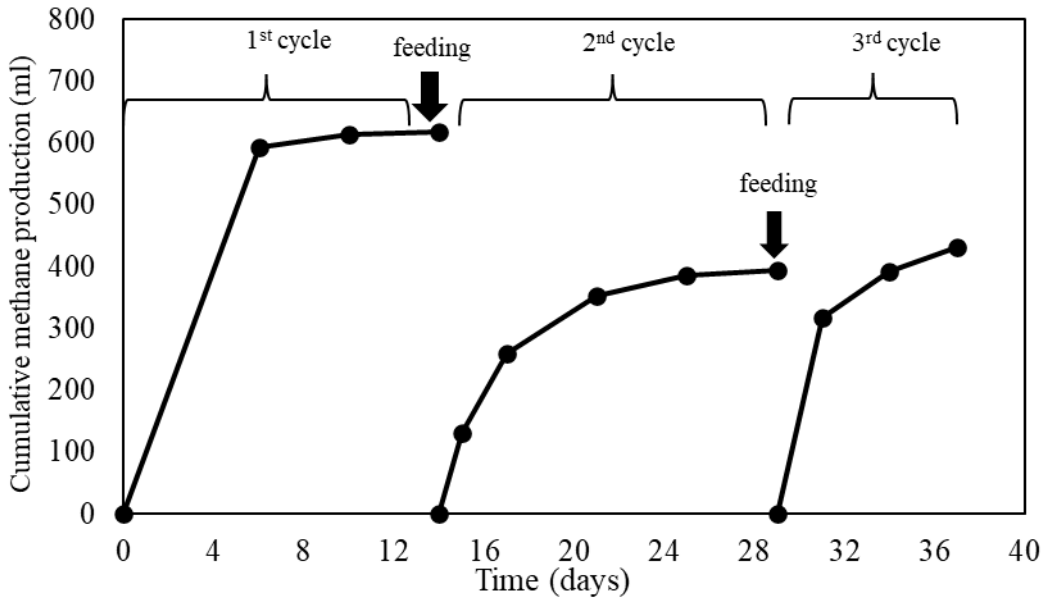

Figure 4.12. Cumulative methane production during the acclimation period

Biofilm Formation on GAC Particles

In order to obtain biofilm attached GAC (BioGAC), the reactors with a working volume of 150 ml and 6 replicates were supplied with 40 g/L of GAC and operated with addition of filtered CM as carbon source prior to start of Set 4. Methane production of the reactors were monitored periodically and when cumulative methane production as compared to previous measurement was less than 10% for two times, new cycle was started by feeding. The operation of the acclimation lasted for two cycles, and cumulative methane production in each cycle is shown in Figure 4.13. At the end of this stage, biofilm attached GAC were taken out of these reactors inside the anaerobic glovebox and were transferred to the reactors of Set 4.

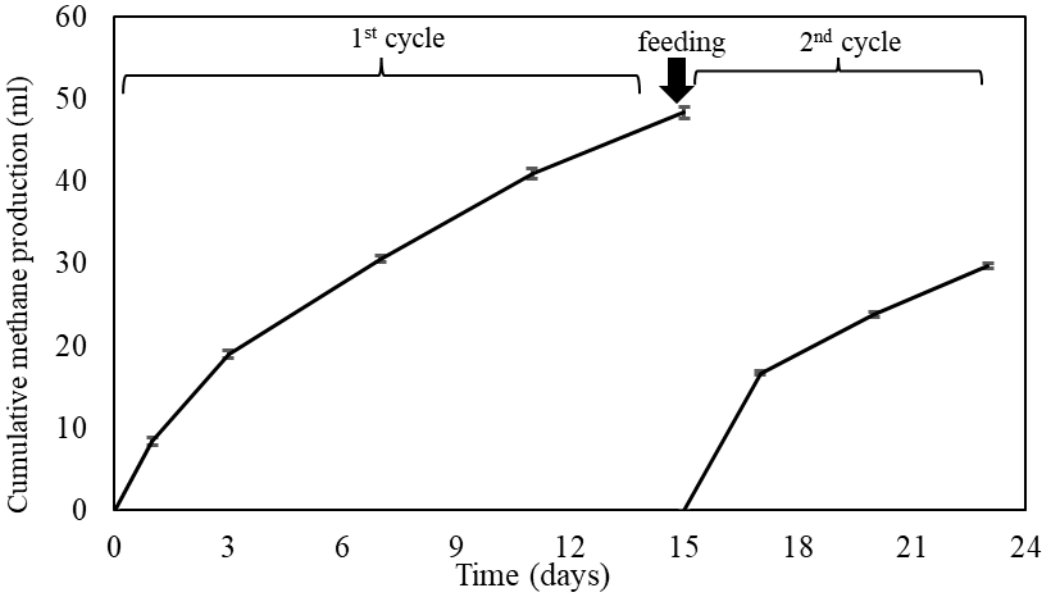

Figure 4.13. Cumulative methane production for biofilm formation reactors

During the operation of the reactors in the scope of Set 4, the temperature was monitored with a data collector (RC-4, Elitech), and the change in temperature during the operation is shown in Figure 4.14. According to the temperature profile during the incubation period, the average temperature was 18.1 ± 1.2 °C. The average temperature value confirmed the application of psychrophilic operation, and this temperature value was used in cost-revenue analysis for the comparison with mesophilic temperature.

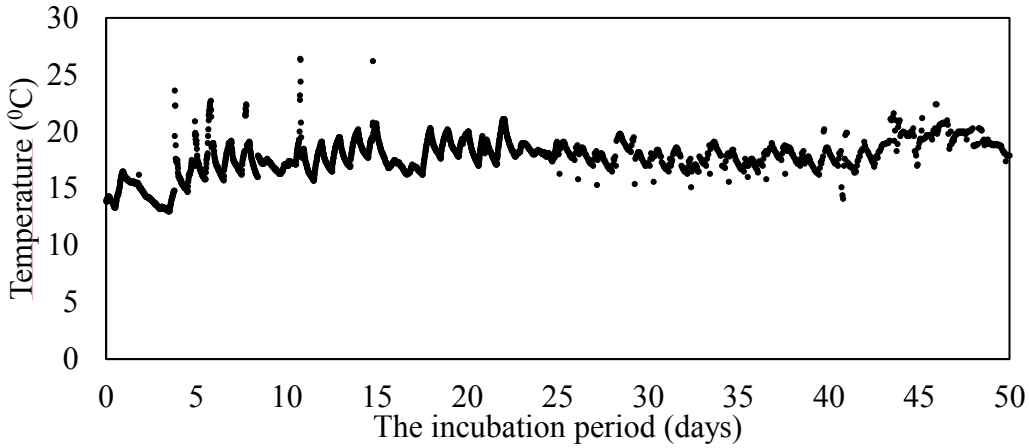

Figure 4.14. Temperature profile of biofilm formation reactors during the incubation

The impact of GAC amendment on biomethane production at psychrophilic temperature

Cumulative methane productions for all reactors are depicted in Figure 4.15a. Among the reactors with F/M ratio of 1, the application of GAC in GAC1 (498 ± 12 mL CH_4) enhanced cumulative methane production 13% in comparison to Control1 (442 ± 8 mL CH_4), while the enhancement is 20% in BioGAC1 (531 ± 6 mL CH_4). Similar findings were obtained for F/M ratio of 3 operation (Figure 4.15b). At F/M ratio of 3, GAC and BioGAC application increased cumulative methane production by 17% and 25% in GAC3 (656 ± 15 mL CH_4) and BioGAC3 (698 ± 15 mL CH_4) as compared to Control3 (560 ± 6 mL CH_4), respectively. In terms of percent methane in total produced biogas, AD1, GAC1 and BioGAC1 had 59.5 ± 0.5%, 53.9 ± 1.9% and 55.9 ± 0.3% methane, respectively for the reactors at F/M ratio of 1. For F/M ratio of 3 operation, the percent methane values are 56.3 ± 1.3%, 52.8 ± 0.4% and 56.9 ± 0.8% methane in AD3, GAC3 and BioGAC3, respectively.

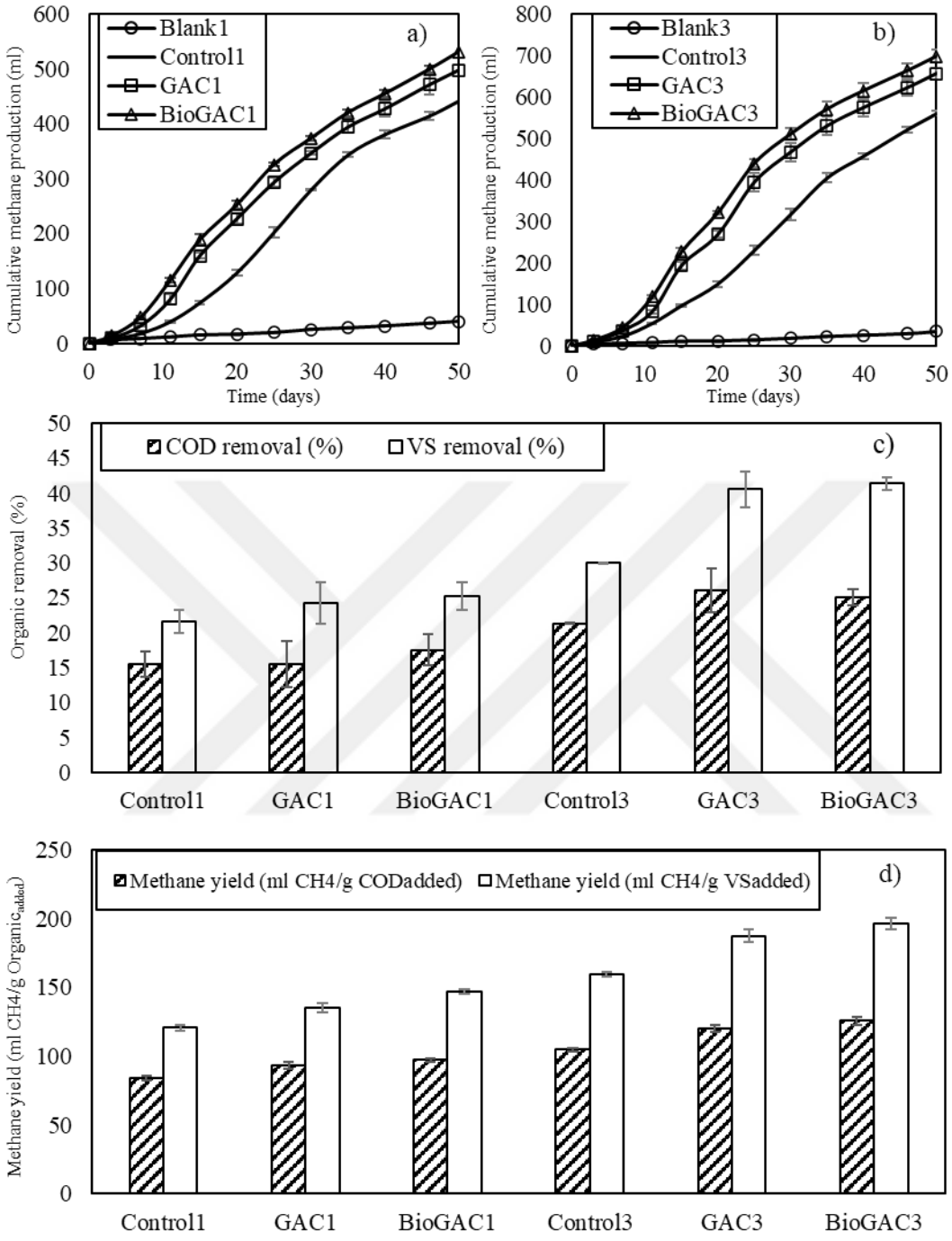

Figure 4.15. Cumulative methane production for a) reactors with F/M of 1 and b) for reactors with F/M ratio of 3, c) organic removal for all reactors and, d) methane yields for all reactors in Set 4

Methane yields (based on both added amount of VS and COD) are presented in Figure 4.15d for all reactors. For the reactor with F/M ratio of 1, the application of GAC and BioGAC in GAC1 (135 ± 3 mL CH_4/g VS_{added}) and BioGAC1(147 ± 2 mL CH_4/g VS_{added}) enhanced methane yield (based on added amount of VS) by 12% and 21% as compared to Control1 (121 ± 2 mL CH_4/g VS_{added}), respectively. Among the reactors with F/M ratio of 3, the improvements via GAC and BioGAC were higher than F/M ratio of 1 operation. Methane yield of Control3 (160 ± 2 mL CH_4/g VS_{added}) was improved 18% via GAC and 23% via BioGAC application.

Organic removals for all reactors are shown in Figure 4.15c. At F/M ratio of 1 no significant change in organic removals were observed, VS removal in Control1 averaged at 22 ± 2 %, in GAC1 averaged at 24 ± 3 % and in BioGAC1 averaged at 25 ± 2 %. For the reactors with F/M ratio of 3, the application of GAC and BioGAC increased organic removal when quantified via VS. In GAC3 (41 ± 3 %) and BioGAC3 (41 ± 1 %) around 37% higher VS removal were attained as compared to the Control3 (30 ± 0 %) (Figure 4.16b). The application of higher F/M ratio resulted in positive impact on organic removals. For VS removals, 36%, 71% and 64% improvements were obtained in Control3, GAC3 and BioGAC3 as compared to Control1, GAC1 and BioGAC1, respectively.

The results of kinetic parameters for all reactors are given in Table 4.8. For the reactors with F/M ratio of 1, R^2 values are ranging in 0.9958-0.9990 for all reactors indicating that the experimental data are well fitted to the model data. The cumulative methane production graphs showing experimental data and the model data are shown in Appendix E. From the point of view of methane production rate, the application of GAC and BioGAC increased the rate over the control. 7% and 10% enhancement in the rate was observed in GAC1 (15.5 ± 0.2 mL CH_4/day) and BioGAC1 (15.9 ± 0.4 mL CH_4/day) as compared to Control1 (14.5 ± 0.4 mL CH_4/day) via GAC and BioGAC application, respectively. In terms of lag time, GAC and BioGAC amendment in GAC1 (5.9 ± 0.6 days) and BioGAC1 (4.3 ± 0.3 days) resulted in 45% and 60% decrease in lag time over Control1 (10.7 ± 0.6 days), respectively.

Table 4.8. The results of kinetic parameters calculated from Gompertz modeling for the reactors in Set 4

Reactor	P (mL)	R_m (mL CH_4/day)	λ (day)	R^2
Control1	495.7 ± 11.0	14.5 ± 0.4	10.7 ± 0.6	0.9990
GAC1	523.6 ± 30.2	15.5 ± 0.2 (7%)	5.9 ± 0.6 (45%)	0.9967
BioGAC1	553.8 ± 7.5	15.9 ± 0.4 (10%)	4.3 ± 0.3 (60%)	0.9958
Control3	697.0 ± 14.5	16.4 ± 0.5	10.7 ± 0.2	0.9993
GAC3	687.4 ± 11.6	21.9 ± 1.3 (34%)	7.3 ± 0.1 (32%)	0.9980
BioGAC3	719.9 ± 20.0	23.4 ± 0.7 (43%)	6.2 ± 0.3 (42%)	0.9982

The number in the parenthesis indicates the enhancement in methane production rate and decrease in lag time as compared to the control.

GAC and BioGAC supplementations in GAC3 (21.9 ± 1.3 mL CH_4/day) and BioGAC3 (23.4 ± 0.7 mL CH_4/day) enhanced the rate 34% and 43% as compared to Control3 (16.4 ± 0.5 mL CH_4/day), respectively. Similarly, GAC and BioGAC addition in GAC3 (7.3 ± 0.1 days) and BioGAC3 (6.2 ± 0.3 days) decreased lag time 32% and 42% as compared to Control3 (10.7 ± 0.2 days), respectively. Significantly further improvement in lag time via BioGAC application can be explained by the fact that BioGAC has biofilm formed with acclimated microorganisms before the operation. This can lead to methane production earlier than bare GAC and results in decrease in lag time.

These results strongly suggest that the application of GAC on AD of CM at psychrophilic temperature is a promising approach for the enhancement of reactor performance in terms of methane yield, rate and start-up time. Similar finding was observed by Park et al. (2020). They found that the application of GAC on AD of activated sludge increased cumulative methane production and methane yield as

compared to the control (without GAC) at psychrophilic temperature (J. H. Park et al., 2020a). These results indicate that GAC and BioGAC addition can enhance methane production from a complex waste over conventional AD process especially at higher loadings *i.e.* higher F/M ratio, even at psychrophilic temperature. Also, in our study, it was observed that further improvement in methane yield can be obtained via BioGAC application for both F/M ratios.

Effect of different organic loading application

When the reactor performances of F/M ratio of 1 and F/M ratio of 3 were compared, we have observed that the methane yield in F/M ratio of 3 are even higher than F/M ratio of 1. The application of GAC and BioGAC at F/M ratio of 3 in GAC3 and BioGAC3 enhanced methane yield 55% and 62% as compared the control at F/M ratio of 1. The application of BioGAC resulted in further enhancement since it provided the acclimated microorganism on GAC particles.

These improvements in the yield via GAC and BioGAC application can be attributed to potential DIET mechanism provided by GAC. GAC and BioGAC can behave as electron and create a syntrophic interaction conduit between microorganisms even at psychrophilic temperature. Although it was observed that GAC application supports potential DIET mechanism in methanogenic environments at mesophilic temperatures (F. Liu et al., 2012; Rotaru et al., 2014a), it is strongly presented that the application of GAC provides enhancement in reactor performance even at psychrophilic temperature and this provides clear indications for the application of psychrophilic temperature for AD of CM.

The impact on electro-active biofilm formation

The results of CV analysis are given in Figure 4.16 for each group of the reactors. Among the reactors with F/M ratio of 1, the reduction peak is significantly higher in BioGAC1 as compared to GAC1 and Control1 (between -0.4 V - -0.6 V vs Ag/AgCl). The similar peaks were observed in Control1 and GAC1. For the reactors with F/M ratio of 3, the difference between reduction peaks of Control3 and GAC3

is very small. Similar to F/M ratio of 1, at F/M ratio of 3 BioGAC showed significantly bigger reduction peak over Control and GAC.

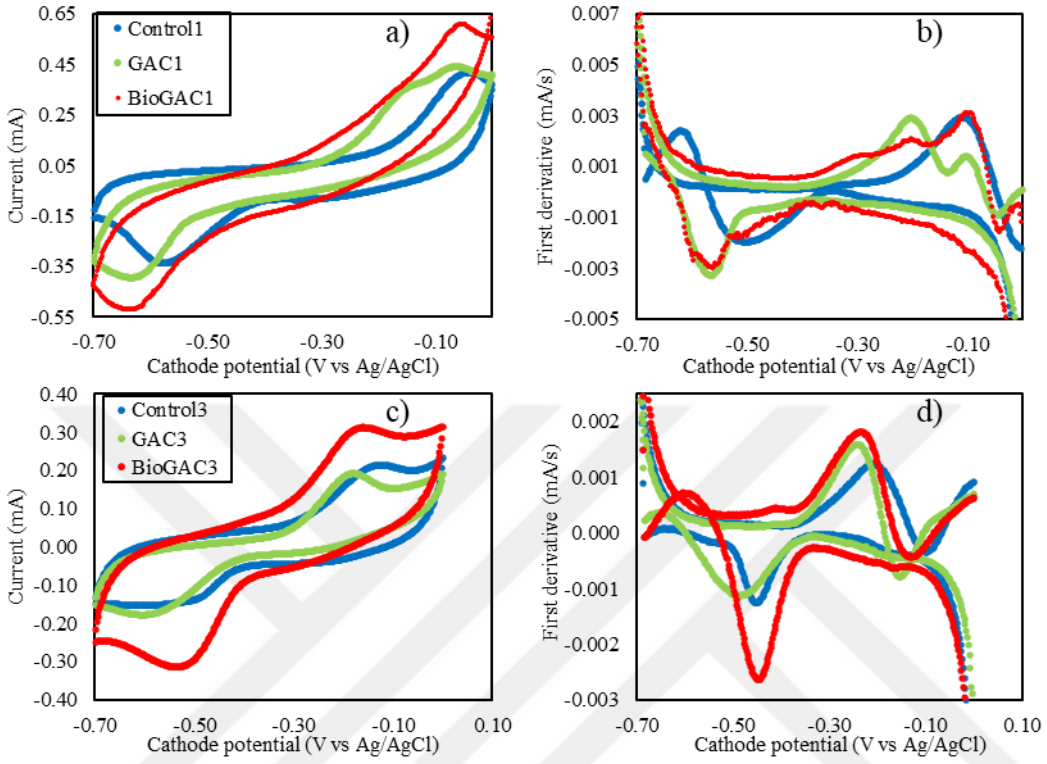

Figure 4.16. a) CV curves for reactors with F/M ratio of 1 b) first derivatives of CV curves of F/M ratio of 1 reactors, c) CV curves for reactors with F/M ratio of 3 (d) first derivatives of CV curves of F/M ratio of 3 reactors

The reduction peaks observed in CV analysis can be correlated to biological methane production via DIET mechanism as mentioned in the literature (Lee et al., 2016). CV analysis suggest that the application of BioGAC and GAC provide an electro active biofilm formation. Further analysis of CV voltammograms of the reactors in terms of 1st derivative of the voltammograms shows that higher reduction peaks were obtained in GAC1 and BioGAC1 over Control1 among the reactor with F/M ratio of 1. On the other hand, for F/M ratio of 3 reactors, BioGAC3 had significantly higher reduction peaks than Control3 and GAC3. For the 1st derivative analysis of the voltammograms, it is strongly suggested that the peak observed in the range of approximately -0.6 V vs Ag/AgCl is an implication of biological methane production

from carbon dioxide reduction via DIET mechanism as stated in the study conducted by (Fu et al., 2015). These results are similar to our observation in Set 3.

VFA concentrations in Set 4 reactors

As one of the important parameters for AD performance, periodic changes in VFAs for each reactor group are given in Figure 4.17 with an interval of 1 week. Among the reactors with F/M ratio of 1, although GAC1 and BioGAC1 peaked acetic acid concentration in the initial, the peak concentration was observed in 2nd week for Control1 (1741 ± 54 mg/L). After 2nd week, degradation of acetic acid was observed in each group of the reactors. Interestingly, acetic acid concentration was lower in GAC1 and BioGAC1 than Control1 except 1st week, and it can be an indication of effective digestion performance of CM via GAC and BioGAC application. Similarly, Jang et al. (2018) found that total VFA concentration was lower during AD of dairy manure in the reactor having biochar as CM than the control without CM at psychrophilic temperature. For butyric acid concentration, although GAC1 and BioGAC1 showed the peak concentrations in 1st week and the degradation started from 1st week, the time for peak concentration in Control1 delayed and it showed in 2nd week. In terms of propionic concentrations, similar to acetic acid concentrations, GAC1 and BioGAC1 reached the peak concentration at the initial and started to the degradation of propionic acid. For Control1, propionic acid concentration was peaked in 2nd week and the degradation was initiated in 3rd week.

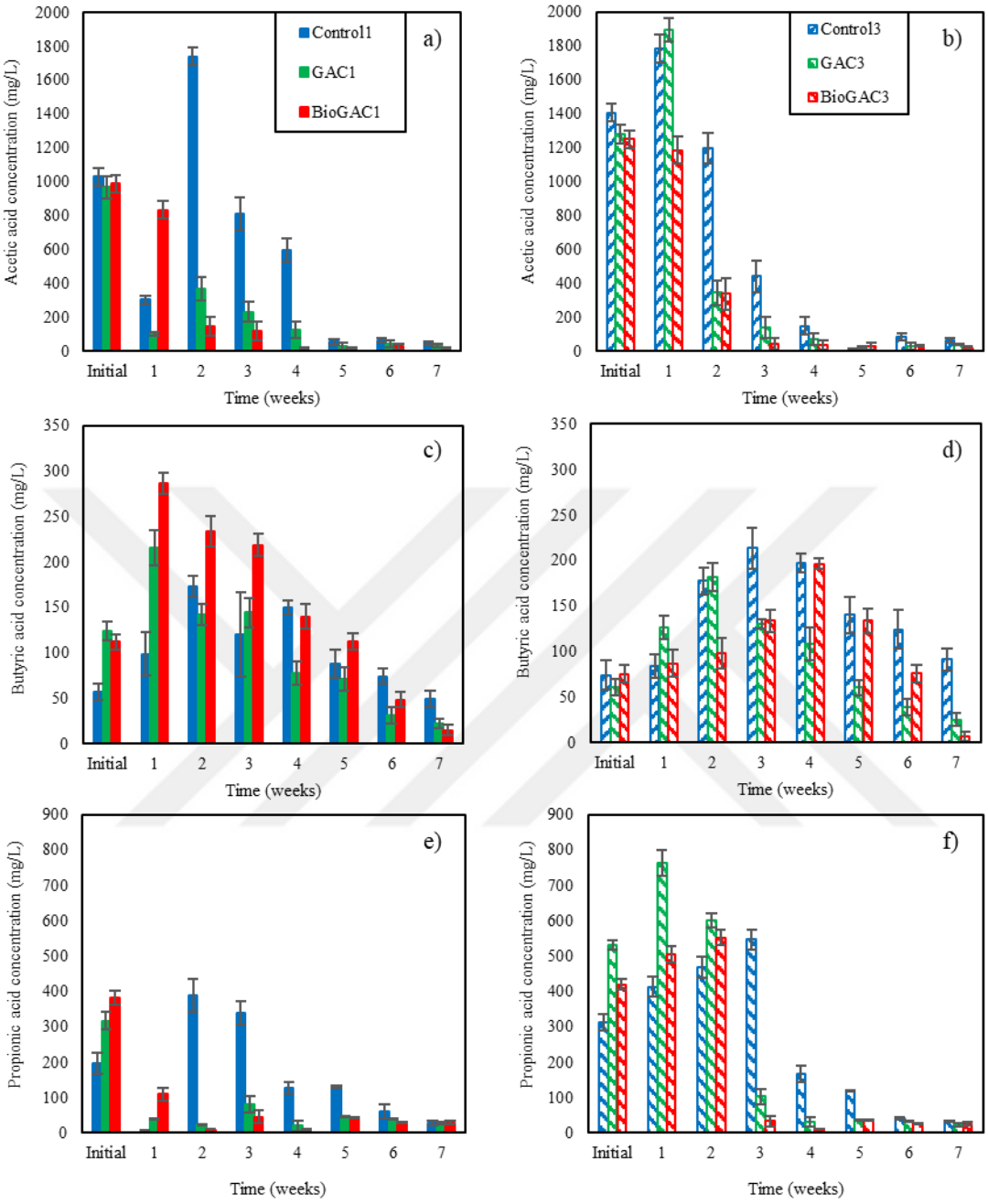

Figure 4.17. a)-b) acetic acid concentrations for F/M of 1 and 3 reactors, c)-d) butyric acid concentrations for F/M of 1 and 3 reactors and e)-f) propionic acid concentrations for F/M of 1 and 3 reactors in Set 4

For the reactors with F/M ratio of 3, acetic acid concentrations followed similar trend for each group of the reactors (Figure 4.17). The peak concentrations of acetic acid

were observed in the initial and 1st week, then the degradation was continued with a small difference in the final concentration. For butyric acid concentration, although similar trends were observed in Control3, GAC3 and BioGAC3, final concentration of butyric acid was significantly higher in Control3 (91 ± 12 mg/L) than GAC3 (25 ± 8 mg/L) and BioGAC3 (7 ± 5 mg/L). In terms of propionic acid concentration, the lagging for peak concentration was observed in Control3 with a peak concentration of 547 ± 27 mg/L. It was reached the peak concentration in 3rd week, although GAC3 and BioGAC3 reached the peak concentrations in 1st week and 2nd week, respectively.

These higher concentrations and delay to reach peak concentration in the controls (Control1 and Control3), especially in propionic acid concentrations, may explain lower methane yield and production rate in controls since it is known that propionic acid can inhibit methanogenic activity independent of pH ((Dang et al., 2017b)). Although the profiles of VFA concentrations in each group of the reactor were different, the inhibition level of about 6000, 8000 and 4000 mg/L for acetic acid, butyric acid and propionic acid was not observed in this study (Yin et al., 2020). Faster propionic acid degradation in the reactors with GAC (GAC1, BioGAC1, GAC3 and BioGAC3) as compared to their controls (Control1 and Control3) is an important indication for a promoted DIET mechanism as stated by (Liang et al.2021). The profiles of total VFA for each reactor are given in Figure 4.18. The results suggest that the application of GAC and BioGAC as CMs resulted in more effective degradation of VFAs and it was strongly supported that enhanced methanogenesis is potentially correlated to DIET mechanism.

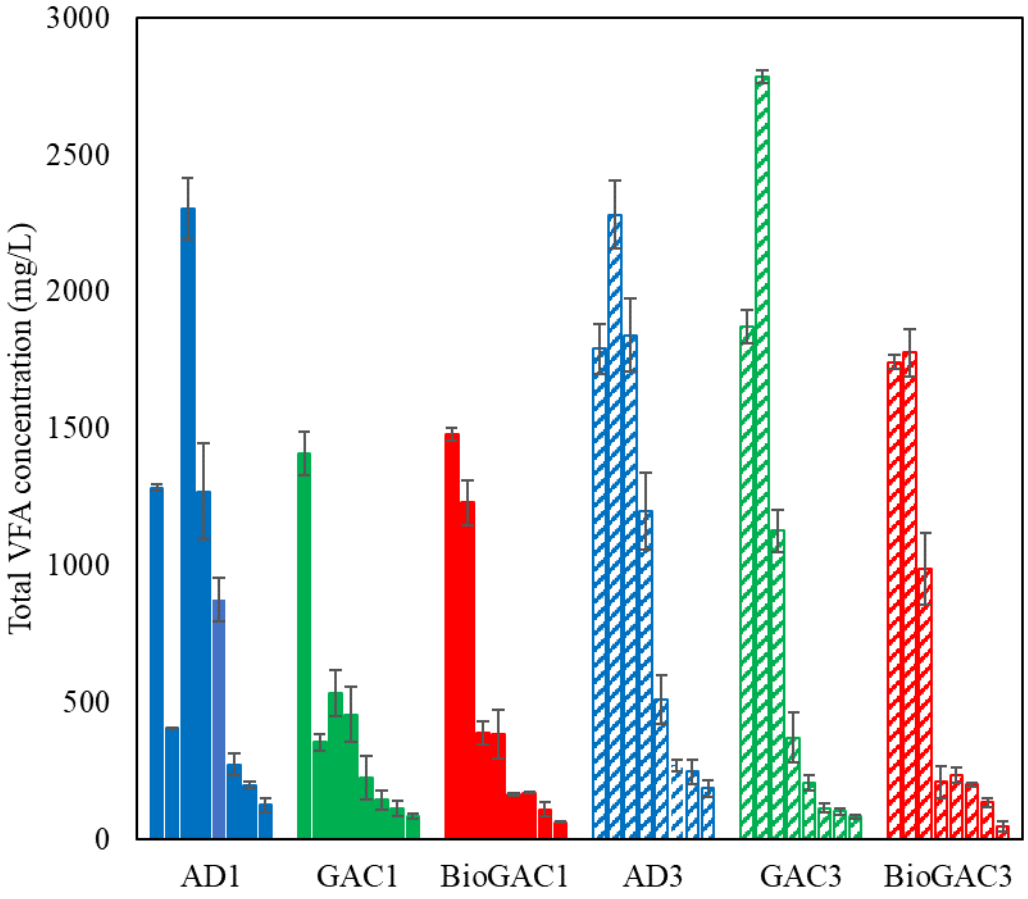

Figure 4.18. Total VFA profile for the reactors in Set 4

With the application of higher organic loading (F/M ratio of 3), higher VFA concentrations during the operation were observed in comparison to the reactors with F/M ratio of 1. Especially for acetic acid and propionic acid concentrations this is the case, which is expected as higher organic loadings may result in VFA accumulation in AD reactors (Yin et al., 2020). After relative accumulations of acetic acid and propionic acid for F/M ratio of 3 as compared to F/M ratio of 1 in the first two weeks, the difference in cumulative methane production became more apparent in F/M ratio of 3 over FM ratio of 1 with the degradation of these VFAs.

Nutrient concentrations in Set 4 reactors

Final ammonium and phosphorus concentrations for all reactors are shown in Figure 4.19. For the reactors with F/M ratio of 1, the highest ammonium concentration was

measured in Control1 (910 ± 36 mg NH_4-N/L). The application of GAC and BioGAC decreased final ammonium concentration 22% and 6% in GAC1 (713 ± 26 mg NH_4-N/L) and BioGAC1 (855 ± 19 mg NH_4-N/L), respectively as compared to Control1. In terms of phosphorus concentrations, the reactors with GAC and BioGAC had higher values than the control. 37% and 16% higher final phosphorus concentrations in GAC1 (67 ± 6 mg PO_4-P/L) and BioGAC1 (57 ± 4 mg PO_4-P/L) were observed than Control1 (49 ± 3 mg PO_4-P/L).

Among the reactors with F/M ratio of 3, similar to F/M ratio of 1, the amendment of GAC and BioGAC decreased final ammonium concentration over the control (Control3) (Figure 4.19). 28% and 31% decrease was observed in GAC3 (752 ± 25 mg NH_4-N/L) and BioGAC3 (722 ± 10 mg NH_4-N/L) as compared to Control3 (1049 ± 18 mg NH_4-N/L), respectively. For final phosphorus measurements, Control3 showed the lowest concentration with 36 ± 3 mg PO_4-P/L among the reactors with F/M ratio of 3. Higher final phosphorus concentrations were measured in GAC3 (62 ± 3 mg PO_4-P/L) and BioGAC3 (67 ± 5 mg PO_4-P/L) than Control3.

Likewise in Set 3, the ammonium concentrations are not higher than inhibition level that was stated as 3000 mg NH_4-N/L, it can be concluded that any inhibition due to ammonium accumulation was not observed (Krakat et al., 2017). Also, any inhibition due to phosphorus accumulation was not observed in this set (R. Wang et al., 2015).

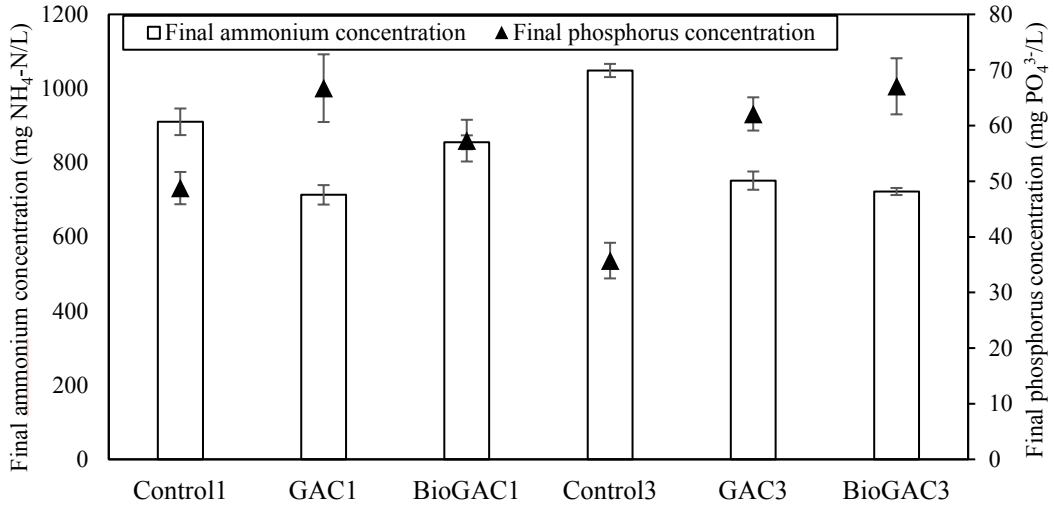

Figure 4.19. Final ammonium and phosphorus concentrations in Set 4

pH, electrical conductivity and ORP measurements of reactors in Set 4

The results of final pH, ORP and electrical conductivity measurements for all reactors are given in Figure 4.20. In the reactors pH ranged between 7.4-7.5, which is in the range of the safe zone for methanogenic activity as mentioned in the literature (Uçkun Kiran et al., 2016b). pH values may also imply that potential inhibition of acid accumulation was not occurred, and the reactors performances were not inhibited. For electrical conductivity measurements, the application of GAC and BioGAC for both F/M ratios increased electrical conductivity as compared to the controls (Control1 and Control3). Among the reactors with F/M ratio of 1, electrical conductivity values followed the order of BioGAC1 (8.2 ± 0.1 mS/cm) and GAC1 (8.2 ± 0.0 mS/cm) that were higher than Control1 (7.7 ± 0.1 mS/cm). In terms of ORP measurement, among the reactors with F/M ratio of 1, GAC and BioGAC amendment resulted in more negative ORP values than AD indicating a more suitable environment for methanogenic activity (Martins et al., 2018). For the reactors with F/M ratio of 1, GAC addition decreased ORP values in Control1 (-419 ± 5 mV) to 449 ± 9 mV. Additionally, further decrease in BioGAC1 (-463 ± 9 mV) was observed via biofilmed GAC particles. Among the reactors with F/M ratio of 3,

ORP values decreased in the control (Control3) from -438 ± 5 mV to 444 ± 6 mV and -463 ± 6 mV, respectively with the application of GAC and BioGAC in GAC3 and BioGAC3, respectively.

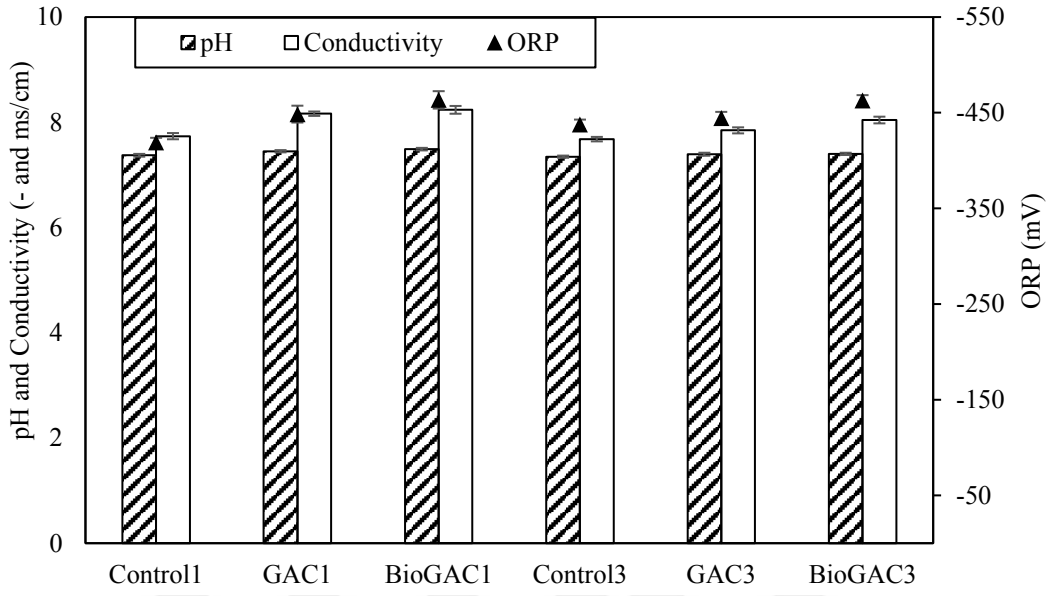

Figure 4.20. Final pH, electrical conductivity and ORP values in Set 4

Microbial community analysis

<u>Archaea</u>

The diversity of microbial community analysis on each sample in terms of archaeal species seems to be different based on the presence of GAC and BioGAC and also F/M ratios. The most abundant archaea were *Methanosaeta* in each sample except GAC3_S (Figure 4.21). The undefined genus belonging to *Methanomassiliicoccaceae* is the most abundant archaea in GAC3_S with 48%. *Methanosaeta* had the abundances of 73%, 78%, 65%, 73% and 49% in AD1, GAC1_A, GAC1_S, BioGAC1_A and BioGAC1_S for the samples of F/M ratio of 1 application. For F/M ratio of 3i the abundances of *Methanosaeta* 57%, 56%, 17, 48% and 53% in AD3, GAC3_A, GAC3_S, BioGAC3_A and BioGAC3_S. *Methanosaeta* is a well-known acetoclastic methanogen consuming acetate for its

metabolism and the production of methane (Mori et al., 2012). Rotaru et al. (2014) suggested that the co-cultures of *Geobacter* and *Methanosaeta* species are capable of performing electron transfer via DIET in anaerobic reactors. It was also suggested that *Geobacter* and *Methanosaeta* species can attach on conductive material such as biochar and can transfer electron to each other as a result of the metabolism of organic substances (Zhao et al., 2016) Our finding supported these findings by the fact that the samples BioGAC1_A, BioGAC3_A, GAC1_A and GAC3_A have *Methanosaeta* as the most abundant specie suggesting that *Methanosaeta* may attach on GAC and participate in anaerobic digestion by performing DIET. The members of family, *Methanoregulaceae*, including the genus *Methanolinea*, were observed in each sample. *Methanolinea* is a hydrogenotrophic methanogen which was stated as well-tolerated to acidic environments and yielding better growing than other methanogens (Y. Li et al., 2018). It was mentioned that *Methanolinea* was the predominant genus on anaerobic biofilm of polyurethane which is a biological filler, indicating that *Methanolinea* can grow on materials and producing a biofilm (Shi et al., 2019). This suggests that on GAC and BioGAC particles, *Methanolinea* could produce an anaerobic biofilm and also this biofilm could be observed in suspended sludge samples. In some of our suspended sludge samples including AD1, BioGAC1_S, GAC1_S and GAC3_S, the members of family, *Methanosarcinaceae*, including the genus, *Methanosarcina*, was observed. (Rotaru et al., 2014a) stated that *Methanosarcina* is one of the methanogens having membrane-bound cytochromes which can lead a potential mechanism for extracellular electron exchange. It was mentioned that *Methanosarcina* is one of the mostly abundant methanogens in anaerobic systems and their ability to DIET mechanism was proven (Kutlar et al., 2022). This can suggest that DIET could be conducted since *Methanosarcina* was observed in our suspended sludge. The genus, *Methanospirillum*, from the family *of Methanospirillaceae*, was enriched only in the samples of BioGAC1_A, GAC1_A and GAC3_A. This situation was associated with the biofilm formation on GAC samples and the possible DIET mechanism. (Yu et al., 2021) observed syntrophic interactions between the hydrogenotrophic

methanogen, *Methanospirillum* and some bacteria. Also, they stated the enrichment of *Methanospirillum* on the biofilm from GAC samples. This supported by the fact that our GAC samples had methanogenic biofilm including *Methanospirillum* and DIET took place on the biofilm of GAC samples. The enrichment of *Methanospirillum* on our working temperature was also supported by another study. L. Zhou et al. (2014) stated that optimal temperature was 25 ^{0}C for the growth of *Methanospirillum* which is quite close to our operational temperature. In terms of F/M ratio, the microbial community analysis shows that at F/M ratio of 3, the genus, *Methanoregula*, from the family of *Methanoregulaceae*, was observed in the samples of BioGAC3_A and GAC3_A. At F/M ratio of 1, *Methanoregula* was not enriched. Similarly, Zhen et al. (2022) observed that when OLR of their system was increased, *Methanoregula* exhibited its activity and abundantly enriched over other methanogens. Abundance of lower than all the other reactors Additionally, Kang & Liu (2021) stated that the abundance of *Methanoregula* was increased when magnetite was used as conductive material for their system which is similar to the amendment of GAC as conductive material in our system.

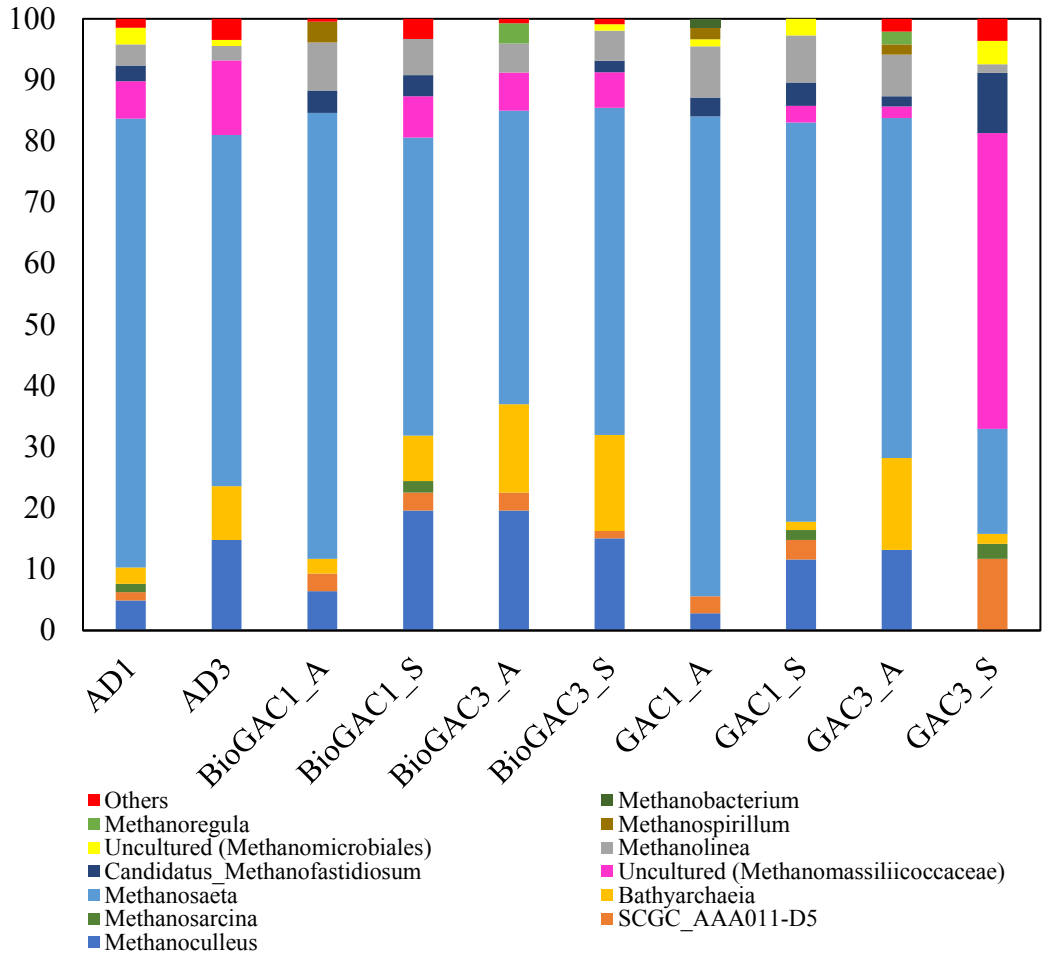

Figure 4.21. Microbial community structure based on relative abundance of 16S rRNA sequences of the sample in Set 4 at archaeal genus level

Bacteria

The microbial community analysis of the samples showed that the bacterial diversity was higher than archaeal diversity for the samples (Figure 4.22). It was revealed that generally the dominant order is *Cloacimonadales*. Although it was stated that the order, *Cloacimonadales* is one of the major players participated in mesophilic anaerobic systems, it was observed in all samples at our working temperature which belongs to psychrophilic range (Arthur et al., 2022). On the other hand, the genus, *Smithella*, belonging to phylum *Desulfobacterota,* was observed in all samples except GAC1_A. Puengrang et al. (2020) showed that *Smithella* is a syntrophic

propionate-oxidizing bacteria which can have syntrophic interactions with hydrogenotrophic methanogens such as *Methanospirillum* and *Methanoculleus*. This finding was supported with our results by the fact that especially, *Methanoculleus* was enriched in our samples except GAC3_S. Except from BioGAC1_S, BioGAC3_S and GAC1_S, *Treponema*, from the family of *Spirochaetaceae*, was observed in the samples. It was stated that *Treponema* is an homoacetogens that can produce acetate by consuming H_2 and CO_2 and it can be a partner with acetoclastic methanogens (W. Wang et al., 2013). Since it has been reported that homoacetogenic activity is typically occurred at psychrophilic temperature and the occurrence of *Treponema* as homoacetogen in our samples is not surprising (L. Li et al., 2016). In BioGAC1_A, BioGAC3_A, GAC1_A and _GAC3_A, the genus, Pseudomonas, was enriched. It was stated that *Pseudomonas* do not have an effective extracellular electron transfer ability although it is an electrogenic bacteria, in other words, it can produce electron by organic degradation (R. Lin et al., 2017). It was reported that the amendment of graphene as CoM on AD operation resulted in direct electron transfer between *Pseudomonas* and methanogens which suggests DIET mechanism can occur via graphene with the occurrence of *Pseudomonas*. In another study, *Pseudomonas* was enriched in the reactor having GAC as CoM, but it was not found in control reactor (Wan et al., 2021). It was mentioned that due to the occurrence of electrogenic bacteria, *Pseudomonas*, DIET mechanism was promoted with the amendment of GAC (Wan et al., 2021). Similar to these findings, in our study, since *Pseudomonas* was found in BioGAC1_A, BioGAC3_A, GAC1_A and _GAC3_A samples, it can be speculated that the addition of GAC and biofilm attached GAC promoted DIET mechanism.

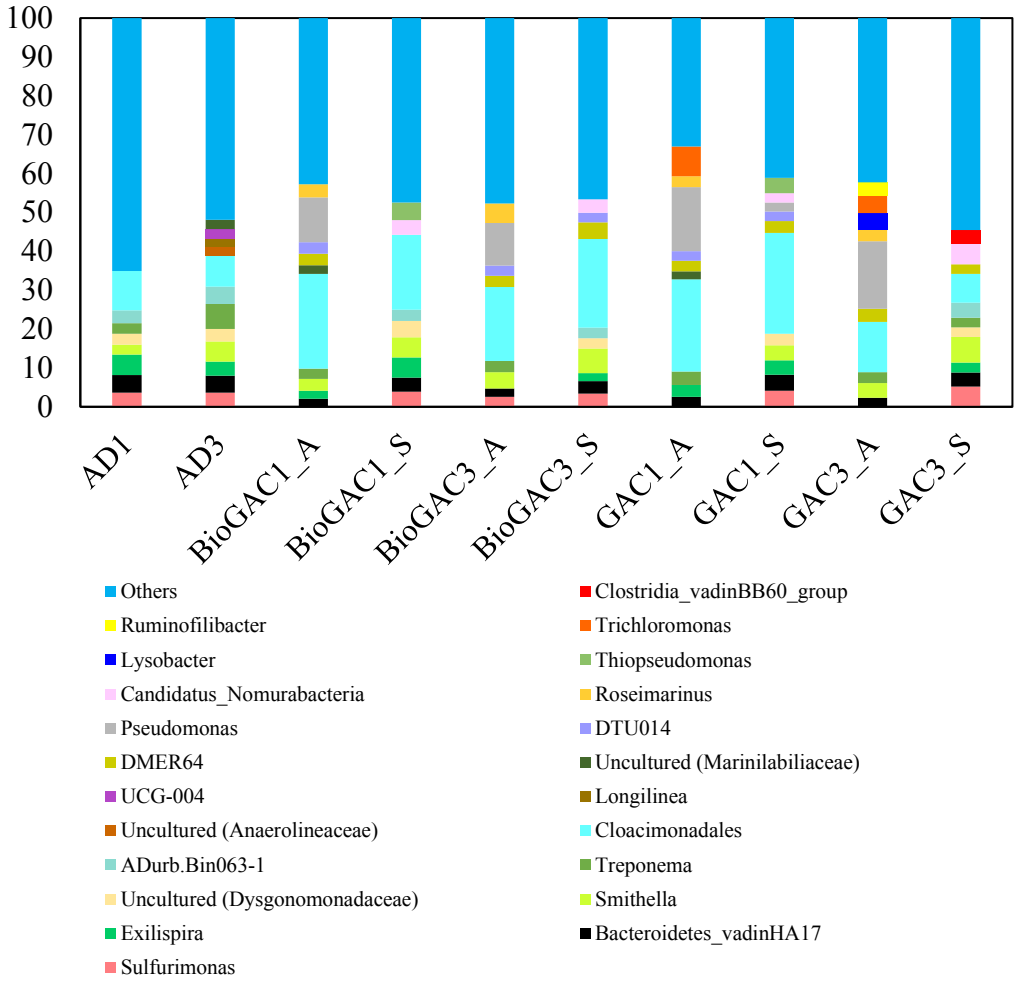

Figure 4.22. Microbial community structure based on relative abundance of 16S rRNA sequences of the sample in Set 4 at bacterial genus level

Comparison of Mesophilic and Psychrophilic AD of CM (Set 3 and Set 4)

In the scope of our study, we also compared the impact of the amendment of GAC as CoM at psychrophilic temperature (Set 4) over conventional AD operation at mesophilic temperature (Set 3). In this comparison, we examined AD1-mix in Set 3 as conventional AD operation and Control 1, GAC1 and BioGAC1 in Set 4 as the reactors amended with GAC at psychrophilic temperature. In order to have a clear comparison, methane yields and methane production rates for AD1-mix, Control 1, GAC1 and BioGAC1 are given in Table 4.9.

Table 4.9. Methane yield and methane production rates for AD1-mix, GAC1 and BioGAC1

Reactor*	Methane yield (mL CH_4/g VS_{added})	Methane production rate (mL CH_4/day)
AD1-mix (mesophilic)	109 ± 2	21.6 ± 0.7
Control1(psychrophilic)	121 ± 2	14.5 ± 0.4
GAC1 (psychrophilic)	135 ± 3	15.5 ± 0.2
BioGAC1 (psychrophilic)	147 ± 2	15.7 ± 0.4

* Mixing was applied to all psychrophilic reactors.

As given in Table 4.9, in terms of methane yield, the operation of psychrophilic AD via GAC amendment in GAC1 and BioGAC1 resulted in 24% and 35% improvement over AD1-mix. Also, conventional AD operation at psychrophilic temperature resulted in 11% enhancement over mesophilic AD operation (AD1-mix). On the other hand, methane production rates were decreased at psychrophilic temperature as compared to mesophilic operation. In Table 4.10, the costs due to GAC application and heating and revenue from methane production rate for AD1-mix, GAC1 and BioGAC1 are given. In this calculation, the dimensions of real biogas plant (Polres) were used. The diameter of the reactor is 12.6 m, and the height of the reactor is 18 m. The active volume of the reactor is 9000 m^3. In order to evaluate the application of GAC amendment at psychrophilic temperature, we calculated the revenue from produced methane and cost due to GAC application (for psychrophilic temperature, Set4) and heating (for mesophilic temperature, Set3), and we compared the difference between cost and revenue for each reactor to obtain which system is costly.

Table 4.10.The costs due to GAC application and heating, revenue from methane production rate and the difference between cost and revenue for AD1-mix, GAC1 and BioGAC1

	GAC cost (thousand dollars/day)	Extra cost due to heating to a higher temperature (thousand dollars/day)	Revenue from methane production rate (dollars/day)	Cost– Revenue (dollars/day)	Cost– Revenue (thousand dollars)
AD1-mix (mesophilic)	-	250	$2.3*10^{-5}$	250	7500
GAC1 (psychrophilic)	30	-	$1.7*10^{-5}$	30	1500
BioGAC1 (psychrophilic)	30	-	$1.7*10^{-5}$	30	1500

As shown in Table 4.10, the difference between cost and revenue for AD1-mix that is conventional AD operation at mesophilic temperature is higher. On the other hand, at psychrophilic temperature, the amendment of GAC and BioGAC decreased the difference between cost and revenue is lower as compared to mesophilic AD operation. Based on our cost calculation, the operation of psychrophilic AD with GAC amendment is 80% less costly than conventional AD operation at mesophilic temperature. To sum up, since there is less heating cost for psychrophilic operation, the cost of methane production is decreased and psychrophilic operation via GAC amendment becomes more feasible and economical. The cost calculations are highly dependent on the lifetime of GAC to be used during AD. Depending on the need for replacement/reloading, the cost calculations may need to be revised.

CHAPTER 5

CONCLUSION

The main objective of this study was the examination of the anaerobic digestibility of CM, and the investigation of the improvement in AD of CM via different CoMs amendment, GAC and hematite. Our study indicated that there is no need for external nutrient supplementation during CM digestion at initial COD concentrations up to 30 g/L. In fact, the addition of BM as external nutrient supplementation decreased methane production rate and caused a longer lag time. For the improvement of CM digestion, it was shown that GAC amendment is better than hematite amendment as it resulted in higher enhancements in both methane yield and methane production rate and lower lag time. In the experimental work, three different GAC dosages of 20 g/L, 40 g/L and 60 g/L were tested and based on the performance parameters of methane production yield, methane production rate and lag time, 40 g/L was selected as optimum dosage under mesophilic conditions. Further, our results suggested that the application of mixing was important when GAC amendment was applied; and higher performances were recorded in the reactors where mixing at a rate of 150 rpm was applied. The conventional AD reactors ideal scenario regarding F/M ratio is 1.0 yet higher F/M ratio may indicate an overloading condition. Therefore, we have tested both F/M ratio of 1 and 3 in the batch reactors at mesophilic conditions. The results show that the improvement via GAC addition with respect to control was higher at F/M ratio of 3 rather than F/M ratio of 1. This may be interpreted as an increased process stability, which may be attributed to the reduced ORP, and increased conductivity values of GAC amended reactors. The changes in ORP and conductivity may suggest that the presence of GAC created a more suitable environment for anaerobic degradation and microbial interaction. Also, the results of CV analysis imply that the addition of GAC on CM digestion had a significant impact on enrichment of electro-active microorganisms in comparison to the control,

and GAC application on AD may promote more effective DIET mechanism for methane production. Lastly, the experiments that were run at psychrophilic conditions (~18 ^{o}C) revealed that the application of GAC enhanced methane production and further improvement was observed via BioGAC application. Similar to mesophilic operation, CV analysis imply that the addition of GAC on AD of CM significantly increased enrichment of electro active microorganisms in comparison to control. Based on the 16S RNA based microbial community analysis, the occurrence of several archaeal genera and the existence of several bacteria suggested that DIET mechanism may be promoted with the application of GAC at psychrophilic temperature. In addition to improvement in methane yield, methane production rate and lag time, the cost-revenue analysis suggested that the application of GAC and BioGAC at psychrophilic temperature may offer a more feasible and economical than operation of CM digestion at mesophilic conditions.

CHAPTER 6

RECOMMENDATIONS

The enhcancement of cattle manure digestion in terms of methane yield, methane production rate and lag time via GAC amendment at both mesophilic and psychrophilic temperature was observed in our study under batch operation conditions. Hence, the impact of GAC amendment on the digestion under continous operation mode should be assessed with different organic loading rates. Further, to prevent biomass and GAC washout from the system, there may be a casing needed for holding the particles. Additionally, from the economical perspective there should be a market search to find GACs produced from local and cheaper raw materials to be used in the experiments.

REFERENCES

An, Z., Feng, Q., Zhao, R., & Wang, X. (2020). Bioelectrochemical methane production from food waste in anaerobic digestion using a carbon-modified copper foam electrode. *Processes*, *8*(4). https://doi.org/10.3390/PR8040416

Anukam, A., Mohammadi, A., Naqvi, M., & Granström, K. (2019). A review of the chemistry of anaerobic digestion: Methods of accelerating and optimizing process efficiency. In *Processes* (Vol. 7, Issue 8, pp. 1–19). MDPI AG. https://doi.org/10.3390/PR7080504

Arthur, R., Antonczyk, S., Off, S., & Scherer, P. A. (2022). Mesophilic and Thermophilic Anaerobic Digestion of Wheat Straw in a CSTR System with 'Synthetic Manure': Impact of Nickel and Tungsten on Methane Yields, Cell Count, and Microbiome. *Bioengineering*, *9*(1). https://doi.org/10.3390/bioengineering9010013

Asztalos, J. R., & Kim, Y. (2015). Enhanced digestion of waste activated sludge using microbial electrolysis cells at ambient temperature. *Water Research*, *87*, 503–512. https://doi.org/10.1016/j.watres.2015.05.045

Baek, G., Saikaly, P. E., & Logan, B. E. (2021). Addition of a carbon fiber brush improves anaerobic digestion compared to external voltage application. *Water Research*, *188*. https://doi.org/10.1016/j.watres.2020.116575

Bougrier, C., Albasi, C., Delgenès, J. P., & Carrère, H. (2006). Effect of ultrasonic, thermal and ozone pre-treatments on waste activated sludge solubilisation and anaerobic biodegradability. *Chemical Engineering and Processing: Process Intensification*, *45*(8), 711–718. https://doi.org/10.1016/j.cep.2006.02.005

Cerrillo, M., Palatsi, J., Comas, J., Vicens, J., & Bonmatí, A. (2015). Struvite precipitation as a technology to be integrated in a manure anaerobic digestion treatment plant - removal efficiency, crystal characterization and agricultural

assessment. *Journal of Chemical Technology and Biotechnology*, *90*(6), 1135–1143. https://doi.org/10.1002/jctb.4459

Chen, H., Wang, W., Xue, L., Chen, C., Liu, G., & Zhang, R. (2016). Effects of Ammonia on Anaerobic Digestion of Food Waste: Process Performance and Microbial Community. *Energy and Fuels*, *30*(7), 5749–5757. https://doi.org/10.1021/acs.energyfuels.6b00715

Dang, Y., Holmes, D. E., Zhao, Z., Woodard, T. L., Zhang, Y., Sun, D., Wang, L. Y., Nevin, K. P., & Lovley, D. R. (2016a). Enhancing anaerobic digestion of complex organic waste with carbon-based conductive materials. *Bioresource Technology*, *220*, 516–522. https://doi.org/10.1016/j.biortech.2016.08.114

Dang, Y., Holmes, D. E., Zhao, Z., Woodard, T. L., Zhang, Y., Sun, D., Wang, L. Y., Nevin, K. P., & Lovley, D. R. (2016b). Enhancing anaerobic digestion of complex organic waste with carbon-based conductive materials. *Bioresource Technology*, *220*, 516–522. https://doi.org/10.1016/j.biortech.2016.08.114

Dang, Y., Sun, D., Woodard, T. L., Wang, L. Y., Nevin, K. P., & Holmes, D. E. (2017a). Stimulation of the anaerobic digestion of the dry organic fraction of municipal solid waste (OFMSW) with carbon-based conductive materials. *Bioresource Technology*, *238*, 30–38. https://doi.org/10.1016/j.biortech.2017.04.021

Dang, Y., Sun, D., Woodard, T. L., Wang, L. Y., Nevin, K. P., & Holmes, D. E. (2017b). Stimulation of the anaerobic digestion of the dry organic fraction of municipal solid waste (OFMSW) with carbon-based conductive materials. *Bioresource Technology*, *238*, 30–38. https://doi.org/10.1016/j.biortech.2017.04.021

Demirer, G. N., Duran, M., Ergüder, T. H., Güven, E., Ugurlu, Ö., & Tezel, U. (2000). Anaerobic treatability and biogas production potential studies of different agro-industrial wastewaters in Turkey. In *Biodegradation* (Vol. 11).

Filer, J., Ding, H. H., & Chang, S. (2019). Biochemical methane potential (BMP) assay method for anaerobic digestion research. In *Water (Switzerland)* (Vol. 11, Issue 5). MDPI AG. https://doi.org/10.3390/w11050921

Fu, Q., Kuramochi, Y., Fukushima, N., Maeda, H., Sato, K., & Kobayashi, H. (2015). Bioelectrochemical analyses of the development of a thermophilic biocathode catalyzing electromethanogenesis. *Environmental Science and Technology*, *49*(2), 1225–1232. https://doi.org/10.1021/es5052233

Ghosh, P., Kumar, M., Kapoor, R., Kumar, S. S., Singh, L., Vijay, V., Vijay, V. K., Kumar, V., & Thakur, I. S. (2020). Enhanced biogas production from municipal solid waste via co-digestion with sewage sludge and metabolic pathway analysis. *Bioresource Technology*, *296*. https://doi.org/10.1016/j.biortech.2019.122275

González, J., Sánchez, M., & Gómez, X. (2018). Enhancing Anaerobic Digestion: The Effect of Carbon Conductive Materials. *C*, *4*(4), 59. https://doi.org/10.3390/c4040059

Güngör-Demirci, G., & Demirer, G. N. (2004). Effect of initial COD concentration, nutrient addition, temperature and microbial acclimation on anaerobic treatability of broiler and cattle manure. *Bioresource Technology*, *93*(2), 109–117. https://doi.org/10.1016/j.biortech.2003.10.019

Harnisch, F., & Freguia, S. (2012). A basic tutorial on cyclic voltammetry for the investigation of electroactive microbial biofilms. In *Chemistry - An Asian Journal* (Vol. 7, Issue 3, pp. 466–475). https://doi.org/10.1002/asia.201100740

He, X., Guo, Z., Lu, J., & Zhang, P. (2021). Carbon-based conductive materials accelerated methane production in anaerobic digestion of waste fat, oil and grease. *Bioresource Technology*, *329*. https://doi.org/10.1016/j.biortech.2021.124871

Herrmann, C., Sánchez, E., Schultze, M., & Borja, R. (2021). Comparative effect of biochar and activated carbon addition on the mesophilic anaerobic digestion of piggery waste in batch mode. *Journal of Environmental Science and Health - Part A Toxic/Hazardous Substances and Environmental Engineering*, *56*(9), 946–952. https://doi.org/10.1080/10934529.2021.1944833

Hirano, S., Matsumoto, N., Morita, M., Sasaki, K., & Ohmura, N. (2013). Electrochemical control of redox potential affects methanogenesis of the hydrogenotrophic methanogen Methanothermobacter thermautotrophicus. *Letters in Applied Microbiology*, *56*(5), 315–321. https://doi.org/10.1111/lam.12059

Holechek, J. L., Geli, H. M. E., Sawalhah, M. N., & Valdez, R. (2022). A Global Assessment: Can Renewable Energy Replace Fossil Fuels by 2050? *Sustainability (Switzerland)*, *14*(8). https://doi.org/10.3390/su14084792

Issah, A. A., Kabera, T., & Kemausuor, F. (2020). Biogas optimisation processes and effluent quality: A review. In *Biomass and Bioenergy* (Vol. 133). Elsevier Ltd. https://doi.org/10.1016/j.biombioe.2019.105449

Jain, S., Jain, S., Wolf, I. T., Lee, J., & Tong, Y. W. (2015). A comprehensive review on operating parameters and different pretreatment methodologies for anaerobic digestion of municipal solid waste. In *Renewable and Sustainable Energy Reviews* (Vol. 52, pp. 142–154). Elsevier Ltd. https://doi.org/10.1016/j.rser.2015.07.091

Jang, H. M., Choi, Y. K., & Kan, E. (2018). Effects of dairy manure-derived biochar on psychrophilic, mesophilic and thermophilic anaerobic digestions of dairy manure. *Bioresource Technology*, *250*, 927–931. https://doi.org/10.1016/j.biortech.2017.11.074

Jeihanipour, A., Aslanzadeh, S., Rajendran, K., Balasubramanian, G., & Taherzadeh, M. J. (2013). High-rate biogas production from waste textiles

using a two-stage process. *Renewable Energy*, *52*, 128–135. https://doi.org/10.1016/j.renene.2012.10.042

Johnravindar, D., Liang, B., Fu, R., Luo, G., Meruvu, H., Yang, S., Yuan, B., & Fei, Q. (2020). Supplementing granular activated carbon for enhanced methane production in anaerobic co-digestion of post-consumer substrates. *Biomass and Bioenergy*, *136*. https://doi.org/10.1016/j.biombioe.2020.105543

Kang, X., & Liu, Y. (2021). Performance and mechanism of conductive magnetite particle-enhanced excess sludge anaerobic digestion for biogas recovery. *RSC Advances*, *11*(56), 35559–35566. https://doi.org/10.1039/d1ra06236k

Kato, S., Hashimoto, K., & Watanabe, K. (2012). Methanogenesis facilitated by electric syntrophy via (semi)conductive iron-oxide minerals. *Environmental Microbiology*, *14*(7), 1646–1654. https://doi.org/10.1111/j.1462-2920.2011.02611.x

Kim, M., Kim, B. C., Choi, Y., & Nam, K. (2017). Minimizing mixing intensity to improve the performance of rice straw anaerobic digestion via enhanced development of microbe-substrate aggregates. *Bioresource Technology*, *245*, 590–597. https://doi.org/10.1016/j.biortech.2017.09.006

Krakat, N., Anjum, R., Dietz, D., & Demirel, B. (2017). Methods of ammonia removal in anaerobic digestion: A review. *Water Science and Technology*, *76*(8), 1925–1938. https://doi.org/10.2166/wst.2017.406

Kumar, S. S., Ghosh, P., Kataria, N., Kumar, D., Thakur, S., Pathania, D., Kumar, V., Nasrullah, M., & Singh, L. (2021). The role of conductive nanoparticles in anaerobic digestion: Mechanism, current status and future perspectives. *Chemosphere*, *280*. https://doi.org/10.1016/j.chemosphere.2021.130601

Kumar, V., Nabaterega, R., Khoei, S., & Eskicioglu, C. (2021). Insight into interactions between syntrophic bacteria and archaea in anaerobic digestion amended with conductive materials. In *Renewable and Sustainable Energy Reviews* (Vol. 144). Elsevier Ltd. https://doi.org/10.1016/j.rser.2021.110965

Kutlar, F. E., Tunca, B., & Yilmazel, Y. D. (2022). Carbon-based conductive materials enhance biomethane recovery from organic wastes: A review of the impacts on anaerobic treatment. *Chemosphere*, *290*. https://doi.org/10.1016/j.chemosphere.2021.133247

Kutlar, F. E., & Yilmazel, Y. D. (n.d.). *Use of low-cost raw materials for the recovery of phosphorus and nitrogen from biogas plant effluents via struvite crystallization*. https://doi.org/10.1016/j

Lee, J. Y., Lee, S. H., & Park, H. D. (2016). Enrichment of specific electro-active microorganisms and enhancement of methane production by adding granular activated carbon in anaerobic reactors. *Bioresource Technology*, *205*, 205–212. https://doi.org/10.1016/j.biortech.2016.01.054

Lei, Y., Sun, D., Dang, Y., Chen, H., Zhao, Z., Zhang, Y., & Holmes, D. E. (2016). Stimulation of methanogenesis in anaerobic digesters treating leachate from a municipal solid waste incineration plant with carbon cloth. *Bioresource Technology*, *222*, 270–276. https://doi.org/10.1016/j.biortech.2016.10.007

Li, H., Chang, J., Liu, P., Fu, L., Ding, D., & Lu, Y. (2015). Direct interspecies electron transfer accelerates syntrophic oxidation of butyrate in paddy soil enrichments. *Environmental Microbiology*, *17*(5), 1533–1547. https://doi.org/10.1111/1462-2920.12576

Li, L., He, Q., Ma, Y., Wang, X., & Peng, X. (2016). A mesophilic anaerobic digester for treating food waste: Process stability and microbial community analysis using pyrosequencing. *Microbial Cell Factories*, *15*(1). https://doi.org/10.1186/s12934-016-0466-y

Li, Y., Sun, Y., Li, L., & Yuan, Z. (2018). Acclimation of acid-tolerant methanogenic propionate-utilizing culture and microbial community dissecting. *Bioresource Technology*, *250*, 117–123. https://doi.org/10.1016/j.biortech.2017.11.034

Li, Y., Zhang, Y., Yang, Y., Quan, X., & Zhao, Z. (2017). Potentially direct interspecies electron transfer of methanogenesis for syntrophic metabolism under sulfate reducing conditions with stainless steel. *Bioresource Technology*, *234*, 303–309. https://doi.org/10.1016/j.biortech.2017.03.054

Liang, J., Luo, L., Li, D., Varjani, S., Xu, Y., & Wong, J. W. C. (2021). Promoting anaerobic co-digestion of sewage sludge and food waste with different types of conductive materials: Performance, stability, and underlying mechanism. *Bioresource Technology*, *337*. https://doi.org/10.1016/j.biortech.2021.125384

Lin, R., Cheng, J., Ding, L., & Murphy, J. D. (2018). Improved efficiency of anaerobic digestion through direct interspecies electron transfer at mesophilic and thermophilic temperature ranges. *Chemical Engineering Journal*, *350*, 681–691. https://doi.org/10.1016/j.cej.2018.05.173

Lin, R., Cheng, J., Zhang, J., Zhou, J., Cen, K., & Murphy, J. D. (2017). Boosting biomethane yield and production rate with graphene: The potential of direct interspecies electron transfer in anaerobic digestion. *Bioresource Technology*, *239*, 345–352. https://doi.org/10.1016/j.biortech.2017.05.017

Lin, Y., Liang, J., Zeng, C., Wang, D., & Lin, H. (2017a). Anaerobic digestion of pulp and paper mill sludge pretreated by microbial consortium OEM1 with simultaneous degradation of lignocellulose and chlorophenols. *Renewable Energy*, *108*, 108–115. https://doi.org/10.1016/j.renene.2017.02.049

Lin, Y., Liang, J., Zeng, C., Wang, D., & Lin, H. (2017b). Anaerobic digestion of pulp and paper mill sludge pretreated by microbial consortium OEM1 with simultaneous degradation of lignocellulose and chlorophenols. *Renewable Energy*, *108*, 108–115. https://doi.org/10.1016/j.renene.2017.02.049

Lindmark, J., Eriksson, P., & Thorin, E. (2014). The effects of different mixing intensities during anaerobic digestion of the organic fraction of municipal solid waste. *Waste Management*, *34*(8), 1391–1397. https://doi.org/10.1016/j.wasman.2014.04.006

Liu, F., Rotaru, A. E., Shrestha, P. M., Malvankar, N. S., Nevin, K. P., & Lovley, D. R. (2012). Promoting direct interspecies electron transfer with activated carbon. *Energy and Environmental Science*, *5*(10), 8982–8989. https://doi.org/10.1039/c2ee22459c

Liu, J., Liu, T., Chen, S., Yu, H., Zhang, Y., & Quan, X. (2020). Enhancing anaerobic digestion in anaerobic integrated floating fixed-film activated sludge (An-IFFAS) system using novel electron mediator suspended biofilm carriers. *Water Research*, *175*. https://doi.org/10.1016/j.watres.2020.115697

Liu, Y., Li, X., Wu, S., Tan, Z., & Yang, C. (2021). Enhancing anaerobic digestion process with addition of conductive materials. *Chemosphere*, *278*. https://doi.org/10.1016/j.chemosphere.2021.130449

Lovley, D. R. (2017). Syntrophy Goes Electric: Direct Interspecies Electron Transfer. *Review in Advance*. https://doi.org/10.1146/annurev-micro-030117

Loyon, L. (2018). Overview of Animal Manure Management for Beef, Pig, and Poultry Farms in France. *Frontiers in Sustainable Food Systems*, *2*. https://doi.org/10.3389/fsufs.2018.00036

Lu, D., Wu, D., Qian, T., Jiang, J., Cao, S., & Zhou, Y. (2020). Liquid and solids separation for target resource recovery from thermal hydrolyzed sludge. *Water Research*, *171*. https://doi.org/10.1016/j.watres.2020.115476

Lu, T., Zhang, J., Wei, Y., & Shen, P. (2019). Effects of ferric oxide on the microbial community and functioning during anaerobic digestion of swine manure. *Bioresource Technology*, *287*. https://doi.org/10.1016/j.biortech.2019.121393

Martínez, E. J., Rosas, J. G., Morán, A., & Gómez, X. (2015). Effect of ultrasound pretreatment on sludge digestion and dewatering characteristics: Application of particle size analysis. *Water (Switzerland)*, *7*(11), 6483–6495. https://doi.org/10.3390/w7116483

Martins, G., Salvador, A. F., Pereira, L., & Alves, M. M. (2018). Methane Production and Conductive Materials: A Critical Review. In *Environmental Science and Technology* (Vol. 52, Issue 18, pp. 10241–10253). American Chemical Society. https://doi.org/10.1021/acs.est.8b01913

Mawson, A. J., Earle, R. L., & Larsen', V. F. (1991). DEGRADATION OF ACETIC AND PROPIONIC ACIDS IN THE METHANE FERMENTATION. In *War. Res* (Vol. 25, Issue 12).

Meegoda, J. N., Li, B., Patel, K., & Wang, L. B. (2018). A review of the processes, parameters, and optimization of anaerobic digestion. In *International Journal of Environmental Research and Public Health* (Vol. 15, Issue 10). MDPI AG. https://doi.org/10.3390/ijerph15102224

Mei, R., Nobu, M. K., Narihiro, T., Yu, J., Sathyagal, A., Willman, E., & Liu, W. T. (2018). Novel Geobacter species and diverse methanogens contribute to enhanced methane production in media-added methanogenic reactors. *Water Research*, *147*, 403–412. https://doi.org/10.1016/j.watres.2018.10.026

Mori, K., Iino, T., Suzuki, K. I., Yamaguchi, K., & Kamagata, Y. (2012). Aceticlastic and NaCl-requiring methanogen "Methanosaeta pelagica" sp. Nov., isolated from marine tidal flat sediment. *Applied and Environmental Microbiology*, *78*(9), 3416–3423. https://doi.org/10.1128/AEM.07484-11

Mostafa, A., Im, S., Song, Y. C., Ahn, Y., & Kim, D. H. (2020). Enhanced anaerobic digestion by stimulating DIET reaction. In *Processes* (Vol. 8, Issue 4). MDPI AG. https://doi.org/10.3390/PR8040424

Namal, O. O. (2020). Investigation of the effects of different conductive materials on the anaerobic digestion. *International Journal of Environmental Science and Technology*, *17*(1), 473–482. https://doi.org/10.1007/s13762-019-02498-x

Nghiem, L. D., Manassa, P., Dawson, M., & Fitzgerald, S. K. (2014). Oxidation reduction potential as a parameter to regulate micro-oxygen injection into anaerobic digester for reducing hydrogen sulphide concentration in biogas.

Bioresource Technology, *173*, 443–447. https://doi.org/10.1016/j.biortech.2014.09.052

Nielsen, H. B., Mladenovska, Z., Westermann, P., & Ahring, B. K. (2004). Comparison of Two-Stage Thermophilic (68°C/55°C) Anaerobic Digestion with One-Stage Thermophilic (55°C) Digestion of Cattle Manure. *Biotechnology and Bioengineering*, *86*(3), 291–300. https://doi.org/10.1002/bit.20037

Nwokolo, N., Mukumba, P., Obileke, K., & Enebe, M. (2020). Waste to energy: A focus on the impact of substrate type in biogas production. In *Processes* (Vol. 8, Issue 10, pp. 1–21). MDPI AG. https://doi.org/10.3390/pr8101224

Orlando, M. Q., & Borja, V. M. (2020). Pretreatment of animal manure biomass to improve biogas production: A review. In *Energies* (Vol. 13, Issue 14). MDPI AG. https://doi.org/10.3390/en13143573

Palominos, N., Castillo, A., Guerrero, L., Borja, R., & Huiliñir, C. (2021). Coupling of Anaerobic Digestion and Struvite Precipitation in the Same Reactor: Effect of Zeolite and Bischofite as Mg2+ Source. *Frontiers in Environmental Science*, *9*. https://doi.org/10.3389/fenvs.2021.706730

Panigrahi, S., & Dubey, B. K. (2019). A critical review on operating parameters and strategies to improve the biogas yield from anaerobic digestion of organic fraction of municipal solid waste. In *Renewable Energy* (Vol. 143, pp. 779–797). Elsevier Ltd. https://doi.org/10.1016/j.renene.2019.05.040

Park, J. H., Kang, H. J., Park, K. H., & Park, H. D. (2018). Direct interspecies electron transfer via conductive materials: A perspective for anaerobic digestion applications. In *Bioresource Technology* (Vol. 254, pp. 300–311). Elsevier Ltd. https://doi.org/10.1016/j.biortech.2018.01.095

Park, J. H., Park, J. H., Je Seong, H., Sul, W. J., Jin, K. H., & Park, H. D. (2018). Metagenomic insight into methanogenic reactors promoting direct interspecies

electron transfer via granular activated carbon. *Bioresource Technology*, *259*, 414–422. https://doi.org/10.1016/j.biortech.2018.03.050

Park, J. H., Park, J. H., Lee, S. H., Jung, S. P., & Kim, S. H. (2020a). Enhancing anaerobic digestion for rural wastewater treatment with granular activated carbon (GAC) supplementation. *Bioresource Technology*, *315*. https://doi.org/10.1016/j.biortech.2020.123890

Park, J. H., Park, J. H., Lee, S. H., Jung, S. P., & Kim, S. H. (2020b). Enhancing anaerobic digestion for rural wastewater treatment with granular activated carbon (GAC) supplementation. *Bioresource Technology*, *315*. https://doi.org/10.1016/j.biortech.2020.123890

Park, J., Lee, B., Tian, D., & Jun, H. (2018). Bioelectrochemical enhancement of methane production from highly concentrated food waste in a combined anaerobic digester and microbial electrolysis cell. *Bioresource Technology*, *247*, 226–233. https://doi.org/10.1016/j.biortech.2017.09.021

Prashanth, S., Kumar, P., & Mehrotra, I. (2006). Anaerobic Degradability: Effect of Particulate COD. *Journal of Environmental Engineering*, *132*(4), 488–496. https://doi.org/10.1061/(asce)0733-9372(2006)132:4(488)

Puengrang, P., Suraraksa, B., Prommeenate, P., Boonapatcharoen, N., Cheevadhanarak, S., Tanticharoen, M., & Kusonmano, K. (2020). Diverse microbial community profiles of propionate-degrading cultures derived from different sludge sources of anaerobic wastewater treatment plants. *Microorganisms*, *8*(2). https://doi.org/10.3390/microorganisms8020277

Ramos-Suárez, J. L., Gómez, D., Regueiro, L., Baeza, A., & Hansen, F. (2017). Alkaline and oxidative pretreatments for the anaerobic digestion of cow manure and maize straw: Factors influencing the process and preliminary economic viability of an industrial application. *Bioresource Technology*, *241*, 10–20. https://doi.org/10.1016/j.biortech.2017.05.054

Rasapoor, M., Young, B., Asadov, A., Brar, R., Sarmah, A. K., Zhuang, W. Q., & Baroutian, S. (2020). Effects of biochar and activated carbon on biogas generation: A thermogravimetric and chemical analysis approach. *Energy Conversion and Management*, *203*. https://doi.org/10.1016/j.enconman.2019.112221

Rittmann, B. E. (2008). Opportunities for renewable bioenergy using microorganisms. In *Biotechnology and Bioengineering* (Vol. 100, Issue 2, pp. 203–212). https://doi.org/10.1002/bit.21875

Romero, R. M., Valenzuela, E. I., Cervantes, F. J., Garcia-Reyes, R. B., Serrano, D., & Alvarez, L. H. (2020). Improved methane production from anaerobic digestion of liquid and raw fractions of swine manure effluent using activated carbon. *Journal of Water Process Engineering*, *38*. https://doi.org/10.1016/j.jwpe.2020.101576

Rotaru, A. E., Shrestha, P. M., Liu, F., Markovaite, B., Chen, S., Nevin, K. P., & Lovley, D. R. (2014a). Direct interspecies electron transfer between Geobacter metallireducens and Methanosarcina barkeri. *Applied and Environmental Microbiology*, *80*(15), 4599–4605. https://doi.org/10.1128/AEM.00895-14

Rotaru, A. E., Shrestha, P. M., Liu, F., Markovaite, B., Chen, S., Nevin, K. P., & Lovley, D. R. (2014b). Direct interspecies electron transfer between Geobacter metallireducens and Methanosarcina barkeri. *Applied and Environmental Microbiology*, *80*(15), 4599–4605. https://doi.org/10.1128/AEM.00895-14

Rotaru, A. E., Shrestha, P. M., Liu, F., Shrestha, M., Shrestha, D., Embree, M., Zengler, K., Wardman, C., Nevin, K. P., & Lovley, D. R. (2014). A new model for electron flow during anaerobic digestion: Direct interspecies electron transfer to Methanosaeta for the reduction of carbon dioxide to methane. *Energy and Environmental Science*, *7*(1), 408–415. https://doi.org/10.1039/c3ee42189a

Rowe, A. R., Xu, S., Gardel, E., Bose, A., Girguis, P., Amend, J. P., El-Naggar, M. Y., & Ribbe, M. W. (2019). *Methane-Linked Mechanisms of Electron Uptake from Cathodes by Methanosarcina barkeri*. https://doi.org/10.1128/mBio

Ryue, J., Lin, L., Liu, Y., Lu, W., McCartney, D., & Dhar, B. R. (2019). Comparative effects of GAC addition on methane productivity and microbial community in mesophilic and thermophilic anaerobic digestion of food waste. *Biochemical Engineering Journal*, *146*, 79–87. https://doi.org/10.1016/j.bej.2019.03.010

Salvador, A. F., Martins, G., Melle-Franco, M., Serpa, R., Stams, A. J. M., Cavaleiro, A. J., Pereira, M. A., & Alves, M. M. (2017). Carbon nanotubes accelerate methane production in pure cultures of methanogens and in a syntrophic coculture. *Environmental Microbiology*, *19*(7), 2727–2739. https://doi.org/10.1111/1462-2920.13774

Shekhar Bose, R., Chowdhury, B., Zakaria, B. S., Kumar Tiwari, M., & Ranjan Dhar, B. (2021). Significance of different mixing conditions on performance and microbial communities in anaerobic digester amended with granular and powdered activated carbon. *Bioresource Technology*, *341*. https://doi.org/10.1016/j.biortech.2021.125768

Shen, N., Liang, Z., Chen, Y., Song, H., & Wan, J. (2020). Enhancement of syntrophic acetate oxidation pathway via single walled carbon nanotubes addition under high acetate concentration and thermophilic condition. *Bioresource Technology*, *306*. https://doi.org/10.1016/j.biortech.2020.123182

Shi, J., Han, Y., Xu, C., & Han, H. (2019). Enhanced biodegradation of coal gasification wastewater with anaerobic biofilm on polyurethane (PU), powdered activated carbon (PAC), and biochar. *Bioresource Technology*, *289*. https://doi.org/10.1016/j.biortech.2019.121487

Speece, R. E. (1983). Anaerobic biotechnology for industrial wastewater treatment. *Environmental Science and Technology*, *17*(9), 416A-427A. https://doi.org/10.1021/es00115a001

Stams, A. J. M., de Bok, F. A. M., Plugge, C. M., van Eekert, M. H. A., Dolfing, J., & Schraa, G. (2006). Exocellular electron transfer in anaerobic microbial communities. In *Environmental Microbiology* (Vol. 8, Issue 3, pp. 371–382). https://doi.org/10.1111/j.1462-2920.2006.00989.x

Standard Methods for the Examination of Water and Wastewater. (1999).

Sudiartha, G. A. W., Imai, T., & Hung, Y. T. (2022). Effects of Stepwise Temperature Shifts in Anaerobic Digestion for Treating Municipal Wastewater Sludge: A Genomic Study. *International Journal of Environmental Research and Public Health*, *19*(9). https://doi.org/10.3390/ijerph19095728

Summers, Z. M., Fogarty, H. E., Leang, C., Franks, A. E., Malvankar, N. S., & Lovley, D. R. (2010). Direct exchange of electrons within aggregates of an evolved syntrophic coculture of anaerobic bacteria. *Science*, *330*(6009), 1413–1415. https://doi.org/10.1126/science.1196526

Sun, M., Zhang, Z., Liu, G., Lv, M., & Feng, Y. (2021). Enhancing methane production of synthetic brewery water with granular activated carbon modified with nanoscale zero-valent iron (NZVI) in anaerobic system. *Science of the Total Environment*, *760*. https://doi.org/10.1016/j.scitotenv.2020.143933

Tezel, U., Pierson, J. A., & Pavlostathis, S. G. (2007). Effect of polyelectrolytes and quaternary ammonium compounds on the anaerobic biological treatment of poultry processing wastewater. *Water Research*, *41*(6), 1334–1342. https://doi.org/10.1016/j.watres.2006.12.005

Thauer, R. K., Kaster, A. K., Seedorf, H., Buckel, W., & Hedderich, R. (2008). Methanogenic archaea: Ecologically relevant differences in energy

conservation. In *Nature Reviews Microbiology* (Vol. 6, Issue 8, pp. 579–591). https://doi.org/10.1038/nrmicro1931

Tiwari, S. B., Dubey, M., Ahmed, B., Gahlot, P., Khan, A. A., Rajpal, A., Kazmi, A. A., & Tyagi, V. K. (2021). Carbon-based conductive materials facilitated anaerobic co-digestion of agro waste under thermophilic conditions. *Waste Management*, *124*, 17–25. https://doi.org/10.1016/j.wasman.2021.01.032

Uçkun Kiran, E., Stamatelatou, K., Antonopoulou, G., & Lyberatos, G. (2016a). Production of biogas via anaerobic digestion. In *Handbook of Biofuels Production: Processes and Technologies: Second Edition* (pp. 259–301). Elsevier Inc. https://doi.org/10.1016/B978-0-08-100455-5.00010-2

Uçkun Kiran, E., Stamatelatou, K., Antonopoulou, G., & Lyberatos, G. (2016b). Production of biogas via anaerobic digestion. In *Handbook of Biofuels Production: Processes and Technologies: Second Edition* (pp. 259–301). Elsevier Inc. https://doi.org/10.1016/B978-0-08-100455-5.00010-2

Wan, H., Wang, F., Chen, Y., Zhao, Z., Zhang, G., Dou, M., & Xue, B. (2021). Enhanced Reactive Red 2 anaerobic degradation through improving electron transfer efficiency by nano-Fe3O4 modified granular activated carbon. *Renewable Energy*, *179*, 696–704. https://doi.org/10.1016/j.renene.2021.07.046

Wang, C., Wang, C., Liu, J., Han, Z., Xu, Q., Xu, X., & Zhu, L. (2020). Role of magnetite in methanogenic degradation of different substances. *Bioresource Technology*, *314*. https://doi.org/10.1016/j.biortech.2020.123720

Wang, R., Li, Y., Wang, W., Chen, Y., & Vanrolleghem, P. A. (2015). Effect of high orthophosphate concentration on mesophilic anaerobic sludge digestion and its modeling. *Chemical Engineering Journal*, *260*, 791–800. https://doi.org/10.1016/j.cej.2014.09.050

Wang, T., Zhang, D., Dai, L., Chen, Y., & Dai, X. (2016). Effects of metal nanoparticles on methane production from waste-activated sludge and

microorganism community shift in anaerobic granular sludge. *Scientific Reports*, *6*. https://doi.org/10.1038/srep25857

Wang, W., Chang, J. S., & Lee, D. J. (2022). Integrating anaerobic digestion with bioelectrochemical system for performance enhancement: A mini review. In *Bioresource Technology* (Vol. 345). Elsevier Ltd. https://doi.org/10.1016/j.biortech.2021.126519

Wang, W., & Lee, D. J. (2021). Direct interspecies electron transfer mechanism in enhanced methanogenesis: A mini-review. In *Bioresource Technology* (Vol. 330). Elsevier Ltd. https://doi.org/10.1016/j.biortech.2021.124980

Wang, W., Xie, L., Luo, G., Zhou, Q., & Angelidaki, I. (2013). Performance and microbial community analysis of the anaerobic reactor with coke oven gas biomethanation and in situ biogas upgrading. *Bioresource Technology*, *146*, 234–239. https://doi.org/10.1016/j.biortech.2013.07.049

Xiao, B., Zhang, W., Yi, H., Qin, Y., Wu, J., Liu, J., & Li, Y. Y. (2019). Biogas production by two-stage thermophilic anaerobic co-digestion of food waste and paper waste: Effect of paper waste ratio. *Renewable Energy*, *132*, 1301–1309. https://doi.org/10.1016/j.renene.2018.09.030

Xie, S., Li, X., Wang, C., Kulandaivelu, J., & Jiang, G. (2020). Enhanced anaerobic digestion of primary sludge with additives: Performance and mechanisms. *Bioresource Technology*, *316*. https://doi.org/10.1016/j.biortech.2020.123970

Xu, N., Liu, S., Xin, F., Zhou, J., Jia, H., Xu, J., Jiang, M., & Dong, W. (2019). Biomethane production from lignocellulose: Biomass recalcitrance and its impacts on anaerobic digestion. *Frontiers in Bioengineering and Biotechnology*, *7*(AUG). https://doi.org/10.3389/fbioe.2019.00191

Xu, S., He, C., Luo, L., Lü, F., He, P., & Cui, L. (2015). Comparing activated carbon of different particle sizes on enhancing methane generation in upflow

anaerobic digester. *Bioresource Technology*, *196*, 606–612. https://doi.org/10.1016/j.biortech.2015.08.018

Yan, W., Mukherjee, M., & Zhou, Y. (2020). Direct interspecies electron transfer (DIET) can be suppressed under ammonia-stressed condition – Reevaluate the role of conductive materials. *Water Research*, *183*. https://doi.org/10.1016/j.watres.2020.116094

Yang, Y., Zhang, Y., Li, Z., Zhao, Z., Quan, X., & Zhao, Z. (2017). Adding granular activated carbon into anaerobic sludge digestion to promote methane production and sludge decomposition. *Journal of Cleaner Production*, *149*, 1101–1108. https://doi.org/10.1016/j.jclepro.2017.02.156

Yang, Z., Guo, R., Shi, X., Wang, C., Wang, L., & Dai, M. (2016). Magnetite nanoparticles enable a rapid conversion of volatile fatty acids to methane. *RSC Advances*, *6*(31), 25662–25668. https://doi.org/10.1039/c6ra02280d

Yasemin Dilsad Yilmazel, B. (2014). *A CALDICELLULOSIRUPTOR BESCII BASED HYPERTHERMOPHILIC BIOPROCESS FOR HYDROGEN PRODUCTION FROM RENEWABLE FEEDSTOCK*.

Ye, J., Hu, A., Ren, G., Chen, M., Tang, J., Zhang, P., Zhou, S., & He, Z. (2018). Enhancing sludge methanogenesis with improved redox activity of extracellular polymeric substances by hematite in red mud. *Water Research*, *134*, 54–62. https://doi.org/10.1016/j.watres.2018.01.062

Yin, Q., Gu, M., & Wu, G. (2020). Inhibition mitigation of methanogenesis processes by conductive materials: A critical review. *Bioresource Technology*, *317*. https://doi.org/10.1016/j.biortech.2020.123977

Yu, N., Guo, B., & Liu, Y. (2021). Shaping biofilm microbiomes by changing GAC location during wastewater anaerobic digestion. *Science of the Total Environment*, *780*. https://doi.org/10.1016/j.scitotenv.2021.146488

Zhang, J., Zhang, R., Wang, H., & Yang, K. (2020). Direct interspecies electron transfer stimulated by granular activated carbon enhances anaerobic methanation efficiency from typical kitchen waste lipid-rapeseed oil. *Science of the Total Environment*, *704*. https://doi.org/10.1016/j.scitotenv.2019.135282

Zhang, L., Zhang, J., & Loh, K. C. (2018). Activated carbon enhanced anaerobic digestion of food waste – Laboratory-scale and Pilot-scale operation. *Waste Management*, *75*, 270–279. https://doi.org/10.1016/j.wasman.2018.02.020

Zhang, S., Chang, J., Lin, C., Pan, Y., Cui, K., Zhang, X., Liang, P., & Huang, X. (2017). Enhancement of methanogenesis via direct interspecies electron transfer between Geobacteraceae and Methanosaetaceae conducted by granular activated carbon. *Bioresource Technology*, *245*, 132–137. https://doi.org/10.1016/j.biortech.2017.08.111

Zhao, Z., Zhang, Y., Woodard, T. L., Nevin, K. P., & Lovley, D. R. (2015). Enhancing syntrophic metabolism in up-flow anaerobic sludge blanket reactors with conductive carbon materials. *Bioresource Technology*, *191*, 140–145. https://doi.org/10.1016/j.biortech.2015.05.007

Zhao, Z., Zhang, Y., Yu, Q., Dang, Y., Li, Y., & Quan, X. (2016). Communities stimulated with ethanol to perform direct interspecies electron transfer for syntrophic metabolism of propionate and butyrate. *Water Research*, *102*, 475–484. https://doi.org/10.1016/j.watres.2016.07.005

Zhen, X., Luo, M., Dong, H., Fang, L., Wang, W., Feng, L., & Yu, Q. (2022). Effect of organic load regulation on anaerobic digestion performance and microbial community of solar-assisted system of food waste. *Water Reuse*, *12*(2), 260–273. https://doi.org/10.2166/wrd.2022.107

Zheng, Z., Liu, J., Yuan, X., Wang, X., Zhu, W., Yang, F., & Cui, Z. (2015). Effect of dairy manure to switchgrass co-digestion ratio on methane production and

the bacterial community in batch anaerobic digestion. *Applied Energy*, *151*, 249–257. https://doi.org/10.1016/j.apenergy.2015.04.078

Zhou, L., Liu, X., & Dong, X. (2014). Methanospirillum psychrodurum sp. nov., isolated from wetland soil. *International Journal of Systematic and Evolutionary Microbiology*, *64*(PART 2), 638–641. https://doi.org/10.1099/ijs.0.057299-0

Zhou, S., Xu, J., Yang, G., & Zhuang, L. (2014). Methanogenesis affected by the co-occurrence of iron(III) oxides and humic substances. *FEMS Microbiology Ecology*, *88*(1), 107–120. https://doi.org/10.1111/1574-6941.12274

Zhuang, L., Tang, J., Wang, Y., Hu, M., & Zhou, S. (2015). Conductive iron oxide minerals accelerate syntrophic cooperation in methanogenic benzoate degradation. *Journal of Hazardous Materials*, *293*, 37–45. https://doi.org/10.1016/j.jhazmat.2015.03.039

Zwietering, M. H., Jongenburger, I., Rombouts, F. M., van ' K., & Riet, T. (1990). Modeling of the Bacterial Growth Curve. In *APPLIED AND ENVIRONMENTAL MICROBIOLOGY*.

APPENDICES

A. Calculation for kinetic parameters

The Modifief Gompertz Modeling was applied to find kinetic parameters of AD such as maximum methane production potential (mL, B_0), methane production rate (mL CH_4/day, R_m) and lag time for the reactor (day, λ) based on the foowing equation:

$$B_{(t)} = B0 * \exp\{[\frac{Rm*e}{B0} * (\lambda - t) + 1]\}, t \geq 0$$

where t is incubation time (day) e is 2.718.

For each sampling day, the equation was applied, and specific methane production (mL, B_t) was calculated After that, the difference between actual cumulative methane production and calculated specific methane production for each sampling day was squared and summed up as sum of square roots (SSR). After this step, the Solver in Excel was used. The objective was determined 'the minimum value' of SSR, and the variables are 'maximum methane production potential' cell, 'methane production rate' cell and 'lag time' cell with the initial value of 1. After we apply the Solver, these three parameters were calculated. Then, to find the correlation between experimental data and calculated data, we used RSQ formula between these two groups of data, and calculated R^2 values for each reactor.

B. Modified Gompertz Model Fittings for Set 1

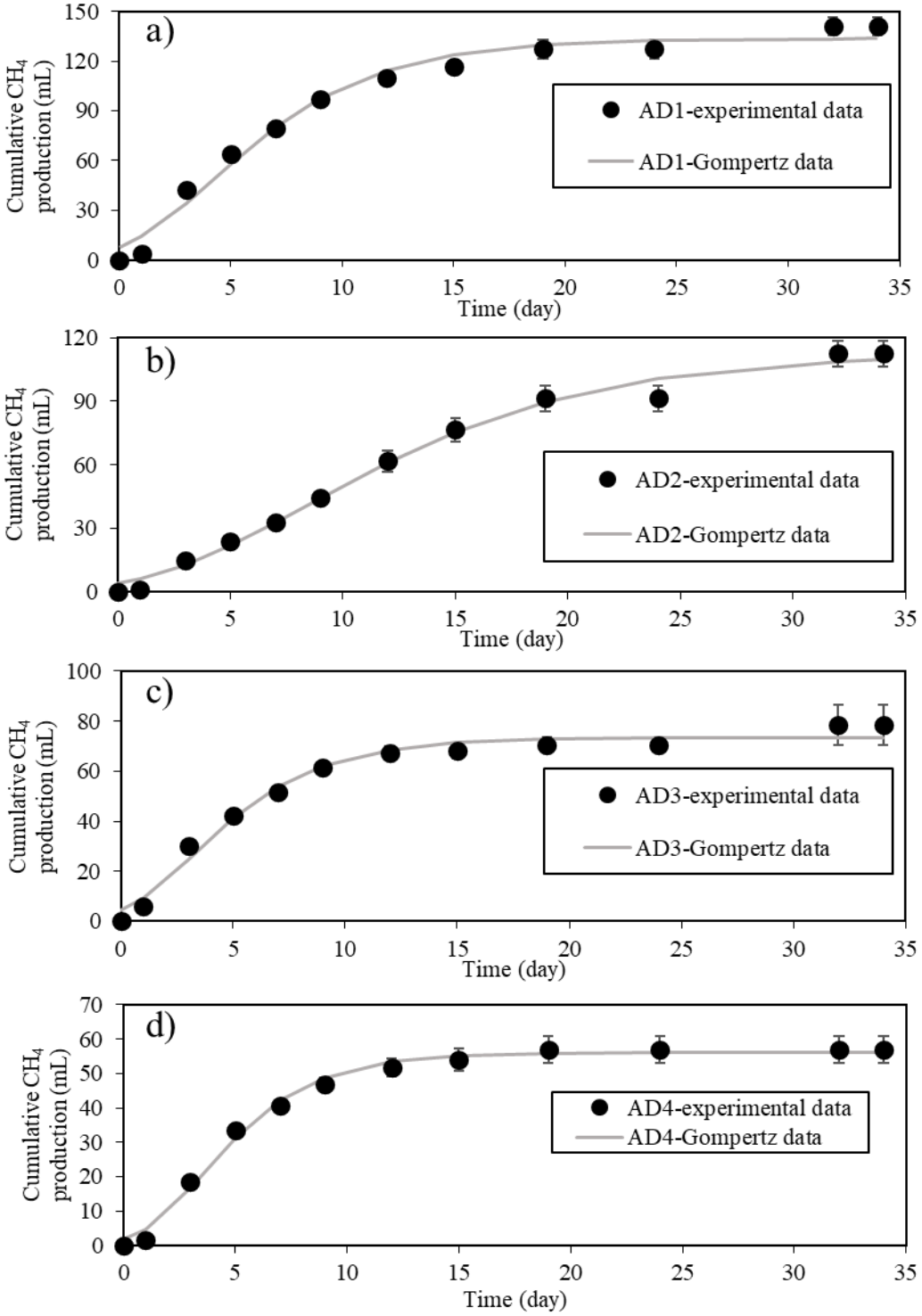

Figure B.1. The fittings of the experimental data and the model data in Set 1

C. Modified Gompertz Model Fittings for Set 2

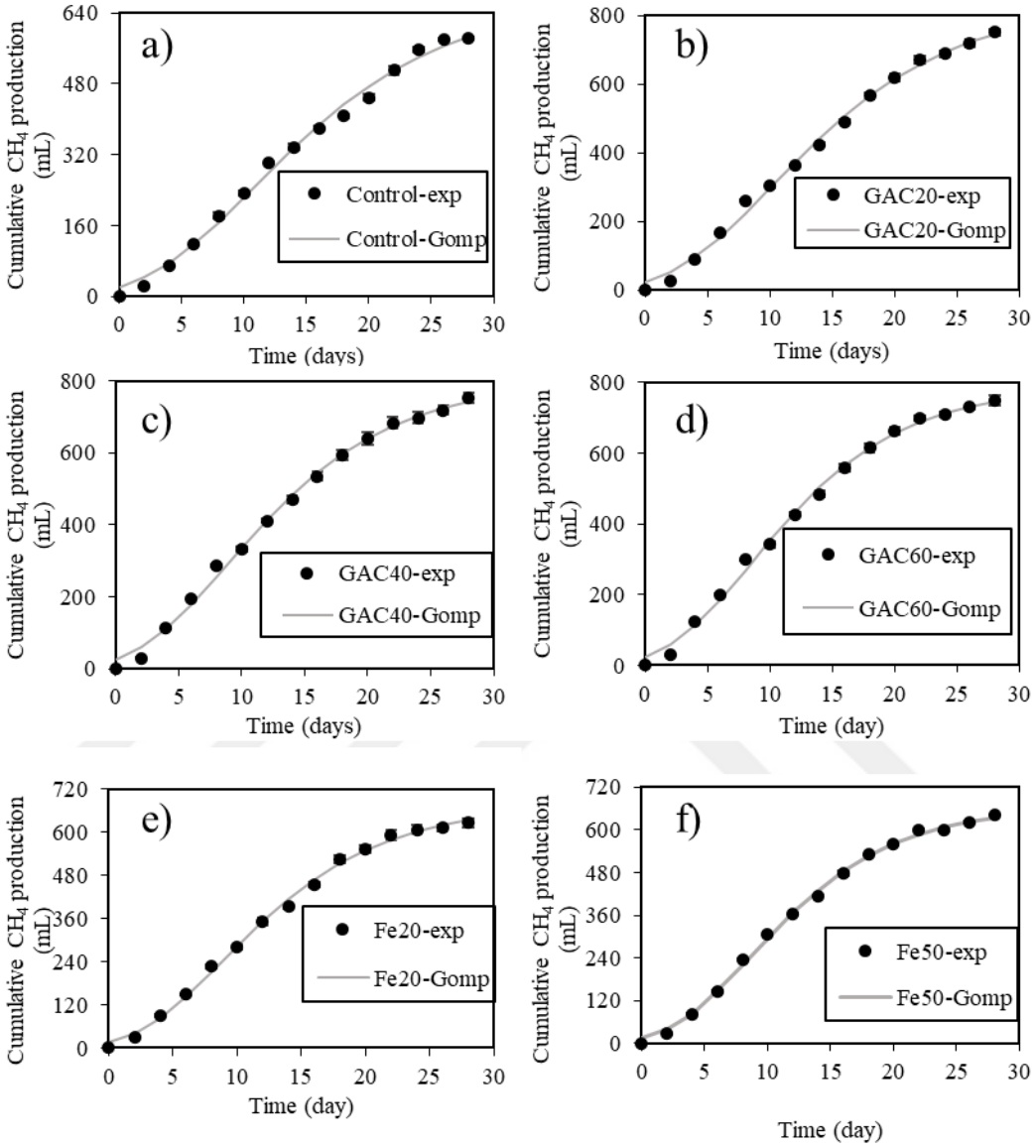

Figure C.1. The fittings of the experimental data and the model data in Set 2

D. Modified Gompertz Model Fittings for Set 3

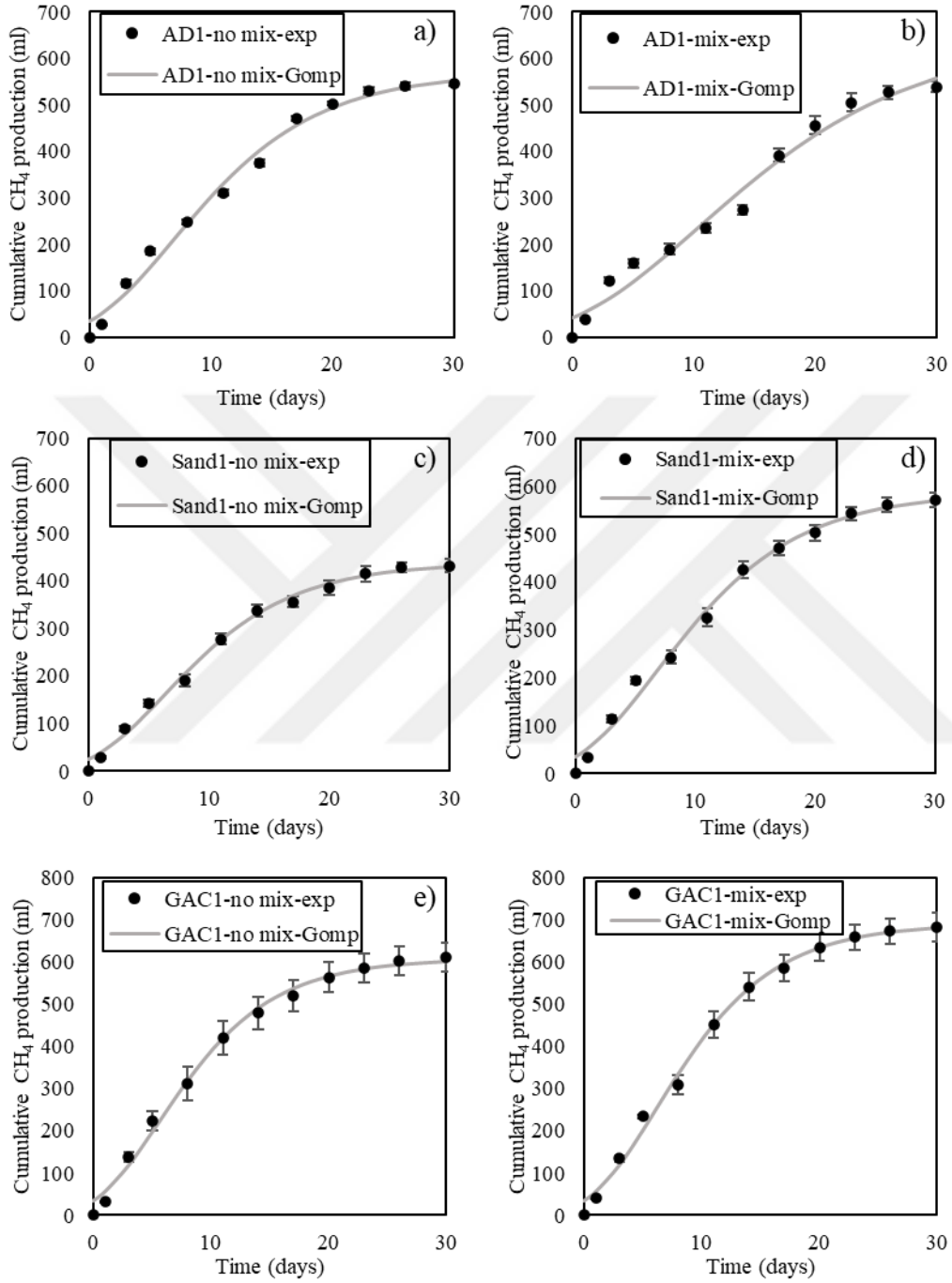

Figure D.1. The fittings of the experimental data and the model data for reactors at F/M ratio of 1 in Set 3

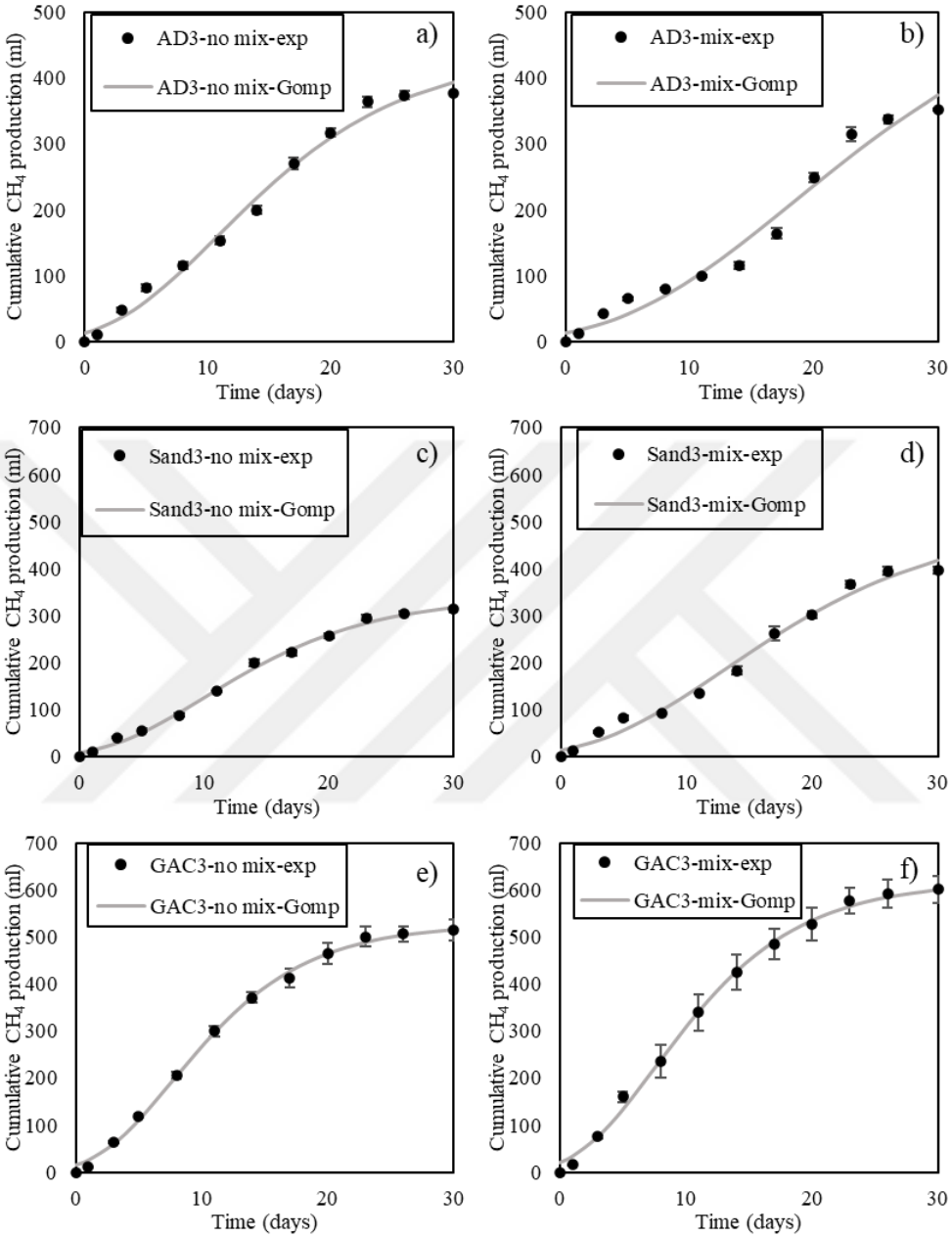

Figure D.2. The fittings of the experimental data and the model data for reactors at F/M ratio of 3 in Set 3

E. Modified Gompertz Model Fittings for Set 4

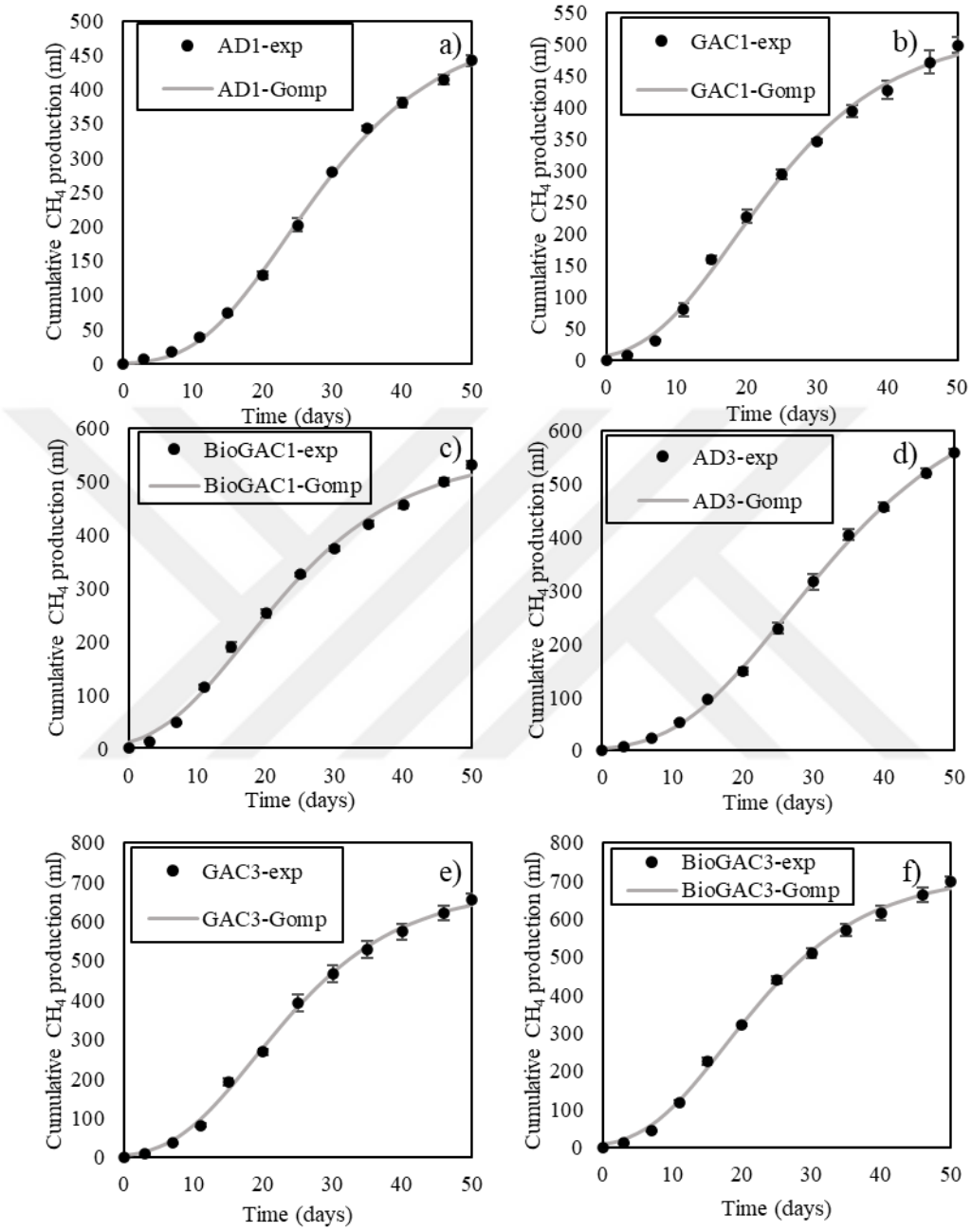

Figure E.1. The fittings of the experimental data and the model data in Set 4